UNCLASSIFIED

AD NUMBER

AD918861

NEW LIMITATION CHANGE

TO

Approved for public release, distribution unlimited

FROM

Distribution authorized to U.S. Gov't. agencies only; Test and Evaluation; Apr 1974. Other requests shall be referred to Air Force Avionics Lab., Wright-Patterson AFB, OH 45433.

AUTHORITY

AFAL LTR, 6 Feb 1976

THIS PAGE IS UNCLASSIFIED

AFAL-TR-73-296

AD918861
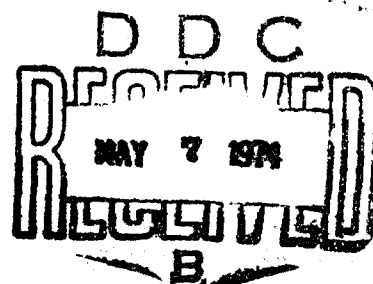
INCREMENTAL LENGTH DIFFRACTION
COEFFICIENTS

K. M. Mitzner

Northrop Corporation
Aircraft Division

TECHNICAL REPORT AFAL-TR-73-296

April 1974

DDC

MAY 7 1974

B

INCREMENTAL LENGTH DIFFRACTION
COEFFICIENTS

K. M. Mitzner

FOREWORD

This document reports a portion of the work performed by Northrop Corporation, Aircraft Division, Hawthorne, California, under USAF Contract F33615-70-C-1820, "Calculation of Radar Cross Sectio.," during the period from 1 December 1970 to 1 June 1973. The work was sponsored by the Electronic Warfare Division, Air Force Avionics Laboratory under Project 7633, Task 13, with Dr. Charles H. Krueger, AFAL/WRP as technical monitor.

This document was prepared by Dr. K. M. Mitzner of the Electronic Systems Research and Technology Group at Northrop. Mr. S. Stanley Locus was Principal Investigator on the contract.

This document has been assigned NOR 73-104 by Northrop for internal control purposes and was submitted by the author in July 1973.

This Technical Report has been reviewed and is approved for publication.

W. J. PORTUNE, JR.
Assistant Chief
Electronic Warfare Division

ABSTRACT

The principal goal of USAF Contract F33615-70-C-1820 is to develop a semi-automated system for computing the radar cross section (RCS) of aerospace vehicles over the frequency range of 500-20,000 MHZ. Such a system requires the use of efficient techniques for calculating the high-frequency scattering from bodies with edges such as wings and ducts.

In calculating the scattering from three-dimensional bodies with edges, it is frequently meaningful and useful to consider the scattering associated with an incremental length of the edge and to describe this scattering in terms of an Incremental Length Edge Diffraction Coefficient (ILEDC). In this report the theory of the ILEDC is developed, taking into account the actual distribution of surface current near the edge. The theory is illustrated by applying it to the problem of scattering from a perfectly conducting polygonal plate. The Incremental Length Diffraction Coefficient (ILDC), which is the generalization of the ILEDC for linear scattering features other than edges, is also treated. It is shown that two-dimensional diffraction coefficients, such as those used by Keller and Ufimtsev, can be considered as special cases of ILDC's.

TABLE OF CONTENTS

LIST OF ILLUSTRATIONS

I. INTRODUCTION AND OVERVIEW

In dealing with high-frequency scattering from three-dimensional bodies with edges, it is often meaningful and useful to treat the edges as diffracting elements. The diffraction from an incremental length of the edge can then be related to the incident field by means of a dyadic quantity* which we shall call the Incremental Length Edge Diffraction Coefficient (ILEDC).

Our principal objective in this report is to evaluate the ILEDC which describes the so-called "fringe wave" scattering from a perfect conductor and to show how this ILEDC is applied. We treat the ILEDC as a special case of a more general dyadic quantity which we call the Incremental Length Diffraction Coefficient (ILDC). The ILDC is defined not just for an edge but for any line diffraction feature, for example, a wire or a rounded edge.

Before considering the ILDC, we first develop many of the concepts of diffraction coefficient theory and much of the nomenclature in a simpler context, that of scattering from an infinitely long cylinder. We describe scattering from such a cylinder - either the total scattering or some physically meaningful contribution to the scattered field - in terms of a dyadic quantity which we call the Two-Dimensional Diffraction Coefficient (2-D DC). The 2-D DC provides a simple and compact way of expressing the well-known edge diffraction results of Ufimtsev (Reference 1) and Keller (Reference 3).

The ILDC, which is defined for all directions of incidence and scattering, is shown to be a generalization of the 2-D DC, which is defined only for certain combinations of incident direction and scattering direction. Wherever the 2-D DC is defined, it is equal to the corresponding ILDC. The fringe wave ILEDC is the generalization of the Ufimtsev 2-D DC and will thus be referred to as the Ufimtsev ILEDC.

The material on the 2-D DC is given in Section II and is backed up by a thorough discussion in the Appendix of scattering from an infinite cylinder. The Ufimtsev 2-D DC is treated in Section 2.2.4 with special cases given in 2.2.5 and 2.2.6.

---

*For those who are not familiar with the term, a dyadic $\underline{\underline{A}}$ is a quantity which effects a linear transformation of a vector $\underline{B}$ into a vector $\underline{C}$. We write the transformation in the form $\underline{C} = \underline{\underline{A}} \cdot \underline{B}$.

1

The ILDC is studied in Section 3.1 and the results are then specialized in Section 3.2 to obtain the Ufimtsev ILEDC for an edge with wedge angle less than 180° (so that there are no internal reflections) on a perfect conductor. Special results for the knife edge case and for backscatter are included in Section 3.2. Section IV illustrates the use of the ILEDC in solving realistic scattering problems.

<p style="text-align:center">✦ ✦ ✦</p>

The sample problem which we consider in Section IV is high-frequency scattering, both monostatic and bistatic, from a flat perfectly conducting plate with a polygonal boundary when both source and observer are in the far-field region. This is an appropriate choice because our investigations of Ufimtsev's approach, the Physical Theory of Diffraction (PTD), and our development of the Ufimtsev ILEDC were originally motivated by our observation that the more commonly-used Geometrical Theory of Diffraction (GTD) was not adequate for rectangular and trapezoidal plate problems. (See Reference 2, Section 2.2.).

We assume in Section IV that edge interactions can be neglected and that we can also neglect the effect of distortions of the surface current near the corners of the plate.

Under these assumptions, the Physical Theory of Diffraction describes the total scattering from the plate as the sum of two contributions, one due to the physical optics surface current on the plate and the other due to the fringe wave surface current concentrated near the edges of the plate. To find the fringe wave current associated with a straight segment of the edge, we assume that the segment is part of the edge of an infinite half-plane and we take the difference between the total surface current and the physical optics surface current for the half-plane problem. It is readily seen that the fringe wave current associated with every incremental length of a straight edge is the same except for phase.

The fringe wave diffraction from a straight segment of length $\overline{L}$ is thus described by the product of the Ufimtsev ILEDC $\underline{d}^U$ with an appropriate $\overline{L}\,\dfrac{\sin X}{X}$ factor obtained by integrating phase along the edge, and the total fringe wave scattering is the sum of analogous contributions from all the straight edges. By decomposing each $\sin X$ term as the sum of two exponentials, we can obtain an equivalent representation in terms of contributions from the corners.

The physical optics contribution to the scattering from the plate has been calculated in Section V of Reference 11, and the most important results are repeated here in Section 4.1. Just as with the fringe wave diffraction, the physical optics scattering can be represented either in terms of edge contributions involving the product of an ILEDC with a $\overline{L} \frac{\sin X}{X}$ factor or in terms of corner contributions. The total scattering can then also be expressed in terms of edge or corner contributions which are the sum of the corresponding fringe wave and physical optics contributions.

Solutions calculated by this approach are compared with experimental results in Section 4.2 and it is confirmed that the approach is accurate over a wide range of conditions.

* * *

It is important to note that the Ufimtsev ILEDC used here is calculated by a method which takes into account the manner in which the fringe wave current is distributed near the edge. This is one of the reasons why the material developed here has a broader range of applicability than the Ryan-Peters theory of Reference 10, in which the total edge diffraction is assumed to originate from a filamentary edge current with a value which is a function of the azimuth of scattering. (The Ryan-Peters theory, on the other hand, has a broader range of applicability than standard GTD.)

* * *

The material in Section IV is an example of how a problem is solved within the framework of Ufimtsev's PTD. The basic idea of PTD is to treat the scattered field as a function of the surface current induced on the scattering body. This surface current is in turn a function of the incident field, and thus we have linked the incident field to the scattered field by way of the surface currents. In many problems the linkage can be described in terms of diffraction coefficients obtained from canonical problems - as has been done for the polygonal plate problem - and it is not necessary in these problems to work directly with surface currents. Thus, even though PTD is based on surface current considerations, the surface currents may only enter a problem implicitly.

The usefulness of the ILEDC is not restricted to simple situations like that of Section IV in which the scattered field can be adequately approximated as the sum of a physical optics contribution plus a fringe wave contribution. The ILEDC can still be used to calculate the fringe wave contributions in more sophisticated versions of PTD which also take into account contributions due to phenomena such as corner currents, creeping waves, and multiple reflection or diffraction. And the more general ILDC can be used similarly for bodies with line diffraction features other than sharp edges.

For many problems, PTD leads to a solution which is simple in form and which, like the corner diffraction representation of the polygonal plate solution, has a physical interpretation in terms of rays emanating from discrete points on the scattering body. For bodies with edges, a necessary though not sufficient condition for the existence of such a scattering center interpretation is that the physical optics scattering can be represented wholly or in part as an edge diffraction phenomenon and that the edge diffraction can be described by a physical optics ILEDC. As examples, the physical optics scattering from any flat perfectly conducting plate can be expressed exactly by the integral of an ILEDC around the edge (See Section 5.4 of Reference 11.), and the physical optics scattering from some doubly curved surfaces with edges can be approximated accurately as the sum of a specular point contribution and the integral of an ILEDC around the edge (Reference 12.) For both types of problem, the edge integral can in many cases be evaluated in terms of contributions from discrete points, but this is not always so.

* * *

We shall concentrate in this report on ILDC's which arise out of the solution of two-dimensional canonical problems, that is, which represent scattering from an incremental length of an infinite cylinder. Since most physical optics diffraction coefficients are not associated with any two-dimensional problem, they are thus outside the pale of this report. We note, however, that efficient techniques for the evaluation of physical optics integrals are crucial to the development of PTD as a practical tool for the treatment of realistic scattering problems and, indeed, much of the advantage of PTD over GTD lies in the ability to treat physical optics diffraction phenomena which have no two-dimensional counterpart. References 11 and 12 give various examples of physical optics calculations.

* * *

4

A good understanding of the 2-D DC makes it much easier to understand the ILDC and the ILEDC. For this reason, we consider the 2-D DC in detail in Section II, developing the general theory in Section 2.1, and then discussing the Keller (GTD) coefficient and the Ufimtsev coefficient in Section 2.2. This study is backed up by a thorough treatment in the Appendix of scattering from an infinitely long cylinder. The Appendix includes not only the material we need for Section II but additional material for use in extending the diffraction coefficient concept to situations in which source or observer or both are at finite distance from the scattering body.

In Sections I.3.3 and 2.1.2, we show that the far-field scattering due to a plane wave incident on an infinitely long cylinder can be interpreted in terms of rays emanating from the cylinder axis and that all scattered rays form the same angle with the cylinder axis. Thus the rays emanating from a point P on the axis all lie on a circular cone with apex at P. The angle which the scattered rays make with the axis is found to be the same as the angle which the incident wave makes with the axis so that, in the nomenclature of Figures 1 and 2, we have $\beta_s = \beta_i$ for all scattered rays.

The 2-D DC which describes this scattering process (both magnitude and polarization changes) has the form of a four-element dyadic which transforms the incident polarization vector into a vector normal to the direction of scattering. If we consider the geometry and composition of the cylinder to be fixed, the 2-D DC is a function of the wave number k, the direction of incidence, and the direction of scattering. But the latter two quantities are not independent because of the requirement that the incident wave and the scattered rays form the same angle with the axis. For a given direction of incidence, the 2-D DC is defined only for those directions of scattering which satisfy this criterion. As to the wave number dependence, we use a normalization in which both the Ufimtsev and Keller diffraction coefficients for a perfectly conducting edge are independent of k.

For incidence normal to the axis, $\beta_i = 0$, the 2-D DC can be expressed in a form in which only two of the four dyadic elements are non-zero. For perfect conductor problems with any value of β_i, we can obtain a form with only two non-zero elements if the diffraction coefficient represents the scattering due to the total surface current on the cylinder (as in the case of the Keller edge diffraction coefficient). We may, however, need a third non-zero element if the coefficient represents the

5

(a) Cross-Sectional View

(b) Side View
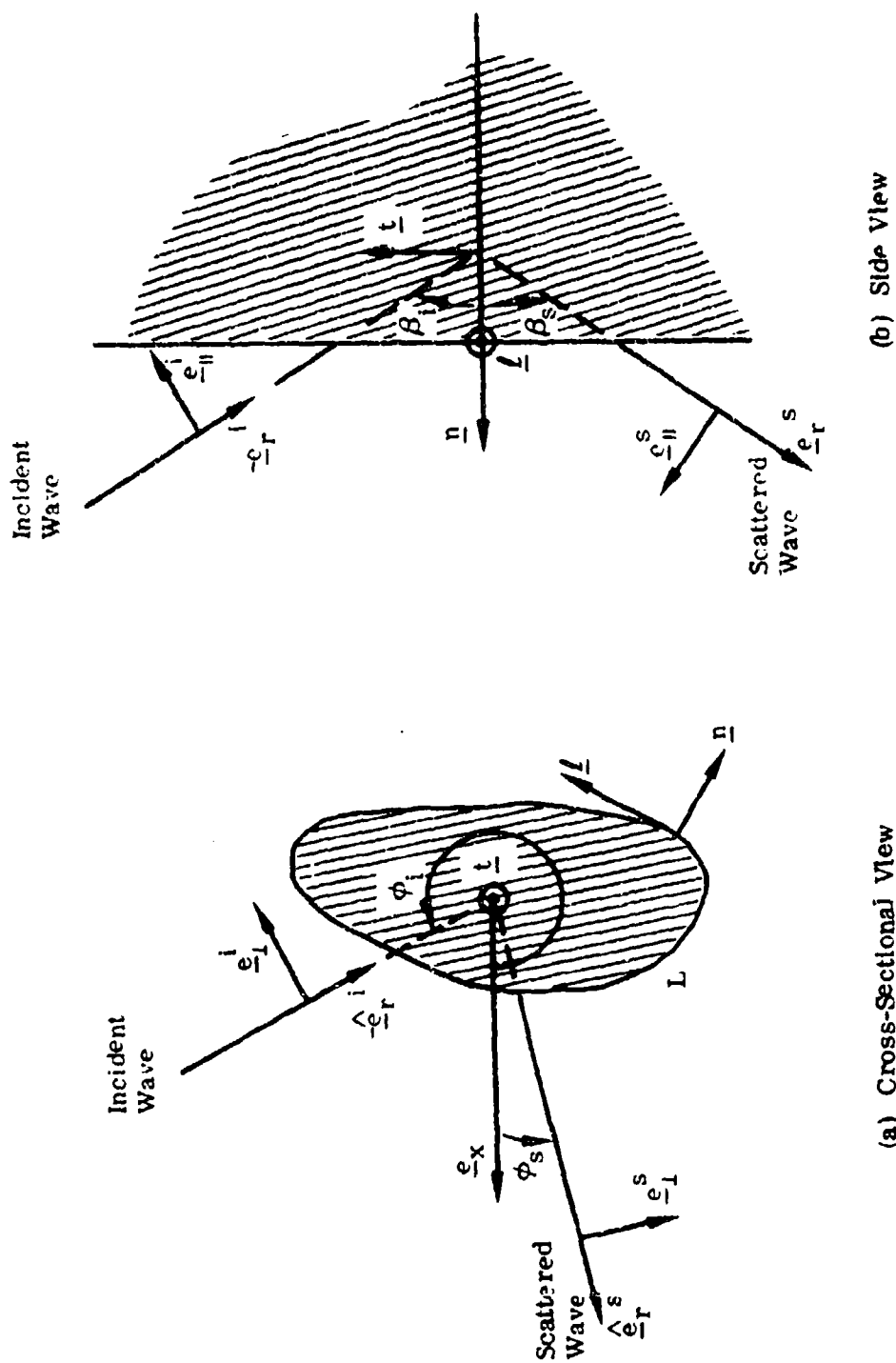
FIGURE 1   SCATTERING FROM A CYLINDER

6
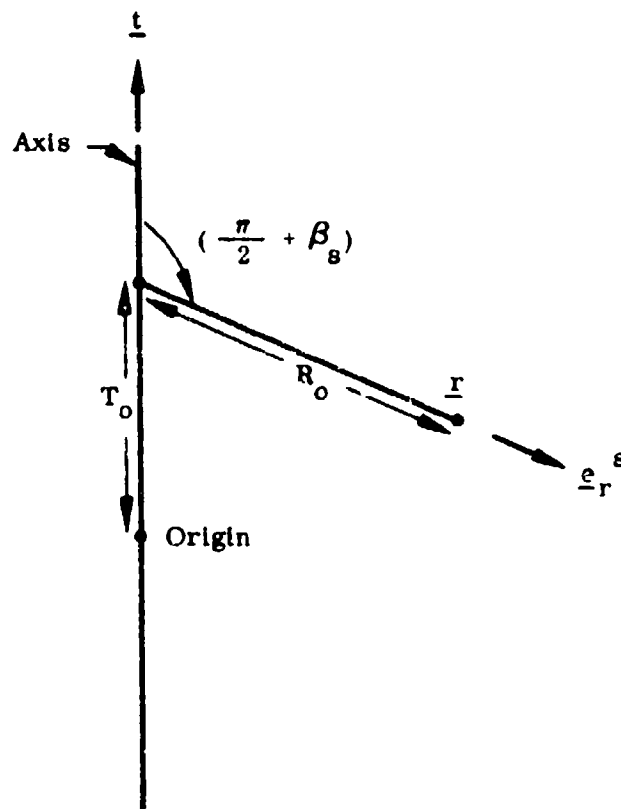
FIGURE 2 DEFINITIONS OF R_o, T_o, $\underline{e}_r^s$

scattering due to some contribution to the total current; existence of such an element means that the diffraction coefficient <u>by itself</u> does not satisfy the requirements of reciprocity.

It turns out that the complete form of the Ufimtsev 2-D DC indeed has the third non-zero element allowed by theory for $\beta_t \neq 0$. Ufimtsev did not consider this element in Reference 1, but its omission does not affect his results for two-dimensional problems - because he considered only problems which can be reduced to equivalent problems with $\beta_t = 0$ (See Section I.3.2) - nor does it affect his single diffraction results for backscatter from bodies with curved edges - because these results involve only the value of the diffraction coefficient for $\beta_s = \beta_t = 0$.

*　*　*

There are many three-dimensional problems which can be solved satisfactorily using a 2-D DC. It is important to understand both why this can be done for some problems and why it cannot be done for others.

Under appropriate circumstances, the far-field diffraction from an edge C which is illuminated by a plane wave can be interpreted in terms of rays emanating from each point on the edge, with all the rays which emanate from a given point P forming a cone with apex at P. Under these same conditions, there will be only a finite number of rays scattered in a given direction, each such ray originating at a different point on the edge. Thus we can say that all the scattering in that direction originates from these points.

The geometry for an incremental length of C, which is the same as the geometry of an incremental length of an infinite wedge, is shown in Figure 3. The cone of scattering angles at the point P is found by identifying the tangent vector to C at P with the axial vector $\underline{t}$ along the edge of the wedge and by then applying the condition $\beta_s = \beta_t$. The wedge angle 2α at P is the angle formed by the tangent planes at P to the two surfaces which meet along C. It can be shown that the amplitude of the field on a ray in the curved edge problem is closely related to the amplitude of the field on the corresponding ray in the infinite wedge problem; it is only necessary to introduce a scalar factor which accounts for the spreading out of energy due to the curvature of C.

8
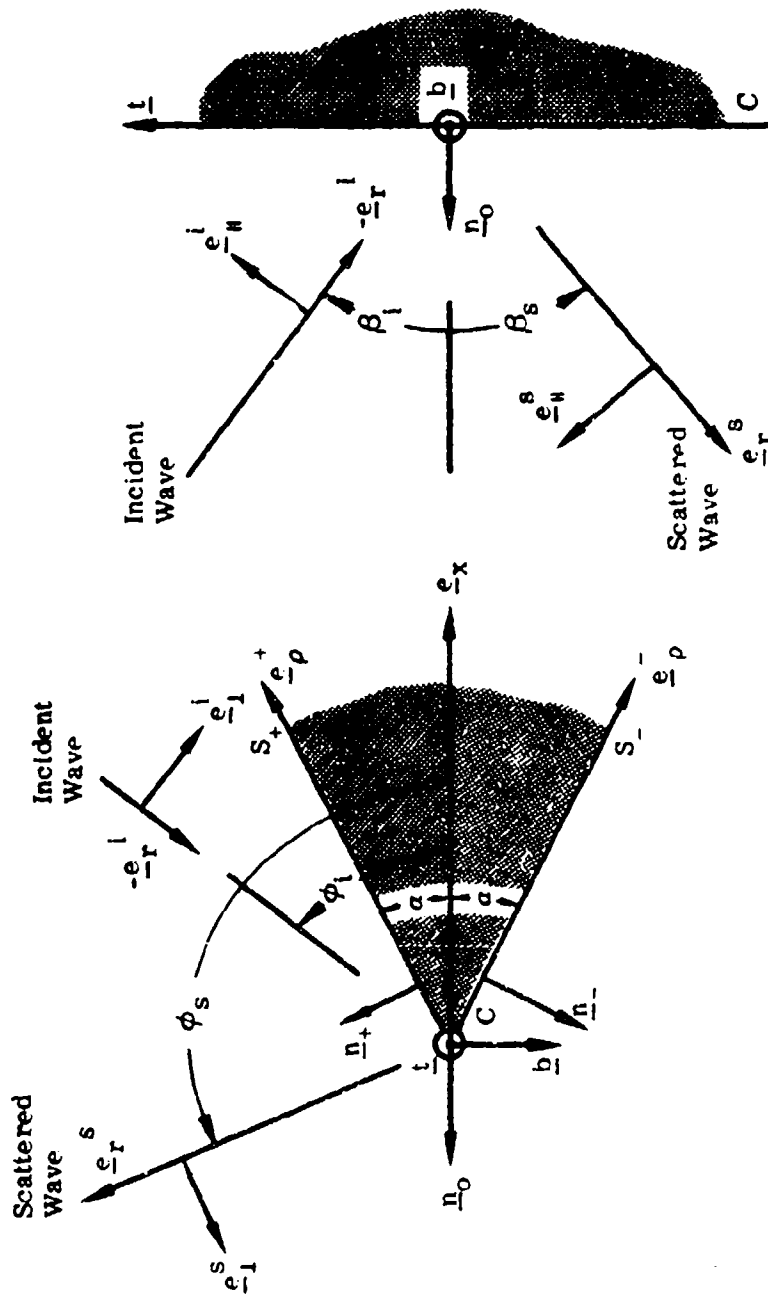
FIGURE 3   SCATTERING FROM A WEDGE

Thus the result of the infinite wedge problem, that is to say, the Two-Dimensional Diffraction Coefficient, can be used to solve the curved edge problem. Indeed, for backscatter we need only the 2-D DC for incidence normal to the axis, $\beta_s = \beta_i = 0$, because the scattering appears to emanate from those points at which the tangent to C is normal to the direction of incidence and scattering. As already noted, the 2-D DC for this special case has only two non-zero elements.

The conditions under which these observations are valid are that the edge C be smooth and of sufficiently high curvature (but not so high that the radius of curvature is of the order of the wavelength) and furthermore that the direction of scattering is sufficiently far removed from any caustic directions of the far-field scattering. (In physical terms, we have a caustic direction when the rays diffracted in this direction from some portion of the edge C are parallel to first order, so that the rays do not appear to be spreading out in the far field region and giving the characteristic 1/R field behavior for large distances R from the edge. The simplest examples are the backscatter and forward scatter directions for normal incidence on a flat plate.)

* * *

When the tangent to C has discontinuities in direction (corners), when segments of C are straight or almost straight, when the direction of scattering is a caustic direction or close to a caustic direction, then the scattering can no longer be described in terms of rays which obey the rules of two-dimensional scattering. If a ray description of the scattering process is still possible, it will involve ray phenomena which have no two-dimensional counterpart, for example, rays scattered in all directions from a corner. Regardless of whether such a description is appropriate, we must proceed toward the solution by first considering scattering from lengths of edge rather than from isolated points.

To do this, we use the Ufimtsev ILEDC.

The Ufimtsev ILEDC describes the scattered field due to the fringe wave currents induced by a plane wave on an incremental length of an infinite wedge. This quantity and its generalization, the ILDC, which describes the scattering due to currents induced on an incremental length of a cylinder of any given cross-

section, are, like the 2-D DC, four-element dyadics which transform the polarization vector of the incident wave into a vector normal to the direction of scattering. If we consider the geometry and composition of the cylinder to be fixed, the ILDC is in general a function of the wave number k, the direction of incidence, and the direction of scattering, with the two directions now independent. The Ufimtsev ILEDC turns out to be independent of k. All perfect conductor ILDC's can be written in a form which has only three non-zero elements; furthermore, for the important case of backscatter, the two diagonal elements are the same as the corresponding elements of the 2-D DC.

The fringe wave diffraction from the edge C is obtained by integrating the ILEDC over C, with proper account taken of phase shift along C. If there is also an ILEDC which describes the physical optics edge diffraction, we can sum the two ILEDC's and then integrate. If there exists a ray description of the edge-diffracted field, it can be found by properly interpreting the result of the integration. That is, in PTD a ray description of the scattering, when appropriate, is a result of the analysis rather than an initial assumption as in GTD.

If C is a closed curve all of which is geometrically illuminated and if the curvature of C is continuous and sufficiently large, then the diffraction will appear to originate from those points on C for which $\beta_s = \beta_i$. Thus we have come back to those cases for which the 2-D DC can be used to solve three-dimensional problems.

*   *   *

In any mathematical writing, it is necessary to strike a balance between, on the one hand, introducing special notation which leads to a simpler form for the final results and, on the other hand, keeping the notation simple so that the exposition is easier to follow. In this report we have leaned heavily toward the use of special notation because we are writing primarily for the person who wants to understand the physical significance of the results and to apply them. A List of Symbols is included for the reader's guidance.

From the applications point of view, the most important material is

(a) The material in Sections 3.1.1 and 3.1.2 which shows how the ILDC and ILEDC relate the far-field scattering to the incident plane wave of (2-3). Key equations are (3-2), (3-3), (3-4), (3-9), (3-10), and (3-12).

(b) The evaluation of the Ufimtsev ILEDC $\underline{\underline{d}}^U$ in Section 3.2.1, for which the key equations are (3-46A), (3-56) to (3-61), the definitions (3-47) to (3-51), the integral forms (3-52) and (3-53) for the functions f and g, and the closed form evaluations of f and g in (3-65) to (3-78) (with appropriate warning that (3-75) to (3-78) have not been verified thoroughly). Also, important special cases of $\underline{\underline{d}}^U$ are treated in Sections 3.2.2 to 3.2.4.

The corresponding material on the 2-D DC is

(a) The material in Section 2.1.2 relating the two-dimensional far-field scattering to the incident wave of (2-3) by means of the 2-D DC. Key equations are (2-19) and (2-22) to (2-24).

(b) The evaluation of the Ufimtsev 2-D DC, also designated $\underline{\underline{d}}^U$, as given in Section 2.2.4. For actual computation the most useful equations are (2-98), (2-100), (2-101), and (2-118). Important special cases are treated in Sections 2.2.5 and 2.2.6.

The Keller 2-D DC $\underline{\underline{d}}^K$ is treated in Section 2.2.3, and some of the results are used in evaluating $\underline{\underline{d}}^U$. The most useful equations for $\underline{\underline{d}}^K$ are (2-80b), (2-82) and (2-83). Important special cases are treated in Sections 2.2.5 and 2.2.6.

II. THE TWO-DIMENSIONAL DIFFRACTION COEFFICIENT

2.1 A FORMALISM FOR TWO-DIMENSIONAL SCATTERING PROBLEMS

2.1.1 THE CYLINDER GEOMETRY AND THE INCIDENT FIELD

Let us consider the problem of an infinite length cylinder with a cross section of finite extent, composed of isotropic material and illuminated by a plane wave. The problem geometry is shown in Figure 1. The unit vector $\underline{t}$ is parallel to the cylinder axis. The cross section of the cylinder is described by the curve L, which we require to be of finite length. The unit outward normal from the cylinder is $\underline{n}$ and the unit tangent to L is $\underline{l}$ so oriented that

$$\underline{n} \times \underline{l} = \underline{t}. \tag{2-1}$$

The length parameter along L, in the direction of $\underline{l}$, is l. The length parameter along the axis is t, and we represent the position of a point $\underline{r}$ in space as

$$\underline{r} = \underline{\rho} + t\underline{t}, \tag{2-2}$$

where $\underline{\rho}$ is the displacement from the axis of the cylinder. The origin $\underline{r} = 0$ can be chosen in any convenient manner. An x-axis normal to $\underline{t}$ and a corresponding unit vector $\underline{e}_x$ can also be chosen in some convenient manner, and we can then introduce a y-axis and a unit vector $\underline{e}_y$ such that $\underline{e}_x \times \underline{e}_y = \underline{t}$.

The incident plane wave will be written

$$\underline{E}_o = E_o \underline{p} \, \exp \left\{ - i \, k \underline{e}_r^i \cdot \underline{r} \right\}, \qquad Z_o \underline{H}_o = - \underline{e}_r^i \times \underline{E}_o. \tag{2-3}$$

Here Z_o is the impedance of free space. As throughout this report, $\exp \left\{ -i\omega t \right\}$ time dependence, with ω the angular frequency and t the time, is assumed and suppressed. The wave number k is given by

$$k = \omega/c \tag{2-3A}$$

where c is the speed of light in free space. The plane wave travels in the $-\underline{e}_r^i$ direction, with $\underline{e}_r^i$ a unit vector. The vector $\underline{p}$ describes the polarization of the wave. It is a complex unit vector and is normal to $\underline{e}_r^i$, that is

13

$$|\underline{p}| = (\underline{p} \cdot \tilde{\underline{p}})^{1/2} = 1 \quad , \quad \underline{p} \cdot \underline{e}_r^i = 0 \quad , \tag{2-4}$$

where $\sim$ indicates the complex conjugate. In dealing with polarization, it is convenient to make use of the unit polarization vectors $\underline{e}_\perp^i$ and $\underline{e}_{\parallel}^i$ defined by

$$\underline{e}_\perp^i = -(\underline{t} \times \underline{e}_r^i) / |\underline{t} \times \underline{e}_r^i| \quad , \quad \underline{e}_{\parallel}^i = \underline{e}_\perp^i \times \underline{e}_r^i \quad . \tag{2-5}$$

The vector $\underline{e}_\perp^i$ is normal to $\underline{t}$ and to $\underline{e}_r^i$, and $\underline{e}_{\parallel}^i$ is normal to $\underline{e}_\perp^i$ and $\underline{e}_r^i$. The vectors $\underline{e}_\perp^i$, $\underline{e}_{\parallel}^i$, $-\underline{e}_r^i$, in that order, form the basis of a right-handed Cartesian coordinate system. We can now write

$$\underline{p} = p_\perp \underline{e}_\perp^i + p_{\parallel} \underline{e}_{\parallel}^i \quad , \tag{2-6}$$

where we call $p_\perp$ the perpendicular-polarized component (because $\underline{e}_\perp^i$ is perpendicular to the cylinder axis) and $p_{\parallel}$ the parallel-polarized component (because $\underline{e}_{\parallel}^i$ has a component parallel to the cylinder axis). Since $\underline{p}$ is a complex unit vector, the components $p_\perp$ and $p_{\parallel}$ are in general complex numbers.

We define the obliquity angle β_i of the incident wave by

$$\beta_i = \sin^{-1} (\underline{e}_r^i \cdot \underline{t}), \qquad -\frac{\pi}{2} < \beta_i < \frac{\pi}{2} \quad . \tag{2-7}$$

For incidence normal to the cylinder axis, $\beta_i = 0$. Otherwise, β_i has the same sign as $\underline{e}_r^i \cdot \underline{t}$.

It is frequently convenient to write $\underline{e}_r^i$ in the form

$$\underline{e}_r^i = \sin \beta_i \, \underline{t} + \cos \beta_i \, \hat{\underline{e}}_r^i \quad , \tag{2-8}$$

where $\hat{\underline{e}}_r^i$ is a unit vector normal to $\underline{t}$. In terms of $\hat{\underline{e}}_r^i$, we have

$$\underline{e}_\perp^i = -\underline{t} \times \hat{\underline{e}}_r^i \quad , \qquad \underline{e}_{\parallel}^i = \cos \beta_i \, \underline{t} - \sin \beta_i \, \hat{\underline{e}}_r^i \quad . \tag{2-9}$$

14

2.1.2 THE FAR-FIELD SCATTERING

Let us now turn our attention to the far-field scattering produced when the wave of (2-3) strikes the cylinder. We will present the results in a manner which is readily generalized to problems involving finite cylinders. Most of the material in Sections 2.1.2 through 2.1.6 is based on material in the Appendix, especially the results compiled in Section I.3.3.

At a point in the far-field, it is meaningful to use a ray interpretation of the scattered field ($\underline{E}^{scat}$, $\underline{H}^{scat}$). The geometry is shown in Figure 2. There appears to be one ray through a given far-field point $\underline{r}$. This ray originates at a point on the cylinder axis and it propagates in a direction which we shall designate by the unit vector $\underline{e}_r^s$. Thus any point $\underline{r}$ can be uniquely represented in the form

$$\underline{r} = R_0 \underline{e}_r^s + T_0 \underline{t} \qquad (2-10)$$

Here $t = T_0$ is the point on the axis at which the ray originates, and we call R_0 the _slant distance_ from the cylinder axis to the point $\underline{r}$.

We designate the angle between $\underline{e}_r^s$ and the axial vector $\underline{t}$ as $(\frac{\pi}{2} + \beta_s)$ and we call β_s the _obliquity angle_ of the scattered ray. We thus have

$$\sin \beta_s = - \underline{e}_r^s \cdot \underline{t} \quad , \quad -\frac{\pi}{2} \le \beta_s \le \frac{\pi}{2} \qquad (2-11)$$

Now, because of the special properties of the infinite cylinder problem, we find that all scattered rays have the same obliquity angle β_s. Thus a cone of rays originates at each point on the cylinder axis and each far-field point lies on one such cone. In the case $\beta_s = 0$, the cones become discs and the rays travel radially outward.

The angle β_s turns out to be equal to β_i,

$$\beta_s = \beta_l \qquad . \qquad (2\text{-}12)$$

Thus, if we were only interested in infinite cylinder problems, we would not even have to distinguish between the quantities β_s and β_l. Nevertheless, we shall treat β_s as though it were an independent quantity so that we can readily generalize from infinite cylinder problems to finite cylinder problems.

It is frequently convenient to write $\underline{e}_r^{\ s}$ in a form analogous to (2-8), namely

$$\underline{e}_r^{\ s} = -\sin\beta_s \underline{t} + \cos\beta_s \ \underline{\hat{e}}_r^{\ s} \qquad , \qquad (2\text{-}13)$$

with $\underline{\hat{e}}_r^{\ s}$ a unit vector normal to $\underline{t}$. (See Figure 1 for the geometrical details of the scattered field.)

It is also useful to define unit polarization vectors $\underline{e}_\perp^{\ s}$ and $\underline{e}_{\parallel}^{\ s}$ such that

$$\underline{e}_\perp^{\ s} = (\underline{t} \times \underline{e}_r^{\ s})/|\underline{t} \times \underline{e}_r^{\ s}| = \underline{t} \times \underline{\hat{e}}_r^{\ s} \qquad , \qquad (2\text{-}14)$$

$$\underline{e}_{\parallel}^{\ s} = \underline{e}_r^{\ s} \times \underline{e}_\perp^{\ s} = \cos\beta_s \underline{t} + \sin\beta_s \ \underline{\hat{e}}_r^{\ s} \qquad , \qquad (2\text{-}15)$$

and $\underline{e}_\perp^{\ s}$, $\underline{e}_{\parallel}^{\ s}$, $\underline{e}_r^{\ s}$, in that order, form the basis of a right-handed Cartesian coordinate system. These definitions are analogous to those of (2-5) and (2-9). For all infinite cylinder problems, $\underline{e}_{\parallel}^{\ s}$ and $\underline{e}_{\parallel}^{\ l}$ are both at the same angle $|\beta_l|$ to the t-axis. Important special cases are

$$\underline{e}_{\parallel}^{\ s} = \underline{e}_{\parallel}^{\ l} = \underline{t} \quad \text{for } \beta_s = \beta_l = 0 \qquad \text{(No obliquity)} \quad (2\text{-}16)$$

and

$$\underline{e}_\perp^{\ s} = -\underline{e}_\perp^{\ l} \text{ for } \beta_s = \beta_l, \ \underline{\hat{e}}_r^{\ s} = \underline{\hat{e}}_r^{\ l} \qquad . \qquad (2\text{-}17)$$

Putting these two cases together, we find

$$\underline{e}_\perp^{\ s} = -\underline{e}_\perp^{\ l} \ , \ \underline{e}_{\parallel}^{\ s} = \underline{e}_{\parallel}^{\ l} - \underline{t} \qquad (2\text{-}18)$$

for backscatter in a two-dimensional problem, where backscatter is only possible for $\beta_s = \beta_l = 0$.

16

We can represent the far-field wave in the form

$$\underline{E}^{scat}(\underline{r}) = \frac{e^{ikR_0}}{R_0^{1/2}} e^{-ik_t T_0} \underline{f} \quad , \qquad Z_0 \underline{H}^{scat} = \underline{e}_r^s \times \underline{E}^{scat} \quad , \tag{2-19}$$

where Z_0 is the wave impedance of free space and k_t is the <u>axial wave number</u>, given by

$$k_t = k \sin \beta_s \quad . \tag{2-20}$$

The <u>radiation vector</u> $\underline{f}$ is independent of R_0 and T_0 and is normal to $\underline{e}_r^s$. It can be expressed in terms of a perpendicular-polarized component and a parallel-polarized component as

$$\underline{f} = f_\perp \underline{e}_\perp^s + f_{||} \underline{e}_{||}^s \quad . \tag{2-21}$$

Furthermore, $\underline{f}$ is a linear function of $E_0 \underline{p}$, and thus we can write

$$\underline{f} = E_0 \frac{1}{k^{1/2} \cos \beta_s} \underline{\underline{d}} \cdot \underline{p} \quad , \tag{2-22}$$

where $\underline{\underline{d}}$ is a dyadic which can be written in terms of its elements as

$$\underline{\underline{d}} = d_{\perp\perp} \underline{e}_\perp^s \underline{e}_\perp^i + d_{\perp||} \underline{e}_\perp^s \underline{e}_{||}^i + d_{||\perp} \underline{e}_{||}^s \underline{e}_\perp^i + d_{||||} \underline{e}_{||}^s \underline{e}_{||}^i \quad . \tag{2-23}$$

The normalization in (2-22) has been chosen so that $\underline{\underline{d}}$ is dimensionless and also so that, for a body of perfect conductivity, $d_{\perp\perp}$ and $d_{||||}$ are independent of the obliquity angle.

If we consider the geometry and the composition of the cylinder to be fixed, then $\underline{\underline{d}}$ is in general a function of the wave number, the direction of incidence, and the direction of scattering. We thus write

$$\underline{\underline{d}} = \underline{\underline{d}} (k; \beta_i, \phi_i; \beta_i, \phi_s) \quad , \tag{2-24}$$

where ϕ_i is the azimuth angle measured from the x-axis to $\hat{\underline{e}}_r^i$, and ϕ_s is the azimuth angle measured from the x-axis to $\hat{\underline{e}}_r^s$. The first β_i tells us the obliquity angle for the incident wave. The second β_i tells us that the

17

obliquity angle is the same for the scattered wave.

The function $\underline{d}$ of (2-24), with the two obliquity angles equal, we shall call the Two-Dimensional Diffraction Coefficient of the problem. The notation is chosen so that the Incremental Length Diffraction Coefficient $\underline{d}$ $(k; \beta_i, \phi_i; \beta_s, \phi_s)$, of Section III reduces to the Two-Dimensional Diffraction Coefficient when $\beta_s = \beta_i$.

2.1.3 THE RELATIONSHIP BETWEEN FAR-FIELD SCATTERING AND EFFECTIVE SURFACE CURRENTS

The radiation vector $\underline{f}$ is also a linear function of the effective electric surface current

$$\underline{K}_e = \underline{n} \times \underline{H} \tag{2-25}$$

(amperes/m) and the effective magnetic surface current

$$\underline{K}_m = -\underline{n} \times \underline{E} \tag{2-26}$$

(volts/m) on the surface of the cylinder. If we write $\underline{K}_e$ and $\underline{K}_m$ in component form as

$$\underline{K}_q = K_{q\ell} \underline{\ell} + K_{qt} \underline{t} \quad \text{for } q = e, m \quad , \tag{2-26A}$$

and if we write $\underline{E}$ and $\underline{H}$ in component form as

$$\underline{A} = A_n \underline{n} + A_\ell \underline{\ell} + A_t \underline{t} \quad \text{for } \underline{A} = \underline{E}, \underline{H}, \tag{2-26B}$$

we find that the component forms of (2-25) and (2-26) are

$$K_{e\ell} = -H_t, \quad K_{et} = H_\ell \quad ; \quad K_{m\ell} = E_t, \quad K_{mt} = -E_\ell . \tag{2-26C}$$

For plane wave incidence , the effective surface currents are linear functions of $E_0 \underline{p}$. In light of this, it is convenient to introduce the electric and magnetic surface current dyadics, $\overset{\wedge}{\underline{\underline{K}}}_e$ and $\overset{\wedge}{\underline{\underline{K}}}_m$ respectively, which are defined by the expressions

18

$$\underline{K}_q = \hat{\underline{K}}_q \exp\{-ikt \sin\beta_i\} \quad , \quad \hat{\underline{K}}_q = E_o \hat{\underline{\underline{K}}}_q \cdot \underline{p} \text{ for } q = e, m \text{ and all } \underline{p} . \tag{2-27}$$

We see that $\hat{\underline{K}}_e$ and $\hat{\underline{K}}_m$ describe those qualities of the surface currents which are independent of position on the axis and of the amplitude and polarization of the incident wave.

The surface current dyadics can be written in element form most simply as

$$\hat{\underline{\underline{K}}} = \hat{K}_{l\perp} \underline{le}_\perp^i + \hat{K}_{l\shortparallel} \ \underline{le}_\shortparallel^i + \hat{K}_{t\perp} \underline{t} \underline{e}_\perp^i + \hat{K}_{t\shortparallel} \underline{t} \ \underline{e}_\shortparallel^i \quad . \tag{2-28}$$

Here the elements $\hat{K}_{ij}$ are functions of wave number, direction of incidence, and position on the cross section curve L; that is,

$$\hat{K}_{ij} = \hat{K}_{ij} (k; \underline{e}_r^i ; l) = \hat{K}_{ij} (k; \beta_i, \phi_i ; l) \quad . \tag{2-29}$$

Let us next define the dyadic

$$\begin{aligned}
\underline{\underline{W}} &= \underline{\underline{W}} \ (k; \beta_i, \phi_i; \beta_s, \phi_s ; l) \\
&= W_{\perp\perp} \underline{e}_\perp^s \underline{e}_\perp^i + W_{\perp\shortparallel} \underline{e}_\perp^s \ \underline{e}_\shortparallel^i + W_{\shortparallel\perp} \underline{e}_\shortparallel^s \ \underline{e}_\perp^i + W_{\shortparallel\shortparallel} \underline{e}_\shortparallel^s \underline{e}_\shortparallel^i \\
&= - [Z_o \underline{e}_r^s \times (\underline{e}_r^s \times \hat{\underline{\underline{K}}}_e) + \underline{e}_r^s \times \hat{\underline{\underline{K}}}_m] \quad .
\end{aligned} \tag{2-30}$$

The elements of $\underline{\underline{W}}$ are

$$\left.
\begin{aligned}
W_{\perp j} &= (\hat{\underline{e}}_r^s \cdot \underline{n}) \ Z_o \hat{K}_{el j} + \cos\beta_s \ \hat{K}_{mtj} \\
&\quad - (\underline{e}_\perp^s \cdot \underline{n}) \sin\beta_s \ \hat{K}_{mlj} \\
W_{\shortparallel j} &= - (\hat{\underline{e}}_r^s \cdot \underline{n}) \ \hat{K}_{mlj} + \cos\beta_s \ Z_o \ \hat{K}_{etj} \\
&\quad - (\underline{e}_\perp^s \cdot \underline{n}) \sin\beta_s Z_o \hat{K}_{elj}
\end{aligned}
\right\} j = \perp, \shortparallel . \tag{2-31}$$

We can now express the two-dimensional diffraction coefficient $\underline{d}$ in terms of $\underline{W}$ and thus in terms of $\hat{\underline{K}}_e$ and $\hat{\underline{K}}_m$. The result is

$$\underline{d} = - \frac{e^{-i\pi/4}}{2(2\pi)^{1/2}} k \int_L dl' \exp\left\{-ik\cos\beta_s \; \hat{\underline{e}}_r^s \cdot \underline{\rho}'\right\} \underline{W}' \; , \qquad (2\text{-}32)$$

where a prime indicates a function of the integration variable. (To derive this result, we start with (I-104), use (2-22) to represent $\underline{f}$ in terms of $\underline{d}$, and express $\underline{W}$ in terms of the closely related dyadic $\underline{\underline{W}}$.) At this point, we are only stating the validity of (2-32) for the case $\beta_s = \beta_i$ which arises in two-dimensional problems. We will see later that (2-32) is also meaningful when $\beta_s \neq \beta_i$.

$$* \quad * \quad *$$

It can be shown by integration by parts that (2-32) still holds if $\underline{W}$ is replaced by a dyadic $\bar{\underline{W}}$ with elements

$$\bar{W}_{\perp j} = (\hat{\underline{e}}_r^s \cdot \underline{n}) \, Z_o \, \hat{K}_{e l j} + \cos\beta_s \, \hat{K}_{m t j}$$

$$+ \frac{1}{ik} \tan\beta_s \, \frac{\partial}{\partial l} \hat{K}_{m l j} \; ,$$

$$\bar{W}_{\parallel j} = - (\hat{\underline{e}}_r^s \cdot \underline{n}) \, \hat{K}_{m l j} + \cos\beta_s \, Z_o \, \hat{K}_{e t j} \qquad \left.\begin{array}{c} \\ \\ \end{array}\right\} \; j = \perp , \parallel . \qquad (2\text{-}33)$$

$$+ \frac{1}{ik} \tan\beta_s \, \frac{\partial}{\partial l} (Z_o \hat{K}_{e l j}) $$

Because $\hat{K}_{e l j}$ and $\hat{K}_{m l j}$ are the true effective surface currents induced by a source which does not lie on the cylinder surface, they are continuous and differentiable in l at all points of finite curvature of the cross section curve. The l-derivatives do go to infinity at edges, but the singularities are integrable. (For a general discussion of fields near edges, see Reference 5.)

20

Matters will not be so simple, however, when we deal with discontinuous $\hat{K}_{e\ell j}$ and $\hat{K}_{m\ell j}$ such as those of the physical optics contribution.

2.1.4 SYMMETRY PROPERTIES

All the elements of $\hat{\underline{K}}_e$ and $\hat{\underline{K}}_m$ are either even or odd functions of β_i. Specifically, we have

$$\begin{aligned}
\hat{K}_q (-\beta_i) &= \hat{K}_q (\beta_i) \text{ for } q = e\ell\perp,\ et\parallel,\ m\ell\parallel,\ mt\perp\ ; \\
&= -\hat{K}_q (\beta_i) \text{ for } q = e\ell\parallel,\ et\perp,\ m\ell\perp,\ mt\parallel\ .
\end{aligned} \tag{2-34}$$

Here we have omitted the arguments which are not varied.

From these symmetry properties and (2-31), we obtain

$$\begin{aligned}
W_q (-\beta_i; -\beta_s) &= W_q (\beta_i; \beta_s) \text{ for } q = \perp\perp,\ \parallel\parallel\ ; \\
&= -W_q (\beta_i; \beta_s) \text{ for } q = \perp\parallel,\ \parallel\perp.
\end{aligned} \tag{2-35}$$

The symmetry properties of $\overline{\overline{W}}$ are the same. Indeed, we see from (2-32) that those of $\underline{d}$ are also the same:

$$\begin{aligned}
d_q (-\beta_i; -\beta_s) &= d_q (\beta_i; \beta_s) \quad \text{for } q = \perp\perp,\ \parallel\parallel \\
&= -d_q (\beta_i; \beta_s) \quad \text{for } q = \perp\parallel,\ \parallel\perp
\end{aligned} \tag{2-36}$$

From this, we immediately obtain the very important result that the cross-terms in $\underline{d}$ vanish for non-oblique incidence and scattering:

$$d_{\perp\parallel} (0; 0) = d_{\parallel\perp} (0; 0) = 0 \quad . \tag{2-37}$$

2.1.5 THE PERFECT CONDUCTOR CASE

For a perfect conductor, we have

$$\hat{\underline{K}}_m = 0\ , \quad \hat{K}_{e\ell\parallel} = 0 \quad . \tag{2-38}$$

Furthermore, we have the expressions

$$\hat{K}_{e\ell\perp}(k; \beta_i, \varphi_i; \ell) = \hat{K}_{e\ell\perp}(k\cos\beta_i; 0, \varphi_i; \ell) \cos\beta_i \quad, \tag{2-39}$$

$$\hat{K}_{et\perp}(k; \beta_i, \varphi_i; \ell) = -\frac{1}{ik}\frac{\partial}{\partial\ell}\hat{K}_{e\ell\perp}(k\cos\beta_i; 0, \varphi_i; \ell)\tan\beta_i \quad, \tag{2-40}$$

$$\hat{K}_{et\parallel}(k; \beta_i, \varphi_i; \ell) = \hat{K}_{et\parallel}(k\cos\beta_i; 0, \varphi_i; \ell) \quad, \tag{2-41}$$

which relate the surface currents of the oblique incidence problem to those
of a non-oblique problem for the shifted wave number $(k\cos\beta_i)$.   (See Section
I.3.2 for a detailed discussion of the relationship between oblique and non-oblique
incidence problems for perfect conductors.)

By using (2-38) to (2-41) in (2-31) and (2-33), we obtain

$$W_{\perp\perp}(k; \beta_i, \varphi_i; \beta_i, \varphi_s; \ell) = W_{\perp\perp}(k\cos\beta_i; 0, \varphi_i; 0, \varphi_s; \ell)\cos\beta_i$$

$$= (\hat{\underline{e}}_r^s \cdot \underline{n})\, Z_0\, \hat{K}_{e\ell\perp}(k\cos\beta_i; 0, \varphi_i; \ell)\cos\beta_i \tag{2-42}$$

$$W_{\perp\parallel}(k; \beta_i, \varphi_i; \beta_i, \varphi_s; \ell) = 0 \quad, \tag{2-43}$$

$$W_{\parallel\perp}(k; \beta_i, \varphi_i; \qquad\qquad) = -\sin\beta_i\left[\cos\beta_i\,(\underline{e}_i^s \cdot \underline{n})\right.$$

$$\left.+ \frac{1}{ik}\frac{\partial}{\partial\ell}\right]Z_0\,\hat{K}_{e\ell\perp}(k\cos\beta_i; 0, \varphi_i; \ell), \tag{2-44}$$

$$W_{\parallel\parallel}(k; \beta_i, \varphi_i; \beta_i, \varphi_s; \ell) = W_{\parallel\parallel}(k\cos\beta_i; 0, \varphi_i; 0, \varphi_s; \ell)\cos\beta_i$$

$$= Z_0\,\hat{K}_{et\parallel}(k\cos\beta_i; 0, \varphi_i; \ell)\cos\beta_i \quad, \tag{2-45}$$

and

$$\bar{W}_q = W_q \quad, \quad q = \perp\perp, \perp\parallel, \parallel\parallel \quad; \tag{2-46}$$

$$\bar{W}_{\parallel\perp}(k; \beta_i, \varphi_i; \beta_i, \varphi_s; \ell) = 0 \quad. \tag{2-47}$$

22

We now readily find from (2-32) that

$$d_q(k; \beta_l, \phi_l; \beta_l, \phi_s) = d_q(k \cos\beta_l; 0, \phi_l; 0, \phi_s) , \quad q = \perp\perp, \parallel\parallel; \tag{2-48}$$

$$d_{\perp\parallel}(k; \beta_l, \phi_l; \beta_l, \phi_s) = 0 \quad ; \tag{2-49}$$

$$d_{\parallel\perp}(k; \beta_l, \phi_l; \beta_l, \phi_s) = 0 \quad . \tag{2-50}$$

This is a statement in diffraction coefficient terminology of the well-known fact that the far-field scattering at oblique incidence on a perfectly conducting cylinder can be found by solving a non-oblique incidence problem at the shifted wave number ($k \cos\beta_l$). (See Section I.3.2 of Appendix I.)

2.1.6 APPROXIMATE SOLUTIONS AND CONTRIBUTIONS TO THE SOLUTION

Thus far, we have assumed that $\underline{\underline{d}}$, $\hat{\underline{\underline{K}}}_e$, $\hat{\underline{\underline{K}}}_m$ and $\underline{W}$ are exact values. Frequently, however, we have to deal with approximations to these quantities.

Equally important, we frequently represent these quantities as the sum of various contributions. For example, in the wedge problem, we express $\hat{\underline{\underline{K}}}_e$ and $\hat{\underline{\underline{K}}}_m$ as the sum of a physical optics contribution and a fringe wave contribution,

$$\hat{\underline{\underline{K}}} = \hat{\underline{\underline{K}}}^{PO} + \hat{\underline{\underline{K}}}^{U} , \tag{2-51}$$

where the superscript U (for Ufimtsev) indicates the fringe wave contribution. We then obtain analogous representations of $\underline{W}$ and $\underline{\underline{d}}$, each as the sum of a physical optics contribution and a fringe wave contribution.

Approximations to contributions are a third important type of non-exact solution.

23

It is important to realize that these contributions and approximations do not necessarily have all the same properties as the true solution.

In practice we try to give the non-exact solution as many properties as possible of the exact solution. Thus we always choose contributions and approximations for $\underline{d}$ and the $\hat{\underline{\underline{K}}}$ so that they have the four-component form of (2-23) and (2-28) respectively, and so that they have the functional dependence of (2-24) and (2-29) respectively. We always require that (2-30), (2-31), and (2-32) — which relate $\underline{\underline{W}}$ to the $\hat{\underline{\underline{K}}}$ and $\underline{d}$ to $\underline{\underline{W}}$ — hold for each individual contribution separately. It then follows that we can always replace $\underline{\underline{W}}$ in (2-32) by $\bar{\underline{\underline{W}}}$ of (2-33) on a term-by-term basis. We must be careful, however, when dealing with a contribution for which the $\hat{K}_{\ell j}$ are discontinuous (as they are in the case of the physical optics contribution for a wedge), to include impulse functions in the $\partial K_{\ell j}/\partial \ell$ terms to account for the discontinuities. (See Section I.2.4.)

We furthermore consider only contributions and approximations for which the symmetry condition (2-34) holds. Thus the symmetry conditions (2-35), (2-36) and (2-37) will also hold for each term.

Summing up, we can without difficulty always work with contributions and approximations for which all the formulas of Sections 2.1.2 to 2.1.4 are valid.

As to the perfect conductor formulas of Section 2.1.5, we always choose contributions and approximations which satisfy (2-38), (2-39), (2-41), (2-42), (2-43), (2-45), (2-46), (2-48), and (2-49). The remaining four equations, for $\hat{K}_{et\perp}$, $W_{\parallel\perp}$, $\bar{W}_{\parallel\perp}$, and $d_{\parallel\perp}$, are, however, frequently not satisfied term-by-term by the contributions which are used in practice. Most importantly, the $d_{\parallel\perp}$ for a contribution or approximation may be non-zero.

As an example, consider the fringe wave contribution to the scattering from a wedge with one face illuminated, the other in shadow, when $\beta_1 \neq 0$. The fringe wave current component $\hat{K}^U_{et\perp}(k; \beta_1, \phi_1; l)$ is finite at the edge. On the other hand, the current component $\hat{K}^U_{e l \perp}(k \cos \beta_1; 0, \phi_1; l)$ is discontinuous at the edge, with the discontinuity equal and opposite to that in the physical optics contribution, and thus the l-derivative of this component has an impulse at the edge. Clearly (2-40) cannot be valid at the edge. It turns out that the two sides of (2-40) differ only by the impulse at the edge, but this difference is enough to invalidate (2-44), (2-47), and (2-50).

(It should be noted that we can eliminate this difficulty by decomposing the surface current into a "modified" physical optics contribution, with the proper impulse function added to $K_{et\perp}$ so that (2-40) will hold, plus a "modified" fringe wave current, with the equal and opposite impulse function included. It is quite possible that this is the procedure we shall adopt in future work. For the present, however, we have decided not to introduce the additional complication of redefining physical optics.)

Whenever (2-40) does not hold, (2-44) and (2-47) must be replaced by the more general expressions

$$W_{\| \perp}(k; \beta_1, \phi_1; \beta_1, \phi_s; l) \tag{2-52}$$
$$= \left[Z_o \hat{K}_{et\perp}(k; \beta_1, \phi_1; l) - (\underline{e}^s_1 \cdot \underline{n}) \, Z_o \hat{K}_{e l \perp}(k \cos \beta_1; 0, \phi_1; l) \sin \beta_1 \right] \cos \beta_1$$

$$\bar{W}_{\| \perp}(k; \beta_1, \phi_1; \beta_1, \phi_s; l) \tag{2-53}$$
$$= Z_o \left[\hat{K}_{et\perp}(k; \beta_1, \phi_1; l) + \frac{1}{ik} \frac{\partial}{\partial l} \hat{K}_{e l \perp}(k \cos \beta_1; 0, \phi_1; l) \tan \beta_1 \right] \cos \beta_1 \ ,$$

which can be derived from (2-31) and (2-33) by use of (2-38) and (2-39). In such cases, $d_{\| \perp}$ will usually be non-zero for $\beta_1 \neq 0$ and can be calculated from (2-32).

2.2 THE UFIMTSEV AND KELLER DIFFRACTION COEFFICIENTS FOR A CON-DUCTING WEDGE

2.2.1 BASIC IDEAS

Let us now consider the case in which our cylinder of infinite length is a wedge whose two faces are infinite half-planes.

We are interested in this problem not just for its own sake but, even more importantly, because the wedge is the simplest body which has an edge. In practice, we treat the wedge problem as a canonical problem, and we use the results in solving a variety of other problems involving bodies with edges. In keeping with this practical emphasis, we shall use the term edge diffraction coefficient rather than wedge diffraction coefficient.

The geometry for scattering from a wedge is shown in Figure 3. The wedge angle is 2α. The t-axis, at which $\rho = 0$, is chosen to coincide with the edge, which we designate as C. The unit vector $\underline{n}_0$ bisects the wedge angle and points out of the wedge. We also define a unit vector

$$\underline{b} = \underline{t} \times \underline{n}_0 \tag{2-54}$$

so that $\underline{n}_0$, $\underline{b}$, $\underline{t}$, in that order, form the basis of a right-handed Cartesian coordinate system. The two faces of the wedge are designated as S_+ and S_-, with $\underline{b}$ pointing from the S_+ side to the S_- side. The unit outward normals to S_+ and S_-, which we designate as $\underline{n}_+$ and $\underline{n}_-$ respectively, are given by

$$\left.\begin{array}{l} \underline{n}_+ = \underline{n}_0 \sin \alpha - \underline{b} \cos \alpha \\ \\ \underline{n}_- = \underline{n}_0 \sin \alpha + \underline{b} \cos \alpha \end{array}\right\} . \tag{2-55}$$

We also define unit tangent vectors $\underline{e}_\rho^+$ and $\underline{e}_\rho^-$ which lie on S_+ and S_- respectively, and which are normal to $\underline{t}$ and directed away from the edge, so that

26

$$e_\rho^+ = -(\underline{n}_o \cos \alpha + \underline{b} \sin \alpha) \Bigg\}$$

$$e_\rho^- = -(\underline{n}_o \cos \alpha - \underline{b} \sin \alpha) \Bigg\} \qquad . \qquad (2\text{-}56)$$

The x-axis from which we measure ϕ_i and ϕ_s is chosen to bisect the wedge angle and is so oriented that

$$\underline{e}_x = -\underline{n}_o \qquad . \qquad (2\text{-}60)$$

The wedge factor

$$\nu = \frac{\pi}{2(\pi - \alpha)} \qquad (2\text{-}58)$$

plays an important role in the wedge diffraction results. This factor has a minimum value of 1/2 for a knife edge and increases with a. We shall limit consideration here to the case of acute wedge angles

$$a < \frac{\pi}{2} \qquad . \qquad (2\text{-}59)$$

Thus we will always have

$$\frac{1}{2} \leq \nu < 1 \qquad . \qquad (2\text{-}57)$$

For values of a greater than $\pi/2$, matters are complicated by the presence of reflections between S_+ and S_-.

We will consider in detail two kinds of diffraction coefficients. The Keller diffraction coefficient $\underline{d}^K$ describes the exact solution of the wedge problem, the far field produced by the total current on the wedge. The Ufimtsev diffraction coefficient $\underline{d}^U$ describes the contribution to the scattered field produced by the "fringe wave" current, which is the difference between the true current and the current predicted by physical optics. For most angles of incidence, the fringe wave current is concentrated near the edge.

Sometimes it is convenient to define a third type of coefficient, the

27

<u>physical optics</u> diffraction coefficient, $\underline{\underline{d}}^{PO}$, which describes the contribution to the scattered field due to the physical optics currents on the wedge. This is related to the other diffraction coefficients by the simple formula

$$\underline{\underline{d}}^{PO} = \underline{\underline{d}}^{K} - \underline{\underline{d}}^{U} \qquad . \qquad (2\text{-}61)$$

In (2-19) and (2-22), we defined $\underline{\underline{d}}$ in terms of the far-field solution. The wedge, however. is a cylinder of infinite cross section, and thus it is not <u>a priori</u> certain that there is indeed a far-field region, that is, a region in which the amplitude and phase of the far-field wave depend on R_o in the manner of (2-19).

It fortunately turns out that, for most combinations of ϕ_i and ϕ_s, there does exist a far-field region.

There are, however, combinations of ϕ_i and ϕ_s for which this is not so. In these cases, no matter how large we make R_o, we never reach a region in which the field decreases as $R_o^{-1/2}$ in the $\underline{e}_r^s$ direction. For these cases, a formal calculation of $\underline{\underline{d}}$ yields an infinite or indeterminate result. One of the advantages of $\underline{\underline{d}}^{U}$ over $\underline{\underline{d}}^{K}$ is that $\underline{\underline{d}}^{K}$ has a singularity whenever ϕ_s lies on a geometrical shadow boundary or reflection boundary, but $\underline{\underline{d}}^{U}$ is finite and uniquely defined except for grazing incidence problems with $\phi_i = \pi \pm a$.

Even though $\underline{\underline{d}}^{K}$ exists for most combinations of ϕ_i and ϕ_s, it cannot be computed using (2-32). The conditions for validity of (2-32) are more stringent than those for existence of a far-field region.

2.2.2 SHADOW BOUNDARIES AND REFLECTION BOUNDARIES

Consider now a wedge with $a > 0$. As we see from Figure 4, there are five types of illumination possible:

Case 1. Only S_+ is illuminated ($a \leq \phi_i < \pi - a$);

Case 2. The incident wave illuminates S_+ and grazes S_- ($\phi_i = \pi - a$);
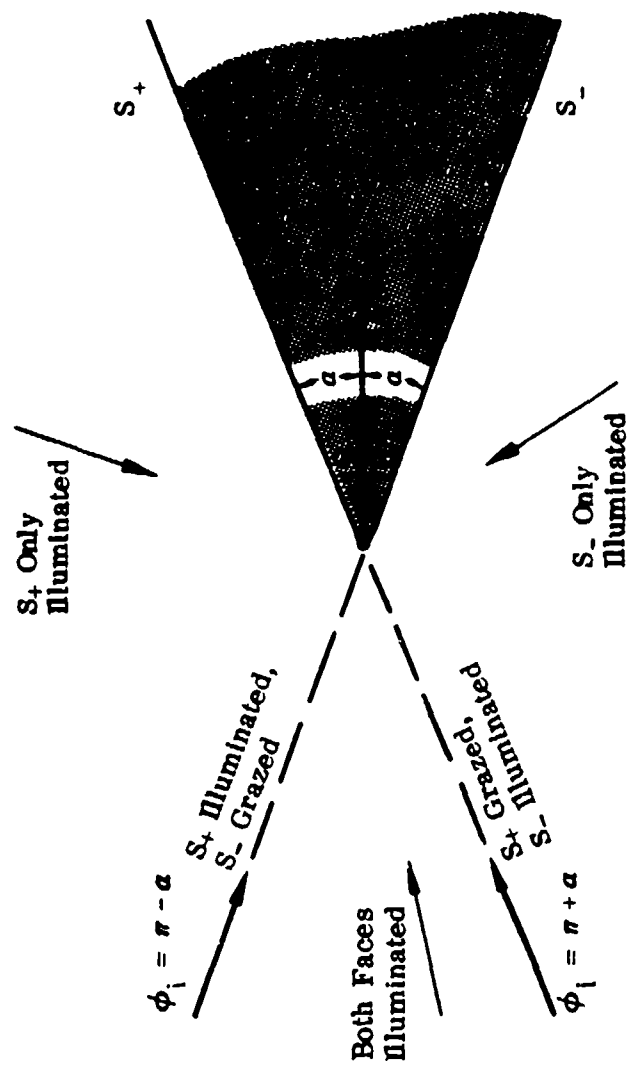
FIGURE 4   FIVE TYPES OF ILLUMINATION AT AN EDGE

Case 3. Both S_+ and S_- are illuminated ($\pi - a < \phi_i < \pi + a$);

Case 4. The incident wave grazes S_+ and illuminates S_- ($\phi_i = \pi + a$);

Case 5. Only S_- is illuminated ($\pi + a < \phi_i \le 2\pi - a$).

We refer to Case 2 and Case 4 as the __transitional cases__.

Let us first consider the other three cases. Cases 1 and 3 are illustrated in Figure 5, and Case 5 is analogous to Case 1. In Case 1, there is a shadow boundary at

$$\phi_s = \phi_{S+} \equiv \phi_i + \pi \qquad . \tag{2-62}$$

That is, in the simple geometrical optics approximation, the region $\varphi_s < (\phi_i + \pi)$ is illuminated by the incident wave and the region $\phi_s > (\phi_i + \pi)$ is in the shadow of S_+. There is also in Case 1 a reflection boundary at

$$\varphi_s = \varphi_{R+} \equiv \pi + 2a - \phi_i \qquad . \tag{2-63}$$

That is, in the simple geometrical optics approximation, a wave reflected from S_+ exists in the region $\phi_s < (\pi + 2a - \phi_i)$ and is absent in the region $\phi_s > (\pi + 2a - \phi_i)$. The two boundaries coincide when $\phi_i = a$.

In Case 3, there are two reflection boundaries, one given by (2-63) and the other by

$$\varphi_s = \varphi_{R-} \equiv 3\pi - 2a - \phi_i \quad \text{(Reflection from } S_-) \quad . \tag{2-64}$$

In Case 5, there is a shadow boundary

$$\phi_s = \phi_{S-} \equiv \phi_i - \pi \qquad \text{(Shadowing by } S_-) \tag{2-65}$$

and a reflection boundary with ϕ_s given by (2-64). The two boundaries coincide when $\phi_i = 2\pi - a$.

We see that there are four different types of geometrical boundaries, the shadow boundary and the reflection boundary for S_+ and the analogous
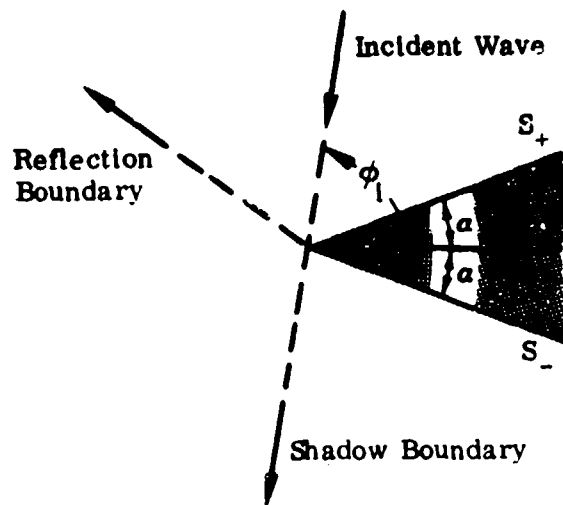
ONE SHADOW AND ONE REFLECTION BOUNDARY
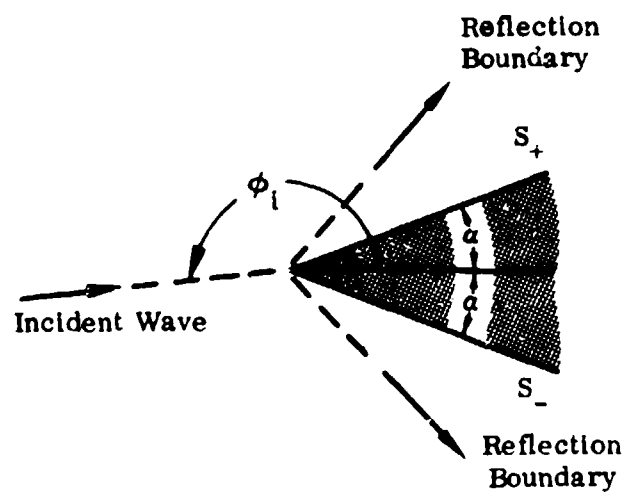
TWO REFLECTION BOUNDARIES

FIGURE 5   SHADOW AND REFLECTION BOUNDARIES

boundaries for S_-. In each case, we actually encounter two of these boundaries. These two we shall call the real boundaries for the given value of ϕ_1.

If we now evaluate ϕ_{R+}, ϕ_{S+}, and ϕ_{R-} for Case 2, which is a transitional case, we find

$$\phi_{R+} = 3\alpha \quad , \quad \phi_{S+} = \phi_{R-} = 2\pi - \alpha \quad . \tag{2-66}$$

We thus see that there is a reflection boundary at

$$\phi_S = \phi_{R+} = 3\alpha \tag{2-67}$$

and a double boundary along S_- at

$$\phi_S = \phi_{S+} = \phi_{R-} = 2\pi - \alpha \tag{2-68}$$

which is both the shadow boundary with reference to face S_+ and the reflection boundary with reference to face S_-.

Similarly, in Case 4, there is a reflection boundary at

$$\phi_S = \phi_{R-} = 2\pi - 3\alpha \tag{2-69}$$

and a double boundary along S_+ at

$$\phi_S = \phi_{S-} = \phi_{R+} = \alpha \tag{2-70}$$

which is both the shadow boundary for S_- and the reflection boundary for S_+.

To unify all these results, we generalize the concept of a geometrical boundary as follows:

For every value of ϕ_1, there exist four geometrical boundaries, given by (2-62) to (2-65). A given boundary may be real, lying in the open range α to $(2\pi - \alpha)$; it may be a grazing boundary at α or $(2\pi - \alpha)$; or it may be a virtual boundary which lies outside the closed range α to $(2\pi - \alpha)$. Grazing boundaries occur in pairs, and the number of virtual boundaries equals the number of real boundaries.

The generalized concepts also hold for the knife edge problem $a = 0$. In this problem, we have Case 1, Case 5, and one transitional case, $\phi_i = \pi$, for which there are two pairs of grazing boundaries, one at 0 and one at 2π.

We now introduce the notation δ_{S+} for the angle from $\hat{\underline{e}}_r^{B}$ to the shadow boundary with reference to face S_+,

$$\delta_{S+} = \phi_{S+} - \phi_s = \pi - \phi_{si} , \qquad (2\text{-}71)$$

and we similarly define

$$\delta_{R+} = \phi_{R+} - \phi_s = (\pi + 2a) - \phi_\Sigma , \qquad (2\text{-}72)$$

$$\delta_{S-} = \phi_{S-} - \phi_s = -(\pi + \phi_{si}), \qquad (2\text{-}73)$$

$$\delta_{R-} = \phi_{R-} - \phi_s = (3\pi - 2a) - \phi_\Sigma . \qquad (2\text{-}74)$$

Here

$$\phi_{si} = \phi_s - \phi_i , \qquad (2\text{-}75)$$

$$\phi_\Sigma = \phi_i + \phi_s . \qquad (2\text{-}76)$$

The δ_j are meaningful even when they correspond to virtual boundaries.

It is important that the δ_j be uniquely and appropriately defined, because we will be considering trigonometric functions of fractions of these angles. As long as we restrict ϕ_i and ϕ_s to be angles outside the wedge, the proper values of the δ_j are obtained by choosing ϕ_i and ϕ_s in the range

$$a \leq \phi_i \leq (2\pi - a) , \qquad (2\text{-}77)$$

33

$$a \leq \phi_s \leq (2\pi - a) \qquad . \qquad (2\text{-}78)$$

In working with the δ_j, the identities

$$\delta_{R+} + \delta_{S+} = 2\,[\,\pi - (\phi_s - a)\,] \quad , \quad \delta_{R+} - \delta_{S+} = 2\,(\phi_1 - a)$$

$$\delta_{R-} + \delta_{S-} = 2\,[\,\pi - (\phi_s + a)\,] \ , \ \delta_{R-} - \delta_{S-} = 2\,[\,2\pi - (\phi_1 + a)\,]$$

$$\delta_{S+} - \delta_{S-} = 2\pi \ , \qquad \delta_{R-} - \delta_{R+} = 2\pi - 4a$$

$$\left.\vphantom{\begin{matrix}1\\1\\1\end{matrix}}\right\} (2\text{-}79)$$

frequently prove useful.

2.2.3 THE KELLER COEFFICIENTS FOR A PERFECT CONDUCTOR

Thus far we have not specialized to the case of a perfectly conducting wedge. Let us now make that specialization.

The Keller diffraction coefficient for a perfect conductor is given in Section 3 of Reference 3. In our notation, these results become

$$\underline{\underline{d}}^K = d_\perp^K \ \underline{e}_\perp^s \ \underline{e}_\perp^i \ + \ d_{\parallel}^K \ \underline{e}_{\parallel}^s \ \underline{e}_{\parallel}^i \qquad (2\text{-}80a)$$

$$= d_a^K \ (\underline{e}_\perp^s \ \underline{e}_\perp^i \ + \ \underline{e}_{\parallel}^s \ \underline{e}_{\parallel}^i \ ) + d_b^K \ (\underline{e}_\perp^s \ \underline{e}_\perp^i \ - \ \underline{e}_{\parallel}^s \ \underline{e}_{\parallel}^i) \qquad , \qquad (2\text{-}80b)$$

where

$$d_\perp^K = d_a^K + d_b^K \ , \ \ d_{\parallel}^K = d_a^K - d_b^K \ ,$$

$$d_a^K = \frac{1}{2}\,(d_\perp^K + d_{\parallel}^K), \ \ d_b^K = \frac{1}{2}\,(d_\perp^K - d_{\parallel}^K) \ . \left.\vphantom{\begin{matrix}1\\1\end{matrix}}\right\} \qquad (2\text{-}81)$$

and

$$d_a^K = \frac{e^{i\pi/4}}{(2\pi)^{1/2}} \ \frac{\nu \sin \nu\pi}{\cos \nu\pi - \cos \nu\,(\phi_1 - \phi_s)} \qquad , \qquad (2\text{-}82)$$

$$d_b^K = \frac{e^{i\pi/4}}{(2\pi)^{1/2}} \frac{\nu \sin \nu\pi}{\cos \nu\pi + \cos\left[\nu\left(2\pi - (\phi_i + \phi_s)\right)\right]} \quad . \tag{2-83}$$

Here we have used the simplified notation $d_\perp$, $d_\parallel$ for $d_{\perp\perp}$, $d_{\parallel\parallel}$. In accord with (2-49) and (2-50) there are no cross-terms in $\underline{d}^K$. Furthermore, $\underline{d}^K$ is independent of k and of β_i. (From (2-48) we see that independence of k implies independence of β_i.)

By straightforward application of standard trigonometric identities, we can obtain the equivalent forms

$$d_a^K = \frac{e^{i\pi/4}}{2(2\pi)^{1/2}} \frac{\nu \sin \nu\pi}{\sin(\frac{\nu}{2}\delta_{S+}) \sin(\frac{\nu}{2}\delta_{S-})} \quad , \tag{2-84}$$

$$d_b^K = -\frac{e^{i\pi/4}}{2(2\pi)^{1/2}} \frac{\nu \sin \nu\pi}{\sin(\frac{\nu}{2}\delta_{R+}) \sin(\frac{\nu}{2}\delta_{R-})} \quad . \tag{2-85}$$

These are not as convenient for computation as (2-82) and (2-83), but they show how simply the diffraction coefficient is related to the positions of the geometrical boundaries.

It is a simple matter to decompose each expression (2-84) and (2-85) into a contribution from the current on S_+ and a contribution from the current on S_-. Let us write

$$\underline{d}^K = \underline{d}^K_+ + \underline{d}^K_- \quad , \quad d_q^K = d_{q+}^K + d_{q-}^K \quad , \quad q = \perp, \parallel, a, b, \text{etc.} \quad , \tag{2-86}$$

where + indicates the S_+ contribution and – indicates the S_- contribution. We then readily find

$$d_{a+}^K = -\frac{e^{i\pi/4}}{2(2\pi)^{1/2}} \nu \cot \frac{\nu}{2}\delta_{S+} \quad , \tag{2-87}$$

$$d_{a-}^K = \frac{e^{i\pi/4}}{2(2\pi)^{1/2}} \nu \cot \frac{\nu}{2}\delta_{S-} \quad , \tag{2-88}$$

$$d_{b+}^K = -\frac{e^{i\pi/4}}{2(2\pi)^{1/2}} \nu \cot \frac{\nu}{2}\delta_{R+} \quad , \tag{2-89}$$

$$d_{b-}^{K} = \frac{e^{i\pi/4}}{2\,(2\pi)^{1/2}}\, \nu \, \cot \frac{\nu}{2}\delta_{R-} \qquad\qquad , \qquad\qquad (2\text{-}90)$$

and

$$d_{1+}^{K} = -\frac{e^{i\pi/4}}{2\,(2\pi)^{1/2}}\, \nu \, \frac{\sin \frac{\nu}{2}(\delta_{S+}+\delta_{R+})}{\sin \frac{\nu}{2}\delta_{S+}\,\sin \frac{\nu}{2}\delta_{R+}} \qquad\qquad (2\text{-}91a)$$

$$= -\frac{e^{i\pi/4}}{(2\pi)^{1/2}}\, \nu \, \frac{\sin \nu[(\pi+\alpha)-\phi_{S}]}{\cos \nu(\phi_{i}-\alpha)-\cos \nu[(\pi+\alpha)-\phi_{S}]} \qquad (2\text{-}91b)$$

$$= \frac{e^{i\pi/4}}{(2\pi)^{1/2}}\, \nu \, \frac{\cos \nu(2\pi-\phi_{S})}{\sin \nu(\pi-\phi_{i})-\sin \nu(2\pi-\phi_{S})} \qquad\qquad , \qquad (2\text{-}91c)$$

$$d_{1-}^{K} = \frac{e^{i\pi/4}}{2(2\pi)^{1/2}}\, \nu \, \frac{\sin \frac{\nu}{2}(\delta_{S-}+\delta_{R-})}{\sin \frac{\nu}{2}\delta_{S-}\,\sin \frac{\nu}{2}\delta_{R-}} \qquad\qquad (2\text{-}92a)$$

$$= \frac{e^{i\pi/4}}{(2\pi)^{1/2}}\, \nu \, \frac{\sin \nu[(\pi-\alpha)-\phi_{S}]}{\cos \nu[(2\pi-\alpha)-\phi_{i}]-\cos \nu[(\pi-\alpha)-\phi_{S}]} \qquad (2\text{-}92b)$$

$$= -\frac{e^{i\pi/4}}{(2\pi)^{1/2}}\, \nu \, \frac{\cos \nu\phi_{S}}{\sin \nu(\pi-\phi_{i})+\sin \nu\phi_{S}} \qquad\qquad , \qquad (2\text{-}92c)$$

$$d_{\|+}^{K} = \frac{e^{i\pi/4}}{2\,(2\pi)^{1/2}}\, \nu \, \frac{\sin \frac{\nu}{2}(\delta_{S+}-\delta_{R+})}{\sin \frac{\nu}{2}\delta_{S+}\,\sin \frac{\nu}{2}\delta_{R+}} \qquad\qquad (2\text{-}93a)$$

$$= \frac{e^{i\pi/4}}{(2\pi)^{1/2}}\, \nu \, \frac{\sin \nu(\phi_{i}-\alpha)}{\cos \nu(\phi_{i}-\alpha)-\cos \nu[(\pi+\alpha)-\phi_{S}]} \qquad (2\text{-}93b)$$

$$= \frac{e^{i\pi/4}}{(2\pi)^{1/2}}\, \nu \, \frac{\cos \nu(\pi-\phi_{i})}{\sin \nu(\pi-\phi_{i})-\sin \nu(2\pi-\phi_{S})} \qquad\qquad , \qquad (2\text{-}93c)$$

$$d_{\|-}^{K} = \frac{e^{i\pi/4}}{2\,(2\pi)^{1/2}}\, \nu \, \frac{\sin \frac{\nu}{2}(\delta_{R-}-\delta_{S-})}{\sin \frac{\nu}{2}\delta_{S-}\,\sin \frac{\nu}{2}\delta_{R-}} \qquad\qquad (2\text{-}94a)$$

$$= \frac{e^{i\pi/4}}{(2\pi)^{1/2}}\, \nu \, \frac{\sin \nu[(2\pi-\alpha)-\phi_{i}]}{\cos \nu[(2\pi-\alpha)-\phi_{i}]-\cos \nu[(\pi-\alpha)-\phi_{S}]} \qquad (2\text{-}94b)$$

$$= -\frac{e^{i\pi/4}}{(2\pi)^{1/2}}\, \nu \, \frac{\cos \nu(\pi-\phi_{i})}{\sin \nu(\pi-\phi_{i})+\sin \nu\phi_{S}} \qquad\qquad . \qquad (2\text{-}94c)$$

In each equation, the sine terms in the numerator of the "a" form and of the "b" form are equal, as can be verified using (2-79).

If now we consider the $d^K_{\perp \pm}$ as functions of ϕ_s, we find that

$d_{\perp +}$ has odd symmetry about $\phi_s = \pi + a$;

$d_{\perp -}$ has odd symmetry about $\phi_s = \pi - a$;

$d_{\parallel +}$ has even symmetry about $\phi_s = \pi + a$;

$d_{\parallel -}$ has even symmetry about $\phi_s = \pi - a$.

These are exactly the symmetry properties we expect from the concept of

each face of the wedge being a radiating current sheet.

It is readily verified that the results given in (2-87) to (2-90) add up to yield

the results given in (2-84) and (2-85). The "a" and "b" forms of (2-91) to (2-94)

are obtained from (2-81) and (2-87) to (2-90) by using the identity

$$\cot x \pm \cot y = \frac{\sin (y \pm x)}{\sin x \sin y} = \frac{2 \sin (y \pm x)}{\cos (y - x) - \cos (y + x)} , \qquad (2\text{-}95)$$

and the "c" forms are then obtained by using the definition (2-58) of ν and

standard trigonometric identities.

We omit here the proof that the terms with subscript + and −

are indeed due to currents on S_+ and S_- respectively, but we note

that this proof is easily made as a by-product of the derivation of the

Incremental Length Diffraction Coefficient.

There is no difficulty in evaluating any of the expressions for

$\underline{\underline{d}}^K$ and its components in the transitional cases

$$\phi_i = \pi \pm a .$$

On the other hand we see from (2-87) to (2-90) that $\underline{d}^K$ is singular

when δ_{S+}, δ_{S-}, δ_{R+}, or δ_{R-} is zero. This confirms our statement in Sec-

tion 2.2.1 that $\underline{\underline{d}}^K$ has a singularity when ϕ_s lies on a shadow boundary or a

reflection boundary. It can furthermore be verified that, because of the con-

dition $a < \frac{\pi}{2}$, the arguments of the cotangents in (2-87) to (2-90) never

reach π or $-\pi$, and thus <u>the shadow boundary and reflection boundary singula-</u>

<u>rities are the only singularities of $\underline{\underline{d}}^K$.</u>

2.2.4 THE UFIMTSEV COEFFICIENTS FOR A PERFECT CONDUCTOR

The Ufimtsev diffraction coefficient $\underline{\underline{d}}^U$ for a perfect conductor has the form

$$\underline{\underline{d}}^U = d_\perp^U \, \underline{e}_\perp^s \, \underline{e}_\perp^i + d_x^U \, \underline{e}_\parallel^s \, \underline{e}_\perp^i + d_\parallel^U \, \underline{e}_\parallel^s \, \underline{e}_\parallel^i \quad , \tag{2-96}$$

where we have used the simplified notations of Section 2.2.3 and also d_x instead of $d_{\parallel \perp}$ for the cross-term. From Section 2.1.6, we see that this is indeed the most general form we ever encounter for a perfect conductor diffraction coefficient; $d_{\perp \parallel}$ is always zero.

It is convenient to proceed as in Section 2.2.3 and define d_a^U and d_b^U such that

$$\left. \begin{aligned} d_\perp^U &= d_a^U + d_b^U \;, \quad d_\parallel^U = d_a^U - d_b^U \;, \\ d_a^U &= \tfrac{1}{2}(d_\perp^U + d_\parallel^U), \quad d_b^U = \tfrac{1}{2}(d_\perp^U - d_\parallel^U). \end{aligned} \right\} \tag{2-97}$$

We then can write

$$\underline{\underline{d}}^U = d_a^U \, (\underline{e}_\perp^s \, \underline{e}_\perp^i + \underline{e}_\parallel^s \, \underline{e}_\parallel^i) + d_b^U \, (\underline{e}_\perp^s \, \underline{e}_\perp^i - \underline{e}_\parallel^s \, \underline{e}_\parallel^i) + d_x^U \, \underline{e}_\parallel^s \, \underline{e}_\perp^i \quad . \tag{2-98}$$

We also proceed analogously to (2-86) and define

$$\underline{\underline{d}}^U = \underline{\underline{d}}_+^U + \underline{\underline{d}}_-^U \quad , \quad d_q^U = d_{q+}^U + d_{q-}^U \quad , \quad q = \perp, \parallel \, x, \, a, \, b, \, \text{etc.} \quad , \tag{2-99}$$

where + and - indicate contributions from S_+ and S_- respectively.

The diagonal elements of $\underline{\underline{d}}^U$ are given in Section 4 of Ufimtsev's book (Reference 1). Expressing Ufimtsev's results in our notation we have

$$d_a^U = d_a^K - \frac{e^{i\pi/4}}{2\,(2\pi)^{1/2}} \, [\, U_+ (\phi_i) - U_- (\phi_i)\,] \, \tan \frac{\phi_i - \phi_s}{2} \quad , \tag{2-100}$$

$$d_b^U = d_b^K + \frac{e^{i\pi/4}}{2(2\pi)^{1/2}} \left[U_+ (\phi_i) \tan \frac{\phi_i + \phi_s - 2\alpha}{2} - U_- (\phi_i) \tan \frac{\phi_i + \phi_s + 2\alpha}{2} \right]. \tag{2-101}$$

Here U_+ and U_- are step functions defined by

$$
\left. \begin{aligned}
U_+(\phi_l) &= 1 \text{ for } (\pi + a) > \phi_l \geq a \\
&\quad \text{undefined for } \phi_l = \pi + a \\
&= 0 \text{ otherwise}
\end{aligned} \right\} \quad , \qquad (2\text{-}102)
$$

$$
\left. \begin{aligned}
U_-(\phi_l) &= 1 \text{ for } (2\pi - a) \geq \phi_l > (\pi - a) \\
&\quad \text{undefined for } \phi_l = \pi - a \\
&= 0 \text{ otherwise}
\end{aligned} \right\} \quad . \qquad (2\text{-}103)
$$

That is, $U_+ = 1$ when S_+ is illuminated, $U_- = 1$ when S_- is illuminated.

We see that $d_a{}^U$ and $d_b{}^U$ are independent of k and β_l, and thus $d_\perp{}^U$ and $d_\parallel{}^U$ are independent of k and β_l. We also note that

$$
d_a{}^U = d_a{}^K \text{ for } (\pi + a) > \phi_s > (\pi - a) \quad .
$$

By making use of the easily-verified identities

$$
\tan \frac{1}{2}(\phi_l - \phi_s) = -\tan \frac{1}{2}\phi_{sl} = -\cot \frac{1}{2}\,\delta_{S+} = -\cot \frac{1}{2}\,\delta_{S-} \quad , \qquad (2\text{-}104)
$$

$$
\left. \begin{aligned}
\tan \frac{1}{2}(\phi_l + \phi_s - 2a) &= \cot \frac{1}{2}\,\delta_{R+} \\
\tan \frac{1}{2}(\phi_l + \phi_s + 2a) &= \cot \frac{1}{2}\,\delta_{R-}
\end{aligned} \right\} \quad , \qquad (2\text{-}105)
$$

we can write (2-100) and (2-101) in the equivalent forms

$$
d_a{}^U = d_a{}^K + \frac{e^{i\pi/4}}{2(2\pi)^{1/2}} \left(U_+ \cot \frac{\delta_{S+}}{2} - U_- \cot \frac{\delta_{S-}}{2} \right) \quad , \qquad (2\text{-}106)
$$

$$
d_b{}^U = d_b{}^K + \frac{e^{i\pi/4}}{2(2\pi)^{1/2}} \left(U_+ \cot \frac{\delta_{R+}}{2} - U_- \cot \frac{\delta_{R-}}{2} \right) \quad . \qquad (2\text{-}107)
$$

39

From these expressions and (2-84) and (2-85), we see how simply the diagonal elements of $\underline{d}^U$ are related to the positions of the geometrical boundaries.

It is now straightforward to separate the S_+ and S_- contributions to d_a^U and d_b^U. We obtain

$$d_{a+}^U = - \frac{e^{i\pi/4}}{2(2\pi)^{1/2}} \left[\nu \cot(\frac{\nu}{2}\delta_{S+}) - U_+ \cot(\frac{1}{2}\delta_{S+}) \right], \tag{2-108}$$

$$d_{a-}^U = \frac{e^{i\pi/4}}{2(2\pi)^{1/2}} \left[\nu \cot(\frac{\nu}{2}\delta_{S-}) - U_- \cot(\frac{1}{2}\delta_{S-}) \right], \tag{2-109}$$

$$d_{b+}^U = - \frac{e^{i\pi/4}}{2(2\pi)^{1/2}} \left[\nu \cot(\frac{\nu}{2}\delta_{R+}) - U_+ \cot(\frac{1}{2}\delta_{R+}) \right], \tag{2-110}$$

$$d_{b-}^U = \frac{e^{i\pi/4}}{2(2\pi)^{1/2}} \left[\nu \cot(\frac{\nu}{2}\delta_{R-}) - U_- \cot(\frac{1}{2}\delta_{R-}) \right]. \tag{2-111}$$

The S_+ and S_- contributions to $d_\perp^U$ and $d_\parallel^U$ are

$$d_{\perp+}^U = - \frac{e^{i\pi/4}}{2(2\pi)^{1/2}} \left[\nu \frac{\sin\frac{\nu}{2}(\delta_{S+}+\delta_{R+})}{\sin\frac{\nu}{2}\delta_{S+}\sin\frac{\nu}{2}\delta_{R+}} - U_+ \frac{\sin\frac{1}{2}(\delta_{S+}+\delta_{R+})}{\sin\frac{1}{2}\delta_{S+}\sin\frac{1}{2}\delta_{R+}} \right], \tag{2-112}$$

$$d_{\perp-}^U = \frac{e^{i\pi/4}}{2(2\pi)^{1/2}} \left[\nu \frac{\sin\frac{\nu}{2}(\delta_{S-}+\delta_{R-})}{\sin\frac{\nu}{2}\delta_{S-}\sin\frac{\nu}{2}\delta_{R-}} - U_- \frac{\sin\frac{1}{2}(\delta_{S-}+\delta_{R-})}{\sin\frac{1}{2}\delta_{S-}\sin\frac{1}{2}\delta_{R-}} \right], \tag{2-113}$$

$$d_{\parallel+}^U = \frac{e^{i\pi/4}}{2(2\pi)^{1/2}} \left[\nu \frac{\sin\frac{\nu}{2}(\delta_{S+}-\delta_{R+})}{\sin\frac{\nu}{2}\delta_{S+}\sin\frac{\nu}{2}\delta_{R+}} - U_+ \frac{\sin\frac{1}{2}(\delta_{S+}-\delta_{R+})}{\sin\frac{1}{2}\delta_{S+}\sin\frac{1}{2}\delta_{R+}} \right], \tag{2-114}$$

$$d_{\parallel-}^U = \frac{e^{i\pi/4}}{2(2\pi)^{1/2}} \left[\nu \frac{\sin\frac{\nu}{2}(\delta_{R-}-\delta_{S-})}{\sin\frac{\nu}{2}\delta_{S-}\sin\frac{\nu}{2}\delta_{R-}} - U_- \frac{\sin\frac{1}{2}(\delta_{R-}-\delta_{S-})}{\sin\frac{1}{2}\delta_{S-}\sin\frac{1}{2}\delta_{R-}} \right]. \tag{2-115}$$

40

The $(\delta \pm \delta)$ terms can be evaluated using (2-79). Note that the coefficient of the step function $U_\pm$ is obtained from the Keller coefficient by substituting 1 for ν. Using this fact, we can readily construct forms of the d^U corresponding to the "b" and "c" forms of (2-91) to (2-94). The symmetry properties of the $d^U_{\frac{1}{\parallel}\pm}$ as functions of ϕ_s are the same as those given in Section 2.2.3 for the $d^K_{\frac{1}{\parallel}\pm}$.

When both ϕ_i and ϕ_s lie outside the wedge, in the range a to $(2\pi - a)$, the forms (2-100) and (2-101) are probably the most useful ones for actual computation. It may also be meaningful in some instances to consider values of ϕ_s inside the wedge, because the fringe wave current alone does produce scattering in these directions. For such directions, we can use (2-108) to (2-115) provided we use the range of angles

$$(2\pi + a) \geq \phi_s \geq a \qquad (2-116)$$

in the expressions for the d_{q+} and the range of angles

$$(2\pi - a) \geq \phi_s \geq -a \qquad (2-117)$$

in the expressions for the d_{q-}. This choice of ranges can be justified by symmetry considerations. In actual computation, (2-108) to (2-111) are probably more convenient than (2-112) to (2-115).

It may be meaningful to consider values of ϕ_i inside the wedge, but this question has not yet been studied.

The cross-term d_x^U is given by

$$d_x^U = -\frac{e^{i\pi/4}}{(2\pi)^{1/2}} \sin\beta_1 \left[U_+ (\phi_i) - U_- (\phi_i) \right] \quad , \qquad (2-118)$$

which vanishes when both faces are illuminated and also for incidence normal to the axis. To verify (2-118), we calculate $\bar{W}_{\parallel\perp}{}^{PO}$ (which is a simple and straightforward procedure), use (2-47) to show that $\bar{W}_{\parallel\perp}{}^{U} = -\bar{W}_{\parallel\perp}{}^{PO}$, and then calculate $d_x{}^U$ from the $\bar{\bar{W}}$ form of (2-32). Since $d_x{}^U$ is independent of ϕ_s, we may use (2-118) for

values of ϕ_s inside the wedge, and it is thus not necessary to consider a decomposition of d_x^U into S_+ and S_- contributions. (In order to carry out the decomposition, we would have to evaluate $\hat{K}_{e\ell\perp}$ at the edge. This would be just an unproductive side issue.)

The cross-term d_x^U does not appear in Ufimtsev's work (Reference 1). This does not affect his results for two-dimensional problems, because a two-dimensional problem involving only perfect conductors can be reduced to an equivalent problem with $\beta_1 = 0$ for which d_x^U vanishes. Similarly, Ufimtsev's results for backscatter from a three-dimensional body are valid whenever the scattering appears to arise from single diffraction at scattering centers, because here $\beta_1 = 0$ in the canonical problem which we utilize at each scattering center. On the other hand, the absence of the cross-term can make an important difference in three-dimensional bistatic scattering problems and in three-dimensional backscatter problems involving multiple diffraction or combined diffraction and reflection.

As noted in Section 2.2.1, $\underline{\underline{d}}^U$ is finite and uniquely defined for all ϕ_s when $\phi_1 \neq \pi \pm a$. To prove this, we refer to (2-108) to (2-111), note that the step function $U_\pm$ is always unity when the arguments of the cotangents are zero, and use the identity

$$\nu \cot (\tfrac{\nu}{2}\delta) - \cot (\tfrac{1}{2}\delta) = \frac{\nu \tan \tfrac{1}{2}\delta - \tan \tfrac{\nu}{2}\delta}{\tan \tfrac{1}{2}\delta \ \tan \tfrac{\nu}{2}\delta} = \tfrac{1}{6}(1 - \nu^2)\delta + O(\delta^3) \qquad (2\text{-}119)$$

to show that there is neither a singularity nor an ambiguity in definition when one of the δ is zero. Furthermore, it can readily be verified that δ_{S+} and δ_{R+} have absolute value less than 2π for all values of ϕ_1 for which $U_+ = 1$, and δ_{S-} and δ_{R-} have absolute value less than 2π for all ϕ_1 for which $U_- = 1$.

42

Thus the terms of form $U \cot \delta/2$ have no singularities other than the one at $\delta = 0$. It follows that the $d^U_{\substack{a \pm \\ b}}$ are uniquely defined and finite for all ϕ_s when $\phi_l \neq \pi \pm a$.

For the transitional or grazing cases $\phi_l = \pi \pm a$, we would expect some difficulty since, for a $\perp$-polarized incident wave, we do not even have a unique separation into physical optics and fringe wave currents. Let us consider the elements of $\underline{\underline{d}}^U$ separately. The simplest to deal with is d^U_x. We see by inspection of (2-118) that, for $\beta_l \neq 0$, d^U_x is not defined for $\phi_l = \pi \pm a$, values which in fact correspond to discontinuities in d^U_x. For $\beta_l = 0$, d^U_x vanishes for all values of ϕ_l, including $\pi \pm a$.

The most efficient way to study $d^U_{\perp+}$ and $d^U_{\parallel+}$ is by means of the expressions (2-108) and (2-110) for d^U_{a+} and d^U_{b+} and the definitions (2-71) and (2-72) for δ_{S+} and δ_{R+}. We find that $d^U_{\perp+}$, as a function of ϕ_l and ϕ_s, has a rather complicated behavior near the points $(\phi_l, \phi_s) = (\pi + a, a)$, $(\pi + a, 2\pi + a)$, a behavior which is probably of no physical significance. For $a < \phi_s < \pi + a$ and $\pi + a < \phi_s < 2\pi + a$, $d^U_{\perp+}$ is not defined when $\phi_l = \pi + a$, because there is a finite discontinuity of $d^U_{\perp+}$ across this value. Only when $\phi_s = \phi_l$ is $d^U_{\perp+}$ defined for $\phi_l = \pi + a$, but this exception is very important because it includes the case of backscatter. As to $d^U_{\parallel+}$, we find that it is defined for $\phi_l = \pi + a$ in all cases but $\phi_s = a$ and $\phi_s = 2\pi + a$, where we encounter the same kind of complicated behavior as for $d^U_{\perp+}$.

In similar manner, we find that $d^U_{\perp-}$ and $d^U_{\parallel-}$ have a rather complicated behavior near the points $(\pi - \alpha, -\alpha)$ and $(\pi - \alpha, 2\pi - \alpha)$; that $d^U_{\perp-}$ is not defined for $(\pi - \alpha, \phi_s)$ when $-\alpha < \phi_s < \pi - \alpha$ or $\pi - \alpha < \phi_s < 2\pi - \alpha$ because these values represent a line of discontinuity; that $d^U_{\perp-}$ is defined for $\phi_s = \phi_i = \pi - \alpha$; and that $d^U_{\parallel-}$ is defined for $\phi_i = \pi - \alpha$ and $-\alpha < \phi_s < 2\pi - \alpha$.

All elements of $\underline{d}^U$ are defined for backscatter at non-oblique incidence,

$$\phi_s = \phi_i = \pi \pm \alpha \;, \quad \beta_i = 0 \qquad ; \tag{2-120}$$

and thus $\underline{d}^U$ is a continuous function of ϕ_i for backscatter.

The fact that a dyadic element does not exist for a given pair of values of ϕ_i and ϕ_s tells us that our simple model of the scattering mechanism is not valid at or near this pair of values. A more complicated model must be used.

2.2.5 SIMPLIFICATIONS FOR A KNIFE EDGE

For a knife edge, we have

$$a = 0, \quad \upsilon = \frac{1}{2} . \tag{2-121}$$

There is no range of ϕ_i for which both S_+ and S_- are illuminated.

There is only one transitional case,

$$\phi_i = \pi . \tag{2-122}$$

There are no angles inside the wedge, and both ϕ_i and ϕ_s

run from 0 to 2π. Also

$$U_- = 1-U_+ . \tag{2-123}$$

The simplest and most important forms of the diffraction coef-

ficient for a knife edge are

$$d_\perp^U = \mp \frac{e^{i\pi/4}}{(2\pi)^{1/2}} \frac{\sin \frac{1}{2}(\pi - \phi_s)}{\sin \frac{1}{2}|\pi - \phi_i| + \cos \frac{1}{2}(\pi - \phi_s)} , \tag{2-124}$$

$$\tag{2-125}$$

$$d_{\perp +}^U = d_{\perp -}^U = \frac{1}{2} d_\perp^U ,$$

$$d_{\parallel}^U = - \frac{e^{i\pi/4}}{(2\pi)^{1/2}} \frac{\cos \frac{1}{2}(\pi - \phi_i)}{\sin \frac{1}{2}|\pi - \phi_i| + \cos \frac{1}{2}(\pi - \phi_s)} , \tag{2-126}$$

$$d_{\parallel +}^U = d_{\parallel -}^U = \frac{1}{2} d_{\parallel}^U , \tag{2-127}$$

$$d_X^U = \mp \frac{e^{i\pi/4}}{(2\pi)^{1/2}} \sin \beta_i , \tag{2-128}$$

where the - sign is used for $\phi_i < \pi$, the + sign for $\phi_i > \pi$. We have written $d_\perp^U$ in a form which emphasizes that it is an odd function of $(\pi - \phi_i)$ and an odd function of $(\pi - \phi_s)$, and we have written $d_{\parallel}^U$ in a form which emphasizes that it is an even function of $(\pi - \phi_i)$ and an even function of $(\pi - \phi_s)$.

We readily see that $\underline{\underline{d}}^U$ is finite and uniquely defined for all ϕ_s except when $\phi_i = \pi$. When $\phi_i = \pi$, $d_{\parallel}{}^U$ is uniquely defined for all values of ϕ_s except 0 and 2π, $d_{\perp}{}^U$ is defined uniquely for $\phi_s = \phi_i = \pi$ but not for any other value of ϕ_s, and $d_x{}^U$ is uniquely defined only when $\beta_i = 0$.

Other diffraction coefficient forms which are of interest include

$$d_a{}^K = -\frac{e^{i\pi/4}}{2(2\pi)^{1/2}} \; \frac{1}{\cos\left[\frac{1}{2}(\phi_i - \phi_s)\right]} \qquad , \qquad (2\text{-}129)$$

$$d_b{}^K = -\frac{e^{i\pi/4}}{2(2\pi)^{1/2}} \; \frac{1}{\cos\left[\frac{1}{2}(\phi_i + \phi_s)\right]} \qquad , \qquad (2\text{-}130)$$

$$c_{a+}{}^K = -\frac{e^{i\pi/4}}{4(2\pi)^{1/2}} \; \cot\frac{1}{4}\,\delta_{S+} = -\frac{e^{i\pi/4}}{4(2\pi)^{1/2}} \; \frac{1+\tan\frac{1}{4}\phi_{si}}{1-\tan\frac{1}{4}\phi_{si}} \qquad , \qquad (2\text{-}131)$$

$$d_{a-}{}^K = +\frac{e^{i\pi/4}}{4(2\pi)^{1/2}} \; \cot\frac{1}{4}\,\delta_{S-} = -\frac{e^{i\pi/4}}{4(2\pi)^{1/2}} \; \frac{1-\tan\frac{1}{4}\phi_{si}}{1+\tan\frac{1}{4}\phi_{si}} \qquad , \qquad (2\text{-}132)$$

$$d_{b+}{}^K = -\frac{e^{i\pi/4}}{4(2\pi)^{1/2}} \cot\frac{1}{4}\,\delta_{R+} = -\frac{e^{i\pi/4}}{4(2\pi)^{1/2}} \; \frac{1+\tan\frac{1}{4}\phi_{\Sigma}}{1-\tan\frac{1}{4}\phi_{\Sigma}} \qquad , \qquad (2\text{-}133)$$

$$d_{b-}{}^K = -\frac{e^{i\pi/4}}{2(2\pi)^{1/2}} \cot\frac{1}{4}\,\delta_{R-} = -\frac{e^{i\pi/4}}{4(2\pi)^{1/2}} \; \frac{1-\tan\frac{1}{4}\phi_{\Sigma}}{1+\tan\frac{1}{4}\phi_{\Sigma}} \qquad ; \qquad (2\text{-}134)$$

$$d_{\perp}{}^K = \frac{2e^{i\pi/4}}{(2\pi)^{1/2}} \; \frac{\sin\frac{1}{2}(\pi-\phi_i)\sin\frac{1}{2}(\pi-\phi_s)}{\cos(\pi-\phi_i)+\cos(\pi-\phi_s)} \qquad , \qquad (2\text{-}135)$$

$$d_{\parallel}{}^K = -\frac{2e^{i\pi/4}}{(2\pi)^{1/2}} \; \frac{\cos\frac{1}{2}(\pi-\phi_i)\cos\frac{1}{2}(\pi-\phi_s)}{\cos(\pi-\phi_i)+\cos(\pi-\phi_s)} \qquad ; \qquad (2\text{-}136)$$

$$d^K_{\perp+} = - \frac{e^{i\pi/4}}{2(2\pi)^{1/2}} \frac{\sin\frac{1}{2}(\pi-\phi_s)}{\sin\frac{1}{2}(\pi-\phi_l) - \cos\frac{1}{2}(\pi-\phi_s)} \quad , \qquad (2\text{-}137)$$

$$d^K_{\perp-} = - \frac{e^{i\pi/4}}{2(2\pi)^{1/2}} \frac{\sin\frac{1}{2}(\pi-\phi_s)}{\sin\frac{1}{2}(\pi-\phi_l) + \cos\frac{1}{2}(\pi-\phi_s)} \quad , \qquad (2\text{-}138)$$

$$d^K_{\parallel+} = \frac{e^{i\pi/4}}{2(2\pi)^{1/2}} \frac{\cos\frac{1}{2}(\pi-\phi_l)}{\sin\frac{1}{2}(\pi-\phi_l) - \cos\frac{1}{2}(\pi-\phi_s)} \quad ; \qquad (2\text{-}139)$$

$$d^K_{\parallel-} = - \frac{e^{i\pi/4}}{2(2\pi)^{1/2}} \frac{\cos\frac{1}{2}(\pi-\phi_l)}{\sin\frac{1}{2}(\pi-\phi_l) + \cos\frac{1}{2}(\pi-\phi_s)} \quad ; \qquad (2\text{-}140)$$

$$d^U_a = - \frac{e^{i\pi/4}}{2(2\pi)^{1/2}} \frac{1}{\cos\frac{1}{2}(\phi_s-\phi_l)} \left[1 \mp \sin\frac{1}{2}(\phi_s-\phi_l) \right], \qquad (2\text{-}141)$$

$$d^U_b = - \frac{e^{i\pi/4}}{2(2\pi)^{1/2}} \frac{1}{\cos\frac{1}{2}(\phi_l+\phi_s)} \left[1 \mp \sin\frac{1}{2}(\phi_l+\phi_s) \right], \qquad (2\text{-}142)$$

with the upper sign used for $\phi_l < \pi$, the lower sign for $\phi_l > \pi$; and

$$d^U_{a+} = - \frac{e^{i\pi/4}}{2(2\pi)^{1/2}} \left(\frac{1}{2}\cot\frac{1}{4}\delta_{S+} - U_+ \cot\frac{1}{2}\delta_{S+} \right) \quad , \qquad (2\text{-}143)$$

$$d^U_{a-} = \frac{e^{i\pi/4}}{2(2\pi)^{1/2}} \left(\frac{1}{2}\cot\frac{1}{4}\delta_{S-} - U_- \cot\frac{1}{2}\delta_{S-} \right) \quad , \qquad (2\text{-}144)$$

$$d^U_{b+} = - \frac{e^{i\pi/4}}{2(2\pi)^{1/2}} \left(\frac{1}{2}\cot\frac{1}{4}\delta_{R+} - U_+ \cot\frac{1}{2}\delta_{R+} \right) \quad , \qquad (2\text{-}145)$$

$$d^U_{b-} = \frac{e^{i\pi/4}}{2(2\pi)^{1/2}} \left(\frac{1}{2}\cot\frac{1}{4}\delta_{R-} - U_- \cot\frac{1}{2}\delta_{R-} \right) \quad . \qquad (2\text{-}146)$$

47

Alternate forms of (2-141) and (2-142) can be obtained by using the identity

$$\frac{1 + \sin x}{\cos x} = \frac{\cos x}{1 - \sin x} = \cot \left(\frac{\pi}{4} - \frac{x}{2}\right) = \frac{1 + \tan \frac{x}{2}}{1 - \tan \frac{x}{2}} \qquad . \tag{2-147}$$

The identity

$$\frac{1}{2} \cot \frac{1}{4} \delta - \cot \frac{1}{2} \delta = \frac{1}{2} \tan \frac{1}{4} \delta \tag{2-148}$$

can be used to simplify (2-143) and (2-145) when $U_+ = 1$ and to simplify (2-144) and (2-146) when $U_- = 1$.

2.2.6 BACKSCATTER AND GENERALIZED BACKSCATTER

We shall define generalized backscatter as the case in which

$$\phi_s = \phi_i = \phi \quad . \tag{2-149}$$

Thus backscatter is a special case of generalized backscatter for which $\beta_i = 0$.

The results for generalized backscatter are no more complicated than those for backscatter alone, except that the relationship of $\underline{e}_{\parallel}^s$ to $\underline{e}_{\parallel}^i$ is given by

$$\underline{e}_{\parallel}^s = (\underline{e}_{\parallel}^i \cdot \underline{t}) \, \underline{t} - \underline{t} \times (\underline{e}_{\parallel}^i \times \underline{t}) \tag{2-150}$$

for generalized backscatter and

$$\underline{e}_{\parallel}^s = \underline{e}_{\parallel}^i = \underline{t} \tag{2-150A}$$

for backscatter. We have

$$\underline{e}_{\perp}^s = - \underline{e}_{\perp}^i = \underline{e}_{\perp} \tag{2-150B}$$

and

$$\delta_{S+} = - \delta_{S-} = \pi \quad , \quad \frac{1}{2} \delta_{R+} = \left(\frac{\pi}{2} + a\right) - \phi \, , \quad \frac{1}{2} \delta_{R-} = \left(\frac{3\pi}{2} - a\right) - \phi \quad . \tag{2-151}$$

Also, since we are assuming that ϕ_i is an angle outside the wedge, we have

$$(2\pi - a) \geq \phi \geq a \qquad . \tag{2-152}$$

The simplest and most important forms of the diffraction coefficient for generalized backscatter are

$$d_{\perp+}^{U} = -\frac{e^{i\pi/4}}{2(2\pi)^{1/2}} \left[\frac{\nu}{\sin \nu \frac{\pi}{2}} \; \frac{\sin \frac{\nu}{2}(\delta_{R+} + \pi)}{\sin \frac{\nu}{2}\delta_{R+}} - U_{+} \cot \frac{1}{2}\delta_{R+} \right]$$

$$= -\frac{e^{i\pi/4}}{2(2\pi)^{1/2}} \left[\frac{\nu}{\sin \nu \pi} \; \frac{2}{1+\tan \nu \frac{\pi}{2}\tan \nu (2\pi - \phi)} - U_{+} \cot \frac{1}{2}\delta_{R+} \right], \qquad (2\text{-}153)$$

$$d_{\perp-}^{U} = -\frac{e^{i\pi/4}}{2(2\pi)^{1/2}} \left[\frac{\nu}{\sin \nu \frac{\pi}{2}} \; \frac{\sin \frac{\nu}{2}(\delta_{R-} - \pi)}{\sin \frac{\nu}{2}\delta_{R-}} + U_{-} \cot \frac{1}{2}\delta_{R-} \right]$$

$$= -\frac{e^{i\pi/4}}{2(2\pi)^{1/2}} \left[\frac{\nu}{\sin \nu \pi} \; \frac{2}{1+\tan \nu \frac{\pi}{2}\tan \nu \phi} + U_{-} \cot \frac{1}{2}\delta_{R-} \right], \qquad (2\text{-}154)$$

and

$$d_{\parallel}^{U} = \frac{e^{i\pi/4}}{2(2\pi)^{1/2}} \left\{ \nu \left[(\cot \frac{\nu}{2}\delta_{R+} - \cot \frac{\nu}{2}\delta_{R-}) - 2\cot \nu \frac{\pi}{2} \right] - U_{+}\cot \frac{1}{2}\delta_{R+} + U_{-}\cot \frac{1}{2}\delta_{R-} \right\}$$

$$= -\frac{e^{i\pi/4}}{2(2\pi)^{1/2}} \left[\frac{\nu}{\sin \nu \pi} \; \frac{4}{1-\tan^{2}\nu \frac{\pi}{2}\;\tan^{2}\nu (\pi - \phi)} + U_{+}\cot \frac{1}{2}\delta_{R+} - U_{-}\cot \frac{1}{2}\delta_{R-} \right]. \qquad (2\text{-}155)$$

The expression (2-118) for d_{x}^{U} does not simplify significantly for the case of generalized backscatter. (For true backscatter, which only occurs when $\beta_{1} = 0$, d_{x}^{U} vanishes.)

In (2-153) to (2-155), the first form can readily be found from (2-112) to (2-115), and the second form can be found from the "b" forms in (2-31) to (2-94).

We can obtain $d_{\perp+}^{K}$, $d_{\perp-}^{K}$, and $d_{\parallel}^{K}$ simply by omitting the terms in U_{+} and U_{-} from (2-153) to (2-155).

Other diffraction coefficient forms which are of interest are

$$d_{a}^{U} = d_{a}^{K} = -\frac{e^{i\pi/4}}{(2\pi)^{1/2}} \nu \cot \nu \frac{\pi}{2} = -\frac{e^{i\pi/4}}{(2\pi)^{1/2}} \; \frac{\nu \sin \nu \pi}{1-\cos \nu \pi}, \qquad (2\text{-}156)$$

$$d_{a+}^{U} = d_{a-}^{U} = d_{a+}^{K} = d_{a-}^{K} = \frac{1}{2} d_{a}^{K} \qquad ; \qquad (2\text{-}157)$$

49

$$d_b^U = \frac{e^{i\pi/4}}{2(2\pi)^{1/2}} \left[\frac{2\nu\sin\nu}{\cos\nu\pi + \cos 2\nu(\pi-\phi)} + U_+ \tan(\phi-a) - U_- \tan(\phi+a) \right] ; \qquad (2\text{-}158)$$

$$d_{\|+}^U = - \frac{e^{i\pi/4}}{2(2\pi)^{1/2}} \left[\frac{\nu}{\sin\nu\pi} \frac{2}{1 - \tan\nu\frac{\pi}{2}\tan\nu(\pi-\phi)} + U_+ \tan(\phi-a) \right] , \qquad (2\text{-}159)$$

$$d_{\|-}^U = - \frac{e^{i\pi/4}}{2(2\pi)^{1/2}} \left[\frac{\nu}{\sin\nu\pi} \frac{2}{1 + \tan\nu\frac{\pi}{2}\tan\nu(\pi-\phi)} - U_- \tan(\phi+a) \right] . \qquad (2\text{-}160)$$

We can obtain d_b^K, $d_{\|+}^K$, $d_{\|-}^K$ from (2-158) to (2-160) by omitting the terms in U_+ and U_-.

We have omitted expressions for the $d_{b\pm}^{K,U}$, which only involve using (2-151) in (2-89), (2-90), (2-110), and (2-111), and for $d_{\perp}^K$ and $d_{\perp}^U$, which are merely the sum of the appropriate $d_{\perp+}$ and $d_{\perp-}$ with no significant simplifications.

It is important to note that $d_{\perp}^U$ and $d_{\|}^U$ are continuous functions of ϕ, specifically that they are not discontinuous as ϕ passes through the grazing angles $\phi = \pi \pm a$.

For generalized backscatter from a knife edge, the simplest and most important forms of the diffraction coefficient are

$$d_{\perp}^U = - \frac{e^{i\pi/4}}{(2\pi)^{1/2}} \frac{1}{1 + \cot\frac{1}{2}|\pi-\phi|} = - \frac{e^{i\pi/4}}{2(2\pi)^{1/2}} \left[1 \mp \tan\left(\frac{\phi}{2} \mp \frac{\pi}{4}\right) \right] , \qquad (2\text{-}161)$$

$$d_{\perp+}^U = d_{\perp-}^U = \frac{1}{2} d_{\perp}^U \qquad , \qquad (2\text{-}162)$$

$$d_{\|}^U = - \frac{e^{i\pi/4}}{(2\pi)^{1/2}} \frac{1}{1 + \tan\frac{1}{2}|\pi-\phi|} = - \frac{e^{i\pi/4}}{2(2\pi)^{1/2}} \left[1 \pm \tan\left(\frac{\phi}{2} \mp \frac{\pi}{4}\right) \right] , \qquad (2\text{-}163)$$

$$d_{\|+}^U = d_{\|-}^U = \frac{1}{2} d_{\|}^U \qquad , \qquad (2\text{-}164)$$

and (2-128) for $d_\chi{}^U$, which does not simplify significantly. In (2-161)and (2-163), the upper signs are used for $\phi < \pi$ and the lower signs for $\phi > \pi$.

Other forms of interest are

$$d_a{}^U = d_a{}^K = -\frac{e^{i\pi/4}}{2(2\pi)^{1/2}} \tag{2-165}$$

$$d_{a+}{}^U = d_{a-}{}^U = d_{a+}{}^K = d_{a-}{}^K = \frac{1}{2} \, d_a{}^K \tag{2-166}$$

$$d_b{}^K = \frac{e^{i\pi/4}}{2(2\pi)^{1/2}} \, \frac{1}{\cos(\pi-\phi)} \tag{2-167}$$

$$d_{b+}{}^K = -\frac{e^{i\pi/4}}{4(2\pi)^{1/2}} \, \frac{1 + \tan\frac{\phi}{2}}{1 - \tan\frac{\phi}{2}} \tag{2-168}$$

$$d_{b-}{}^K = -\frac{e^{i\pi/4}}{4(2\pi)^{1/2}} \cdot \frac{1 - \tan\frac{\phi}{2}}{1 + \tan\frac{\phi}{2}} \tag{2-169}$$

$$d_b{}^U = \frac{e^{i\pi/4}}{2(2\pi)^{1/2}} \, \frac{1}{\cos(\pi-\phi)} \left[1 - \left| \sin(\pi-\phi) \right| \right], \tag{2-170}$$

$$d_{b+}{}^U = -\frac{e^{i\pi/4}}{2(2\pi)^{1/2}} \left[\frac{1}{2} \, \frac{1 + \tan\frac{\phi}{2}}{1 - \tan\frac{\phi}{2}} - U_+ \tan\phi \right] , \tag{2-171}$$

$$d_{b-}{}^U = -\frac{e^{i\pi/4}}{2(2\pi)^{1/2}} \left[\frac{1}{2} \, \frac{1 - \tan\frac{\phi}{2}}{1 + \tan\frac{\phi}{2}} + U_- \tan\phi \right] ; \tag{2-172}$$

$$d_1{}^K = \frac{e^{i\pi/4}}{2(2\pi)^{1/2}} \, \frac{1 - \cos(\pi-\phi)}{\cos(\pi-\phi)} \tag{2-173}$$

$$d_{1+}{}^K = -\frac{e^{i\pi/4}}{2(2\pi)^{1/2}} \, \frac{1}{1 - \cot\frac{1}{2}(\pi-\phi)} \tag{2-174}$$

51

$$d_{\perp-}^{K} = -\frac{e^{i\pi/4}}{2(2\pi)^{1/2}} \frac{1}{1 + \cot \frac{1}{2}(\pi - \phi)} \qquad ; \qquad (2\text{-}175)$$

and
$$d_{\parallel}^{K} = -\frac{e^{i\pi/4}}{2(2\pi)^{1/2}} \frac{1 + \cos(\pi - \phi)}{\cos(\pi - \phi)} \qquad , \qquad (2\text{-}176)$$

$$d_{\parallel+}^{K} = \frac{e^{i\pi/4}}{2(2\pi)^{1/2}} \frac{1}{\tan \frac{1}{2}(\pi - \phi) - 1} \qquad , \qquad (2\text{-}177)$$

$$d_{\parallel-}^{K} = -\frac{e^{i\pi/4}}{2(2\pi)^{1/2}} \frac{1}{\tan \frac{1}{2}(\pi - \phi) + 1} \qquad . \qquad (2\text{-}178)$$

III. THE INCREMENTAL LENGTH DIFFRACTION COEFFICIENT

3.1 THE GENERAL THEORY

3.1.1 DEFINITION OF THE INCREMENTAL LENGTH DIFFRACTION COEFFICIENT

Let us now define the Incremental Length Diffraction Coefficient as a mathematical entity. We shall do so without reference to its applications or to the considerations motivating the definition, matters which we defer until Section 3.1.2.

We shall use the standard formalism for three-dimensional scattering problems, in which the scattered field $(\underline{E}^{scat}, \underline{H}^{scat})$ at a point

$$\underline{r} = R_0 \, \underline{e}_r^{\,s} \tag{3-1}$$

in the far-field region is written in the form

$$\underline{E}^{scat} = \frac{\exp\{ikR_0\}}{R_0} \, \underline{F} \quad , \quad \underline{H}^{scat} = \frac{1}{Z_0} \, \underline{e}_r^{\,s} \times \underline{E}^{scat} \quad , \tag{3-2}$$

· where the radiation vector $\underline{F}$ is independent of R_0 and normal to the unit vector $\underline{e}_r^{\,s}$ in the direction of scattering.

By using (2-146) of Reference 4, we can write $\underline{F}$ as an integral of the effective surface currents $\underline{K}_e$ and $\underline{K}_m$ over the surface S of the scattering body,

$$\underline{F} = -\frac{ik}{4\pi} \, \underline{e}_r^{\,s} \times \int_S dS' \, \exp\{-ike_r^{\,s} \cdot \underline{r}'\} \, (\underline{K}'_m + Z\underline{e}_r^{\,s} \times \underline{K}'_e). \tag{3-2A}$$

When the incident wave is a plane wave of the form (2-3), $\underline{K}_e$ and $\underline{K}_m$ are linear functions of $E_0 \underline{p}$, which we can write in the form

$$\underline{K}_q = E_o \underline{\underline{K}}_q \cdot \underline{p} \quad \text{for} \quad q = e, m. \tag{3-2B}$$

On substituting (3-2B) into (3-2A), we see that we can write $\underline{F}$ in the form

$$\underline{F} = E_o \frac{1}{k} \underline{\underline{D}} \cdot \underline{p} \quad , \tag{3-3}$$

where the dyadic $\underline{\underline{D}}$ is dimensionless and is independent of E_o and $\underline{p}$. Indeed, so long as we consider the geometry and composition of the body to be fixed, $\underline{\underline{D}}$ is a function only of the wave number, the direction of incidence, and the direction of scattering,

$$\underline{\underline{D}} = \underline{\underline{D}} \ (k; \underline{e}_r^i; \underline{e}_r^s) \quad . \tag{3-4}$$

We shall call $\underline{\underline{D}}$ the <u>Three-Dimensional Diffraction Coefficient</u> of the problem. The notation $\underline{\underline{D}}$, with appropriate subscript, super-script, or other modification, can also be used to designate an approximation or a contribution to the true value of $\underline{\underline{D}}$.

Now let us consider again the infinite cylinder problem of Section 2.1.1, as illustrated in Figure 1. We use the definitions of Section 2.1.1 for the quantities $\underline{t}$, $\underline{n}$, $\underline{l}$, t, l, L, ϱ, $\underline{e}_x$, $\underline{e}_y$, which refer to the cylinder geometry, and the quantities $\underline{e}_r^i$, $\hat{\underline{e}}_r^i$, $\underline{e}_\perp^i$, $\underline{e}_\parallel^i$, $\underline{p}$, β_i, and ϕ_i, which refer to the incident field. But now, instead of treating the scattering from the entire cylinder, we consider the scattering due to the effective surface currents on the incremental length element of the cylinder which lies between the planes

$$t = \pm \frac{1}{2} dt \quad . \tag{3-5}$$

The incremental element will scatter in all directions, so now the scattering direction $\underline{e}_r{}^s$ is independent of $\underline{e}_r{}^i$. Nevertheless, once we have specified a value of $\underline{e}_r{}^s$, we can still define β_s, $\hat{\underline{e}}_r{}^s$, $\underline{e}_\perp{}^s$, and $\underline{e}_\parallel{}^s$ by (2-11), (2-13), (2-14), and (2-15) respectively, where now β_s is independent of β_i. We can also still define ϕ_s as the azimuth angle measured from the x-axis to $\hat{\underline{e}}_r{}^s$.

Let us assume that $\underline{e}_r{}^i$ and $\underline{e}_r{}^s$ have been so chosen that a far-field region exists. (In the case of a finite cross-section cylinder, a far-field region exists for all values of $\underline{e}_r{}^i$ and $\underline{e}_r{}^s$.) The far-field scattering can be described in terms of a radiation vector $d\underline{F}_\infty$, which we can write in component form as

$$d\,\underline{F}_\infty = d\,F_{\infty\perp}\,\underline{e}_\perp{}^s + d\,F_{\infty\parallel}\,\underline{e}_\parallel{}^s \qquad .$$

(3-6)

This radiation vector can in turn be expressed in terms of a Three-Dimensional Diffraction Coefficient $d\underline{\underline{D}}_\infty$ by

$$d\,\underline{F}_\infty = E_o\,\frac{1}{k}\,d\underline{\underline{D}}_\infty \cdot \underline{P} \qquad ,$$

(3-7)

which is of the same form as (3-3).

It is clear that $d\underline{\underline{D}}_\infty$ is a linear function of the length dt of the incremental element, and thus we can write

$$d\,\underline{\underline{D}}_\infty = \left[\frac{e^{-i\,\pi/4}}{(2\pi)^{1/2}}\,k\,\underline{\underline{d}}\right] dt \qquad ,$$

(3-8)

where $\underline{d}$ is a dimensionless dyadic which describes the scattering properties of an incremental element. The formula (3-8) holds for that particular element of cylinder which is symmetric about $t = 0$. For any other element, we must introduce a phase factor. (See (3-12).)

We shall refer to the quantity $\underline{d}$ as the Incremental Length Diffraction Coefficient for the cylinder of interest. If we consider the geometry and composition of the cylinder and the orientation of the axis to be fixed, then $\underline{d}$ is in general a function of the wave number, the direction of incidence and the direction of scattering,

$$\underline{\underline{d}} = \underline{\underline{d}} \ (k; \ \beta_{\iota}, \ \phi_{\iota}, \ \beta_{s}, \phi_{s}) \qquad . \tag{3-9}$$

For $\beta_{s} = \beta_{\iota}$ the Incremental Length Diffraction Coefficient is equal to the Two-Dimensional Diffraction Coefficient of Section II. This fact, which is verified in Section 3.1.3, motivated the choice of normalization factor in (3-8) and the use of the same symbol $\underline{d}$ for both types of diffraction coefficient.

From (2-6) and (3-6) we see that $\underline{d}$ can be written in component form using (2-23). But now, of course, $\underline{e}_{\parallel}^{s}$ and $\underline{e}_{\parallel}^{\iota}$ are no longer constrained to both form the same angle with the t-axis.

The notation $\underline{d}$, with appropriate subscript, superscript, or other modification, will also be used to designate an approximation or contribution to the true value of the Incremental Length Diffraction Coefficient.

3.1.2 APPLICATIONS

We shall now motivate our definition of the incremental length diffraction coefficient by briefly discussing some important applications.

The most straightforward application is to scattering from a cylinder of finite length. Let us assume that the cylinder is sufficiently long so that there is no interaction between the two ends. Then we can consider the total effective surface currents on the cylinder to be the sum of the currents $\underline{K}_{e\infty}$, $\underline{K}_{m\infty}$ which would exist on an infinitely long cylinder plus correction currents, both on the end plates and near the ends of the shaft, which are independent of the cylinder length. In many problems, the end effects are negligible.

The contribution to the scattered field due to the currents $\underline{K}_{e\infty}$ and $\underline{K}_{m\infty}$ can be described by a Three-Dimensional Diffraction Coefficient $\underline{D}_{\infty}$. We can readily verify that $\underline{D}_{\infty}$ is related to the Incremental Length Diffraction Coefficient $\underline{d}$ by the simple formula

$$\underline{D}_{\infty} = \exp\left\{-ik(e_{\underline{r}}^{s} + e_{\underline{r}}^{i}) \cdot \underline{r}_{0}\right\} \frac{e^{-i\pi/4}}{(2\pi)^{1/2}} kT \frac{\sin X}{X} \underline{d}(k; \beta_{i}, \phi_{i}; \beta_{s}, \phi_{s}) . \tag{3-10}$$

Here T is the length of the cylinder, $\underline{r}_{0}$ is that point on the axis of the cylinder which lies halfway between the ends, and

$$X = \frac{1}{2} kT \left| \sin \beta_{i} - \sin \beta_{s} \right| \tag{3-11}$$

is half the phase difference in radians between far-field returns from the two ends of the cylinder.

The important problem of scattering from a thin straight wire is of course a special case of scattering from a cylinder of finite length.

Another class of applications is to scattering from a curved rod, which we can define as the body produced when we bend the axis of a finite cylinder but keep the cross section perpendicular to the axis constant at every point of the axis. If the radius of curvature of the bent axis is large enough and if there is no significant interaction between parts of the cylinder, then we can assume that

(1) The total current on the shaft can be approximated satis-factorily by the sum of the currents $\underset{\sim}{K}_{e\infty}$, $\underset{\sim}{K}_{m\infty}$ which are found from the corresponding infinite cylinder problem plus end-effect currents which are independent of the length and curvature of the rod;

(2) The compression and stretching of the surface when the cylinder is bent can be neglected.

Because of the second assumption, the contribution to the scattered field from the currents $\underset{\sim}{K}_{e\infty}$, $\underset{\sim}{K}_{m\infty}$ can be approximated by the three-dimensional diffraction coefficient

$$\underset{\equiv}{D}_\infty = \frac{e^{-i\,\pi/4}}{(2\pi)^{1/2}}\,k \int_T dt' \exp\left\{-ik(\underset{\sim}{e}_r^{\,s} + \underset{\sim}{e}_r^{\,i}) \cdot \underset{\sim}{r}'\right\}\quad \underset{\equiv}{d}' \tag{3-12}$$

Here t is the length parameter along the axis, $\underline{r}$ is the position of a point on the axis and is a function of t, and the integration is taken over the length T of the axis. The diffraction coefficient $\underline{d}$ is a function of the five arguments of (3-3) and also of the unit vector $\underline{t}$ along the axis. In turn, $\underline{t}$ and the arguments β_i, ϕ_i, β_s, and ϕ_s are functions of t.

Frequently the integral of (3-12) can be approximated satisfactorily by stationary phase techniques. In many of these cases, the only significant contributions to the integral come from the neighborhood of those points on the axis at which $\beta_s = \beta_i$. Thus many curved rod problems can be solved adequately using the two-dimensional diffraction coefficient of the corresponding cylinder. This was done for the curved wire problem in a recent paper by Keller and Ahluwalia (Reference 6).

The formula (3-12) can also be applied to curved rods of slowly varying cross section, in which case $\underline{d}$ is a function of the local cross section as well as of the axial direction and the angles of incidence and scattering.

One of the most important applications is to scattering from bodies with edges, both wedge-like edges and rounded edges. Consider, for example, the problem of scattering from a flat plate. If the plate dimensions are large enough compared to the wavelength and if the directions of incidence and scattering are not too close to grazing, we can approximate the total current on the plate as the sum of the current predicted by physical optics plus the fringe wave currents associated with the edges. We have shown in Section V of Reference 11 how to calculate the scattering due to the physical optics current. The scattering due to the fringe wave currents is calculated using (3-10) for straight edges and (3-12) for curved edges, with $\underline{d}$ replaced by the Ufimtsev diffraction coefficient $\underline{d}^U$. In Section IV we use this approach to solve the polygonal plate problem.

The idea of breaking the solution up into a physical optics term plus fringe wave scattering terms is, as we have noted in Section I, also basic to the solution of a large variety of other problems.

The original three-dimensional body work of Ufimtsev (Reference 1) was limited to problems involving curved edges for which the only significant contributions to the edge scattering come from the neighborhood of points where $\beta_s = \beta_i$. Thus good results were obtained using two-dimensional diffraction coefficients.

3.1.3 THE DIFFRACTION COEFFICIENT AS A FUNCTION OF THE EFFECTIVE SURFACE CURRENTS

Let us use (2-27) and (2-28) to define surface current dyadics $\hat{\underline{\underline{K}}}_e$ and $\hat{\underline{\underline{K}}}_m$ on the shaft of a cylinder, and let us also introduce the dyadic function $\underline{\underline{W}}$ which is related to $\hat{\underline{\underline{K}}}_e$ and $\hat{\underline{\underline{K}}}_m$ by (2-30) and (2-31). We can then show that the Incremental Length Diffraction Coefficient $\underline{\underline{d}}$ for the cylinder is given in terms of $\underline{\underline{W}}$ - and thus ultimately in terms of $\hat{\underline{\underline{K}}}_e$ and $\hat{\underline{\underline{K}}}_m$ - by (2-32). The proof is obtained by applying (3-2A) to find $d\underline{F}_\infty$ for an incremental length of the cylinder, using (2-27) to express $\underline{K}_e$ and $\underline{K}_m$ in terms of $\hat{\underline{\underline{K}}}_e$ and $\hat{\underline{\underline{K}}}_m$ respectively, and then finding $\underline{\underline{d}}$ from $d\underline{F}_\infty$ by use of (3-7) and (3-8).

The expression (2-32) can also be used to calculate the ILDC associated with an approximation or contribution to the effective surface currents. Furthermore, we can verify by integration by parts that (2-32) is still valid when $\underline{\underline{W}}$ is replaced by the $\overline{\underline{\underline{W}}}$ of (2-33). Care must be taken, when calculating $\overline{\underline{\underline{W}}}$ for a surface current contribution with discontinuities in the $\hat{K}_{ij}$, to account for the discontinuities by including appropriate impulse functions in the $\hat{K}_{ij}/\partial \ell$ terms.

To verify the important fact that the 2-D DC is equal to the ILDC for

$\beta_s = \beta_i$, we merely note that both are given by (2-32).

$$* \quad * \quad *$$

We always work with surface current dyadics for which the symmetry conditions of (2-34) hold. As a result, $\underline{\underline{W}}$ and $\underline{\overline{\overline{W}}}$ have the symmetry properties given in (2-35) and the ILDC $\underline{d}$ has the symmetry properties given in (2-36).

We should keep in mind that the true infinite cylinder currents are not the true total currents on an element of a finite cylinder or curved rod. This is why we have used the subscript ∞ when we refer to infinite cylinder currents in Section 3.1.2. Of course, in many cases the infinite cylinder currents are a very good approximation to the true currents.

3.1.4 SCATTERING INTO THE FORWARD AND BACK CONES

We shall refer to the cone

$$\beta_s = \beta_i \tag{3-13}$$

as the <u>forward cone</u> and shall refer to the cone

$$\beta_s = - \beta_i \tag{3-14}$$

as the <u>back cone</u>. For $\beta_i = 0$, they are the same.

Scattering into the forward cone can be treated using only the two dimensional diffraction coefficient. An important special case is forward scatter, for which

$$\left| \phi_s - \phi_i \right| = \pi \quad . \tag{3-15}$$

Scattering into the back cone includes the extremely important special case of backscatter, for which

$$\phi_s = \phi_i \qquad . \tag{3-16}$$

Let us now consider how scattering into the back cone is related to scattering into the forward cone. Using (2-31) to (2-33), we readily find the expression

$$d_q(\beta_i; -\beta_i) = d_q(\beta_i; \beta_i) + \delta\, d_q(\beta_i)\, \sin\beta_i \quad \text{for } q = \perp\perp, \perp\parallel, \parallel\perp, \parallel\parallel\, , \tag{3-17}$$

where

$$\delta d_q(\beta_i) = -\frac{e^{-i\pi/4}}{2(2\pi)^{1/2}} k \int_L d\ell' \exp\left\{-ik\cos\beta_i\, \hat{\underline{e}}_r^s \cdot \underline{\rho}'\right\} \delta W'_q \tag{3-18}$$

and

$$\left.\begin{array}{l} \delta W_{\perp j} = 2(\underline{e}_{}^s \cdot \underline{n})\, \hat{K}_{m\ell j} \\[2mm] \delta W_{\parallel j} = 2(\underline{e}_{\perp}^s \cdot \underline{n})\, Z_o\, \hat{K}_{e\ell j} \end{array}\right\} j = \perp, \parallel \qquad . \tag{3-19}$$

Here we have omitted those arguments of $\underline{d}$ which are not pertinent.

We see from (3-17) that, for β_i sufficiently small, the elements of the diffraction coefficient for scattering into the back cone can be approximated by the elements of the two-dimensional diffraction coefficient.

3.1.5 THE PERFECT CONDUCTOR CASE

The true infinite cylinder currents on a perfect conductor satisfy (2-38) to (2-41). We then readily find from (2-31) and (2-33) that, for a perfect conductor,

$$W_{\perp\perp}(k; \beta_l, \phi_l; \beta_s, \phi_s; l) = W_{\perp\perp}^{*}(k \cos \beta_l; \phi_l; \phi_s; l) \cos \beta_l \quad , \tag{3-20}$$

$$W_{\perp\parallel}(k; \beta_l, \phi_l; \beta_s, \phi_s; l) = 0, \tag{3-21}$$

$$W_{\parallel\perp}(k; \beta_l, \phi_l; \beta_s, \phi_s; l) = -\Big[\sin \beta_s \cos \beta_l (\underline{e}_\perp^s \cdot \underline{n})$$

$$+ \cos \beta_s \sin \beta_l \frac{1}{ik \cos \beta_l} \frac{\partial}{\partial l}\Big] Z_o \hat{K}_{e l \perp}(k \cos \beta_l; 0, \phi_l; l), \tag{3-22}$$

$$W_{\parallel\parallel}(k; \beta_l, \phi_l; \beta_s, \phi_s; l) = W_{\parallel\parallel}^{*}(k \cos \beta_l; \phi_l; l) \cos \beta_s \quad , \tag{3-23}$$

and

$$\overline{W}_q = W_q \quad , \qquad q = \perp\perp, \perp\parallel, \parallel\parallel \quad , \tag{3-24}$$

$$\overline{W}_{\parallel\perp}(k; \beta_l, \phi_l; \beta_s, \phi_s; l) = \overline{W}_{\parallel\perp}^{*}(k \cos \beta_l; \phi_l; l) \, h(\beta_l, \beta_s) \tag{3-25}$$

where

$$W_{\perp\perp}^{*}(k; \phi_l, \phi_s; l) = (\underline{\hat{e}}_r^s \cdot \underline{n}) \, Z_o \hat{K}_{e l \perp}(k; 0, \phi_l; l), \tag{3-26}$$

$$W_{\parallel\parallel}^{*}(k; \phi_l; l) = Z_o \hat{K}_{e t \parallel}(k; 0, \phi_l; l) \quad , \tag{3-27}$$

$$\overline{W}_{\parallel\perp}^{*}(k; \phi_l; l) = \frac{1}{ik} \frac{\partial}{\partial l} \Big[Z_o \hat{K}_{e l \perp}(k; 0, \phi_l; l) \Big] \quad , \tag{3-28}$$

and

$$h(\beta_l, \beta_s) = \tan \beta_s \cos \beta_l - \tan \beta_l \cos \beta_s = \frac{1 + \sin \beta_s \sin \beta_l}{\cos \beta_s \cos \beta_l} (\sin \beta_s - \sin \beta_l)$$

$$= 2 \frac{1 + \sin \beta_s \sin \beta_l}{\cos \beta_s \cos \beta_l} \cos \tfrac{1}{2}(\beta_s + \beta_l) \sin \tfrac{1}{2}(\beta_s - \beta_l) \quad . \tag{3-29}$$

By using (3-20), (3-21), (3-23), and (3-25) in (2-32), we can readily verify the important identities

$$d_q (k; \beta_l, \varphi_l; \pm \beta_s, \phi_s) = d_q (k \cos \beta_l; 0, \varphi_l; \beta_s^*, \phi_s) , \quad q = \perp\perp, \|\| ; \quad (3\text{-}30)$$

$$d_{\perp\|} (k; \beta_l, \phi_l; \beta_s, \phi_s) = 0 \quad (3\text{-}31)$$

$$d_{\|\perp} (k; \beta_l, \phi_l; \beta_s, \phi_s) = d_{\|\perp}{}^* (k \cos \beta_l; \phi_l; \beta_s^*, \phi_s) \quad h(\beta_l, \beta_s) . \quad (3\text{-}32)$$

Here

$$d_{\|\perp}{}^* (k; \phi_l; \beta_s, \phi_s) =$$

$$-\frac{e^{-i\pi/4}}{2(2\pi)^{1/2}} k \int_L dl' \exp\left\{ -i k \cos \beta_s \, \hat{\underline{e}}_r^s \cdot \underline{\rho}' \right\} \overline{W}_{\|\perp}{}^* (k; \phi_l; l') \quad (3\text{-}33)$$

and β_s^* is defined by

$$\cos \beta_s^* = \frac{\cos \beta_s}{\cos \beta_l} \quad (3\text{-}34)$$

It is clear from the right-hand side of (3-34) that we have to let $\cos \beta_s^*$ take all positive values from 0 to ∞, and this means we must allow imaginary values of β_s^*. We can let β_s^* range either through all positive imaginary values or through all negative imaginary values. It does not matter which branch we choose, since β_s^* enters into the expressions for the d_q only in the form of single-valued functions of $\cos \beta_s^*$.

The most important information contained in (3-30) to (3-32) is that $d_{\perp\|}$ vanishes; that $d_{\perp\perp}$ and $d_{\|\|}$ can be expressed as functions of the four variables $k \cos \beta_l$, $\cos \beta_s^*$, ϕ_l, and ϕ_s instead of the five variables k, β_l, β_s, ϕ_l and φ_s, a fact which can be used to greatly simplify the computation of a diffraction coefficient; and that $d_{\|\perp}$ can be expressed as a function of four variables times a standard geometrical factor.

When $\beta_s = \beta_l$, (3-30) to (3-33) reduce to (2-48) to (2-50).

For scattering into the back cone, we have

$$d_q (k; \beta_l, \phi_l; -\beta_l, \phi_s) = d_q (k \cos \beta_l; 0, \phi_l; 0, \phi_s), \quad q = \perp\perp, \parallel\parallel \quad ; \qquad (3\text{-}35)$$

$$d_{\perp\parallel} (k; \beta_l, \phi_l; -\beta_l, \phi_s) = 0 \quad ; \qquad (3\text{-}36)$$

$$d_{\parallel\perp} (k; \beta_l, \phi_l; -\beta_l, \phi_s) = -2 \, d_{\parallel\perp}^* (k \cos \beta_l; \phi_l; 0, \phi_s) \sin \beta_l . \qquad (3\text{-}37)$$

These formulas tell us that <u>the diagonal elements of $\underline{d}$ for scattering into the back cone are the diagonal elements of the two-dimensional diffraction coefficient.</u> Thus, in the perfect conductor case, there is a very close relationship between three-dimensional backscattering problems and two-dimensional problems.

We have been working thus far with the <u>true</u> infinite cylinder currents on a perfect conductor and the resulting $\underline{d}$. Now let us consider approximations and contributions to the current.

Following the plan of Section 2.1.6, we will consider only approximations and contributions which satisfy (2-38), (2-39) and (2-41), but we will not require that the approximations and contributions satisfy (2-40). These approximations and contributions will then clearly satisfy the equations

(3-20), (3-21), (3-23), and (3-24) for the W_q and $\bar{W}_q$, the equations (3-30) and (3-31) for the d_q, the equations (2-48) and (2-49) for the d_q when $\beta_s = \beta_l$, and the equations (3-35) and (3-36) for the d_q when $\beta_s = -\beta_l$. On the other hand, the contributions and approximations may not satisfy (3-22), (3-25), (3-32), (2-50), and (3-37) for $W_{\parallel\perp}$, $\bar{W}_{\parallel\perp}$, and $d_{\parallel\perp}$.

In place of (3-22) and (3-25), we have the expressions

$$W_{\parallel\perp}(k; \beta_l, \phi_l; \beta_s, \phi_s; l)$$

$$= Z_o \hat{K}_{et\perp}(k; \beta_l, \phi_l; l)\cos\beta_s - (\underline{e}_\perp^s \cdot \underline{u}) \, Z_o \hat{K}_{ell}(k\cos\beta_l; 0, \phi_l; l) \sin\beta_s\cos\beta_l \quad (3\text{-}38)$$

and

$$\overline{W}_{\parallel\perp}(k; \beta_l; \phi_l; \beta_s, \phi_s; l)$$

$$= 2\overline{W}_{\parallel\perp}^{*}(k\cos\beta_l; \phi_l; l) \, \frac{1+\sin\beta_s\sin\beta_l}{\cos\beta_s} \cos\frac{1}{2}(\beta_s+\beta_l)\sin\frac{1}{2}(\beta_s-\beta_l)$$

$$+ \overline{W}_{\parallel\perp}^{**}(k; \beta_l, \phi_l; l) \, \cos\beta_s \quad , \quad\quad\quad (3\text{-}39)$$

With

$$\overline{W}_{\parallel\perp}^{**}(k; \beta_l, \phi_l; l)$$

$$= Z_o \hat{K}_{et\perp}(k; \beta_l, \phi_l; l) + \frac{1}{ik\cos\beta_l} \, \frac{\partial}{\partial l} \, Z_o \hat{K}_{ell}(k\cos\beta_l; 0, \phi_l; l)\sin\beta_l . \quad (3\text{-}40)$$

Note that $\overline{W}_{\parallel\perp}^{**}$ is an odd function of β_l,

$$\overline{W}_{\parallel\perp}^{**}(k; -\beta_l, \phi_l; l) = - \overline{W}_{\parallel\perp}^{**}(k; \beta_l, \phi_l; l) \, . \quad\quad (3\text{-}41)$$

It is readily seen that (3-38) and (3-39) reduce to (2-52) and (2-53) respectively when $\beta_s = \beta_l$.

The equation which replaces (3-32) is

$$d_{\parallel\perp}(k; \beta_l, \phi_l; \beta_s, \phi_s) = 2 \, d_{\parallel\perp}^{*}(k\cos\beta_l; \phi_l; \beta_s^{*}, \phi_s) \, \frac{1+\sin\beta_s\sin\beta_l}{\cos\beta_s\cos\beta_l} \cos\frac{1}{2}(\beta_s+\beta_l)\sin\frac{1}{2}(\beta_s-\beta_l)$$

$$+ d_{\parallel\perp}^{**}(k; \beta_l, \phi_l; \beta_s, \phi_s) \, , \quad\quad\quad\quad (3\text{-}42)$$

with $d_{\parallel\perp}^{*}$ defined by (3-33) and

$$d_{\parallel\perp}^{**}(k;\beta_l,\phi_l;\beta_s,\phi_s)$$

$$= - \frac{e^{-i\pi/4}}{2(2\pi)^{1/2}} \, k \cos\beta_s \int_L d\ell' \exp\{-i k \cos\beta_s \, \hat{\underline{e}}_r^{\,s} \cdot \underline{\rho}'\} \overline{W}_{\parallel\perp}^{**}(k;\beta_l,\phi_l;\ell') \, . \qquad (3\text{-}43)$$

Note that $d_{\parallel\perp}^{**}$ is an even function of β_s and an odd function of β_l,

$$d_{\parallel\perp}^{**}(k;\beta_l,\phi_l;-\beta_s,\phi_s)$$

$$= - d_{\parallel\perp}^{**}(k;-\beta_l,\phi_l;\pm\beta_s,\phi_s) = d_{\parallel\perp}^{**}(k;\beta_l,\phi_l;\beta_s,\phi_s). \qquad (3\text{-}44)$$

Though $d_{\parallel\perp}^{**}$ is in general a function of five variables, it can be quite simple to evaluate in practice. For example, in calculating the fringe wave ILEDC $\underline{d}^{U}$, the integration over ℓ' indicated in (3-43) becomes trivial because W_{i}^{**U} is an impulse function at the edge.

For $\beta_s = \beta_l$, (3-42) reduces to

$$d_{\parallel\perp}(k;\beta_l,\phi_l;\beta_l,\phi_s) = d_{\parallel\perp}^{**}(k;\beta_l,\phi_l;\beta_l,\phi_s) \, , \qquad (3\text{-}45)$$

and for $\beta_s = -\beta_l$, we have

$$d_{\parallel\perp}(k;\beta_l,\phi_l;-\beta_l,\phi_s) = - 2 d_{\parallel\perp}^{*}(k \cos\beta_l;\phi_l;0,\phi_s) \sin\beta_l$$

$$+ d_{\parallel\perp}^{**}(k;\beta_l,\phi_l;\beta_l,\phi_s) \, . \qquad (3\text{-}46)$$

If we consider the physical optics contribution to the surface current, we find that the corresponding $d_{\parallel\perp}$ vanishes for backscatter. This result, which is a special case of the general observation that physical optics backscatter is not depolarized, can be obtained by using the physical optics surface currents in calculating $d_{\parallel\perp}^*$ and $d_{\parallel\perp}^{**}$ and then applying (3-46).

3.2 THE EDGE DIFFRACTION COEFFICIENT FOR A PERFECT CONDUCTOR

3.2.1 THE GENERAL CASE

Let us now return to the problem of Section 2.2 and Figure 3, scattering from a perfectly conducting wedge whose two faces are infinite half-planes. We will concentrate here on the Ufimtsev ILEDC $\underline{\underline{d}}^U$, which describes the contribution to the scattered field produced by the fringe wave current. We have discussed in Section I how $\underline{\underline{d}}^U$ is used in solving scattering problems and we shall give an example in Section IV.

From Section 3.1.5, we see that $d_{\perp\parallel}^U$ vanishes. Thus we can express the incremental length $\underline{\underline{d}}^U$ in terms of three elements $d_\perp^U$, $d_\parallel^U$, and d_χ^U by means of (2-96), an expression we originally wrote down for the two-dimensional diffraction coefficient. Furthermore, we can use (2-99) to express $d_\perp^U$ and $d_\parallel^U$ each as the sum of a + contribution from S_+ and a − contribution from S_-, and we can use (3-42) to express d_χ^U in terms of d_χ^* and d_χ^{**}. We thus find that $\underline{\underline{d}}^U$ can be written in the form

$$\underline{\underline{d}}^U = (d_{\perp +}^U + d_{\perp -}^U)\, \underline{e}_\perp^s\, \underline{e}_\perp^i + (d_{\parallel +}^U + d_{\parallel -}^U)\, \underline{e}_\parallel^s\, \underline{e}_\parallel^i$$
$$+ \left[2\, d_\chi^* \, \frac{1 + \sin\beta_s \sin\beta_i}{\cos\beta_s \cos\beta_i} \, \cos\tfrac{1}{2}(\beta_s + \beta_i)\sin\tfrac{1}{2}(\beta_s + \beta_i) + d_\chi^{**} \right] \underline{e}_\parallel^s\, \underline{e}_\perp^i. \quad (3\text{-}46A)$$

Let us now evaluate the six scalar d which appear in (3-46A). In order to express these quantities in a convenient and compact form, we introduce two pairs of

68

parameters, (V_+, ψ_+) and (V_-, ψ_-), which are defined in terms of the geometry of the problem by

$$V_+ = \frac{\cos\beta_s}{\cos\beta_l} \cos\left[(\pi+\alpha) - \phi_s\right] = -\cos\beta_s^* \cos(\phi_s - \alpha), \quad \psi_+ = \phi_l - \alpha ; \qquad (3-47)$$

$$V_- = \frac{\cos\beta_s}{\cos\beta_l} \cos\left[(\pi-\alpha) - \phi_s\right] = -\cos\beta_s^* \cos(\phi_s + \alpha), \quad \psi_- = 2\pi - \alpha - \phi_l . \qquad (3-48)$$

Since $\cos\beta_s^*$ can take all positive values from 0 to ∞, V_+ and V_- will both take all real values from $-\infty$ to $+\infty$. If we consider only values of ϕ_l outside the wedge, that is, $\alpha \leq \phi_l \leq (2\pi - \alpha)$, then the range of both ψ_+ and ψ_- will be

$$2(\pi - \alpha) \geq \psi_\pm \geq 0 \qquad . \qquad (3-49)$$

We also define parameters v_+, v_-, such that

$$v = \cos^{-1} V \quad , \qquad (3-50)$$

with the branch of $\cos^{-1} V$ so chosen that

$$\left.\begin{array}{l} v = \zeta , \pi \geq \zeta \geq 0 \;\; ; \;\; V = \cos\zeta \text{ for } |V| \leq 1 \\[4pt] v = iw, \;\; w > 0 \;\; ; \;\; V = \cosh w \text{ for } V > 1 \\[4pt] v = \pi - iu, \;\; u > 0 \;\; ; \;\; V = -\cosh u \text{ for } V < -1 \end{array}\right\} \;\; ; \qquad (3-51)$$

here we have suppressed the subscripts $+$ and $-$ on v, V, ζ, w and u.

We now define functions f and g such that

$$f(V, \psi) = \frac{e^{-i\pi/4}}{(2\pi)^{1/2}} \int_0^\infty dx \; \exp\{iVx\} \widetilde{v}_B(x, \psi) \quad , \tag{3-52}$$

$$g(V, \psi) = -\frac{e^{-i\pi/4}}{(2\pi)^{1/2}} \int_0^\infty dx \; \exp\{iVx\} \frac{1}{ix} \widetilde{v}'_B(x, \psi) , \tag{3-53}$$

Here $\widetilde{v}_B$ is the complex conjugate of the function v_B which Pauli uses in Reference 9 to describe the fringe wave current (Pauli's paper, published in 1938, does not, of course, use the term "fringe wave current.")
and

$$\widetilde{v}'_B = \partial \widetilde{v}_B(x, \psi) / \partial \psi \quad . \tag{3-54}$$

We also define

$$\left.\begin{aligned}
f_+ &= f(V_+, \psi_+) \quad , \quad f_- = f(V_-, \psi_-) \\[2em]
g_+ &= g(V_+, \psi_+) \quad , \quad g_- = g(V_-, \psi_-)
\end{aligned}\right\} . \tag{3-55}$$

Starting from the general results of Section 3.1.5, we can show in a straightforward manner that the d_q^U are related to $f_\pm$ and $g_\pm$ by

$$d_{\perp+}^U = f_+ \sin\left[(\pi + \alpha) - \phi_s\right] = f_+ \sin(\phi_s - \alpha), \tag{3-56}$$

$$d_{\perp-}^U = -f_- \sin\left[(\pi - \alpha) - \phi_s\right] = -f_- \sin(\phi_s + \alpha), \tag{3-57}$$

$$d_{\parallel+}^U = g_+ \frac{\cos\beta_s}{\cos\beta_i} = g_+ \cos\beta_s^* \quad , \tag{3-58}$$

$$d_{\parallel-}^U = g_- \frac{\cos\beta_s}{\cos\beta_i} = g_- \cos\beta_s^* \quad , \tag{3-59}$$

and that

$$d_X^* = d_{||\perp}^* (k \cos\beta_1; \phi_1; \beta_s^*, \phi_s) = \left\{ f_+ \cos\left[(\pi+\alpha)-\phi_s\right] - f_- \cos\left[(\pi-\alpha)-\phi_s\right]\right\} \cos\beta_s^*$$

$$= -\left[f_+ \cos(\phi_s - \alpha) - f_- \cos(\phi_s + \alpha)\right] \cos\beta_s^* \quad , \tag{3-60}$$

$$d_X^{**} = d_{||\perp}^{**}(k;\beta_1, \phi_1; \beta_s, \phi_s) = -\frac{e^{i\pi/4}}{(2\pi)^{1/2}} \left[U_+(\phi_1) - U_-(\phi_1)\right] \cos\beta_s \tan\beta_1. \tag{3-61}$$

Here the arguments $(k; \beta_1, \phi_1; \beta_s, \phi_s)$ are to be understood on the d^U in (3-56) to (3-59). The range of ϕ_s in (3-56) and (3-58) is

$$(2\pi+\alpha) \geq \phi_s \geq \alpha \quad , \tag{3-62}$$

and the range in (3-57) and (3-59) is

$$(2\pi-\alpha) \geq \phi_s \geq -\alpha \quad . \tag{3-63}$$

It now remains to evaluate f and g in closed form. The evaluation for

$$-1 < V \leq 1 \tag{3-64}$$

can be carried out by matching (3-56) to (3-59) against the formulas of Section II for the case $\beta_s = \beta_1$. In this manner we obtain

$$f(V, \psi) = \frac{e^{i\pi/4}}{(2\pi)^{1/2}} \quad \frac{1}{\sin \nu} \left[\frac{\nu \sin \nu v}{\cos \nu v - \cos \nu \psi} - U(\pi - \psi)\frac{\sin v}{\cos v - \cos \psi}\right] \tag{3-65}$$

and

$$g(V, \psi) = -\frac{e^{i\pi/4}}{(2\pi)^{1/2}} \left[\frac{\nu \sin \nu \psi}{\cos \nu v - \cos \nu \psi} - U(\pi-\psi) \frac{\sin \psi}{\cos v - \cos \psi}\right] , \tag{3-66}$$

where ν is defined in terms of the wedge half-angle a by (2-58), and U is a step function defined by

$$U(\theta) = 1 \quad \text{for } \pi \ge \theta > 0$$

$$\left. \begin{array}{l} \text{undefined for} \quad \theta = 0 \\[4pt] = 0 \text{ otherwise} \end{array} \right\} \qquad . \tag{3-67}$$

It is useful to note that U is related to U_+ and U_- of (2-102) and (2-103) by

$$U(\pi - \psi_+) = U_+(\phi_1) \qquad , \tag{3-68}$$

$$U(\pi - \psi_-) = U_-(\phi_1) \qquad . \tag{3-69}$$

The apparent singularity of f at $v = 0$ and the apparent singularities of f and g at $v = \psi$ are removable. Specifically, we have

$$f(1,\psi) = \frac{e^{i\pi/4}}{2(2\pi)^{1/2}} \left[\frac{\nu^2}{\sin^2 \frac{\nu}{2}\psi} - U(\pi - \psi) \frac{1}{\sin^2 \frac{1}{2}\psi} \right] \quad \text{for } \psi \ne 0, \pi \quad , \tag{3-70}$$

$$f(\cos \psi, \psi) = - \frac{e^{i\pi/4}}{2(2\pi)^{1/2}} \frac{\nu \cot \nu\psi - \cot \psi}{\sin \psi} \quad \text{for } \pi > \psi > 0, \tag{3-71}$$

$$f(1,0) = - \frac{e^{i\pi/4}}{6(2\pi)^{1/2}} (1 - \nu^2) \quad ; \tag{3-72}$$

and

$$g(\cos \psi, \psi) = - \frac{e^{i\pi/4}}{2(2\pi)^{1/2}} \frac{\nu \cot \nu\psi - \cot \psi}{\nu} \quad \text{for } \pi > \psi > 0, \tag{3-73}$$

$$g(1,0) = 0. \tag{3-74}$$

Furthermore, we see that f is discontinuous in ψ at $\psi = \pi$ and goes to infinity as $V \to -1$ for arbitrary ψ. On the other hand, g is continuous in V and ψ for $|V| < 1$ and goes to infinity only for the case $(V, \psi) \to (-1, \pi)$.

It has been established that f and g have no singularities for $|V| > 1$, but f and g have not yet been evaluated rigorously for this range of V . Preliminary results indicate that (3-65) and (3-66), with v defined by (3-50) and (3-51), are probably still valid for $|V| > 1$. In terms of the variables w and u of (3-51), we would then have

$$f(V, \psi) = \frac{e^{i\pi/4}}{(2\pi)^{1/2}} \frac{1}{\sinh w} \left[\frac{\nu \sinh \nu w}{\cosh \nu w - \cos \nu \psi} - U(\pi - \psi) \frac{\sinh w}{\cosh w - \cos \psi} \right] \quad , \quad (3\text{-}75)$$

$$g(V, \psi) = - \frac{e^{i\pi/4}}{(2\pi)^{1/2}} \left[\frac{\nu \sin \nu \psi}{\cosh \nu w - \cos \nu \psi} - U(\pi - \psi) \frac{\sin \psi}{\cosh w - \cos \psi} \right] \quad , \quad (3\text{-}76)$$

for $\bar{V} > 1$, and

$$f(V, \psi) = \frac{e^{i\pi/4}}{(2\pi)^{1/2}} \frac{1}{\sinh u} \left[\frac{\nu (\sin \nu \pi \cosh \nu u - i \cos \nu \pi \sinh \nu u)}{(\cos \nu \pi \cosh \nu u + i \sin \nu \pi \sinh \nu u) - \cos \nu \psi} \right.$$
$$\left. + U(\pi - \psi) \frac{\sinh u}{\cosh u + \cos \psi} \right] \quad , \quad (3\text{-}77)$$

$$g(V, \psi) = - \frac{e^{i\pi/4}}{(2\pi)^{1/2}} \left[\frac{\nu \sin \nu \psi}{(\cos \nu \pi \cos \nu u + i \sin \nu \pi \sinh \nu u) - \cos \nu \psi} \right.$$
$$\left. + U(\pi - \psi) \frac{\sin \psi}{\cosh u + \cos \psi} \right], \quad (3\text{-}78)$$

for $V < -1$.

Let us now turn our attention from the functions f and g to the diffraction coefficients. We find that both $d_{\parallel+}^{U}$ and $d_{\parallel-}^{U}$ will be infinite for

$$\beta_i = \pm \frac{\pi}{2} \quad , \quad (3\text{-}79)$$

that is, for an incident wave which grazes the edge. This is to be expected, since our simple model of the scattering mechanism is not adequate for this case. Also, $d_{\parallel+}^{U}$ is singular when

$$\phi_i = \pi + \alpha \quad , \quad \cos(\phi_s - \alpha)\cos\beta_s = \cos\beta_i \quad , \quad (3\text{-}80)$$

73

and $d_{\parallel -}{}^U$ is singular when

$$\phi_i = \pi - \alpha \, , \quad \cos(\phi_s + \alpha) \cos \beta_s = \cos \beta_i \quad . \tag{3-81}$$

What (3-80) tells us is that, for grazing incidence at obliquity angle β_i and scattering at any obliquity angle β_s such that

$$|\beta_s| \leq |\beta_i| \quad , \tag{3-82}$$

there exist two values of the scattering azimuth angle ϕ_s, one in the range

$$(\tfrac{\pi}{2} + \alpha) > \phi_s \geq \alpha \quad , \tag{3-83}$$

the other in the range

$$(2\pi + \alpha) \geq \phi_s > (\tfrac{3\pi}{2} + \alpha) \quad , \tag{3-84}$$

for which $d_{\parallel +}{}^U$ is infinite. When $\beta_s = \pm \beta_i$, the two critical values of ϕ_s are α and $(2\pi + \alpha)$, which is consistent with the results observed in Section 2.2.4. Again, a more sophisticated model of the scattering mechanism is necessary in order to handle the critical cases. The interpretation of (3-81) is completely analogous to that of (3-80).

The coefficient $d_{\perp +}{}^U$ is singular whenever

$$\cos(\phi_s - \alpha) \cos \beta_s = \cos \beta_i \quad \text{with} \quad |\beta_s| = |\beta_i| \quad , \tag{3-85}$$

and when

$$\phi_i = \pi + \alpha \, , \quad \phi_s = \begin{cases} \alpha \\ 2\pi + \alpha \end{cases}, \quad \beta_s = \pm \beta_i \quad . \tag{3-86}$$

In the case of (3-85), the singularity is caused by the $\sin v$ term in (3-65) going to zero, an effect which is cancelled by the $\sin(\phi_s - \alpha)$ term in (3-56) when $|\beta_s| = |\beta_i|$. In the case of (3-86), we have a higher order of singularity because

74

$$\sin v = 0 \ , \quad \cos \nu \, v - \cos \nu \dot{\psi} = 0, \quad \text{and} \quad \cos v - \cos \psi = 0, \tag{3-87}$$

and we find that the behavior of $d_{\perp +}{}^{U}$ is quite complicated near the singular points.

We also see that $d_{\perp +}{}^{U}$ is discontinuous for grazing incidence on S_{+},

$$\varphi_{l} = \pi + \alpha \quad , \tag{3-88}$$

except when

$$\text{(a)} \quad \varphi_{s} = \pi + \alpha \ , \tag{3-89}$$

or

$$\text{(b)} \quad \varphi_{s} = \alpha \ \text{ and } \ |\beta_{s}| \neq |\beta_{l}| \ , \tag{3-90}$$

or

$$\text{(c)} \quad \varphi_{s} = (2\pi + \alpha) \ \text{ and } \ |\beta_{s}| \neq |\beta_{l}| \quad , \tag{3-91}$$

in which cases $d_{\perp +}{}^{U} = 0$. (Even if (3-75) and (3-77) should prove incorrect, physical considerations tell us that the discontinuity exists for $|v| > 1$.)

The behavior of $d_{\perp -}{}^{U}$ is completely analogous. It is singular when

$$\cos(\varphi_{s} + \alpha) \cos \beta_{s} = \cos \beta_{l} \ \text{ with } \ |\beta_{s}| < |\beta_{l}| \tag{3-92}$$

and when

$$\varphi_{l} = \pi - \alpha, \quad \phi_{s} = \begin{cases} -\alpha \\ 2\pi - \alpha \end{cases} , \quad \beta_{s} = \pm \beta_{l} \quad . \tag{3-93}$$

It is discontinuous for grazing incidence on S_{-},

$$\phi_{l} = \pi - \alpha \tag{3-94}$$

except when

$$\tag{3-95}$$
$$\text{a)} \quad \varphi_{s} = \pi - \alpha \quad ,$$

75

<u>or</u>

b) $\phi_s = -\alpha$ and $\left|\beta_s\right| \neq \left|\beta_l\right|$, $\qquad$ (3-96)

<u>or</u>

c) $\phi_s = (2\pi - \alpha)$ and $\left|\beta_s\right| \neq \left|\beta_l\right|$. $\qquad$ (3-97)

These results are consistent with those of Section 2.2.4.

A more sophisticated model of the scattering mechanism is needed to handle singular, near-singular, and discontinuous cases.

The coefficient $d_x{}^U$ is discontinuous for grazing incidence on either S_+ or S_- unless we have both $\beta_s = \beta_l = 0$ and $\phi_s \neq -\alpha, \alpha, 2\pi - \alpha, 2\pi + \alpha$. It is singular for an incident wave which grazes the edge,

$$\beta_l = \pm \frac{\pi}{2} \quad , \qquad (3-98)$$

and whenever

$$\cos(\phi_s - \alpha) \cos \beta_s = \cos \beta_l \quad . \qquad (3-99)$$

A more sophisticated model of the scattering mechanism is needed to handle singular, near-singular, and discontinuous cases.

3.2.2 SIMPLIFICATIONS FOR A KNIFE EDGE

For a knife edge, we have

$$\alpha = 0, \quad V = V_+ = V_- = \cos \beta_s{}^* \cos(\pi - \phi_s), \quad \psi_+ = \phi_l, \quad \psi_- = 2\pi - \phi_l . \qquad (3-100)$$

and (3-56) to (3-60) thus become

$$d_\perp{}^U = 2f(V, \psi_+) \sin(\pi - \phi_s) \quad . \qquad (3-101)$$

$$d_{\perp+}{}^U = d_{\perp-}{}^U = \frac{1}{2} d_\perp{}^U \quad , \qquad (3-102)$$

$$d_\parallel{}^U = 2g(V, \psi_\pm) \cos \beta_s{}^* \quad . \qquad (3-103)$$

$$d_{\parallel+}{}^U = d_{\parallel-}{}^U = \frac{1}{2} d_\parallel{}^U \quad , \qquad (3-104)$$

$$d_X^* = -2f(V, \psi_+) \cos \phi_s \cos \beta_s^* = -d_\perp^U \cot \phi_s \cos \beta_s^* \quad . \tag{3-105}$$

In obtaining these results we have used the fact that, for a knife edge, we have

$$f(V, \psi_+) = -f(V, \psi_-), \quad g(V, \psi_+) = g(V, \psi_-). \tag{3-105A}$$

For $|V| \leq 1$, we obtain from (3-65) and (3-66) the expressions

$$f(V, \psi_\pm) = \mp \frac{e^{i\pi/4}}{4(2\pi)^{1/2}} \frac{1}{\cos \frac{1}{2}v} \frac{1}{\sin \frac{1}{2}\left|\pi - \phi_1\right| + \cos \frac{1}{2}v} \quad , \tag{3-106}$$

$$g(V, \psi_\pm) = -\frac{e^{i\pi/4}}{2(2\pi)^{1/2}} \frac{\cos \frac{1}{2}(\pi - \phi_1)}{\sin \frac{1}{2}\left|\pi - \phi_1\right| + \cos \frac{1}{2}v} \quad . \tag{3-107}$$

We can express these results in terms of V using

$$\cos \frac{1}{2}v = \left(\frac{1+V}{2}\right)^{1/2} \tag{3-108}$$

If we assume the validity of (3-65) and (3-66) for $|V| > 1$, we find that (3-106) and (3-107) still hold, with $\cos \frac{1}{2}v$ given by (3-108) for $V > 1$ and

$$\cos \frac{1}{2}v = i \left(\frac{|V|-1}{2}\right)^{1/2} \quad \text{for} \quad V < -1 \quad . \tag{3-109}$$

3.2.3 SCATTERING INTO THE FORWARD AND BACK CONES

For scattering into the forward cone, $\beta_s = \beta_1$, the incremental length edge diffraction coefficient reduces to the two-dimensional diffraction coefficient which has already been discussed at length in Section 2.2.

For scattering into the back cone, $\beta_s = -\beta_1$, we have, from (3-35), (3-45), (3-46), and (3-60),

77

$$\underline{\underline{d}}^U(k;\beta_l,\phi_l;-\beta_l,\phi_s) = d_\perp^U(k;\beta_l,\phi_l;\beta_l,\phi_s)\,\underline{e}_\perp^s\,\underline{e}_\perp^l + d_\parallel^U(k;\beta_l,\phi_l;\beta_l,\phi_s)\,\underline{e}_\parallel^s\,\underline{e}_\parallel^l$$

$$+ d_x^U(k,\beta_l,\phi_l;-\beta_l,\phi_s)\,\underline{e}_\parallel^s\,\underline{e}_\perp^l \qquad , \tag{3-110}$$

with

$$d_x^U(k,\beta_l,\phi_l;-\beta_l,\phi_s) = d_x^U(k,\beta_l,\phi_l;\beta_l,\phi_s) - 2\,d_x^*(\phi_l,\phi_s)\sin\beta_l, \tag{3-111}$$

$$d_x^*(\phi_l,\phi_s) = -\,f(\cos v_+,\ \psi_+)\cos(\phi_s-\alpha) + f(\cos v_-,\ \psi_-)\cos(\phi_s+\alpha), \tag{3-112}$$

and

$$v_\pm = \left|(\pi\pm\alpha)-\phi_s\right| \quad . \tag{3-113}$$

The unit vectors $\underline{e}_\perp^l$, $\underline{e}_\parallel^l$, $\underline{e}_\perp^s$ are the same as for scattering into the forward cone. Thus we see that the dyadic form of the incremental length edge diffraction coefficient for scattering into the back cone differs from the result for scattering into the forward cone only in the definition of $\underline{e}_\parallel^s$ and in the presence of the d_x^* term.

It should be noted that $d_\perp^U(k;\beta_l,\phi_l;\beta_l,\phi_s)$ and

$d_\parallel^U(k;\beta_l,\phi_l;\beta_l,\phi_s)$ are actually independent of k, that $d_x^U(k;\beta_l,\phi_l;\beta_l,\phi_s)$

is in actuality a function only of β_l and ϕ_l, and that $d_x^U(k;\beta_l,\phi_l;-\beta_l,\phi_s)$

is in actuality a function only of β_l, ϕ_l, and ϕ_s. The full complement of arguments has been used to stress the similarity of the two-dimensional results and the three-dimensional back cone results.

It should also be noted that, as we can see from (3-56) and (3-57), the $f(\cos v_\pm,\ \psi_\pm)$ of (3-112) can be expressed in terms of the values for $\beta_s=\beta_l$ of $d_{\perp+}^U$ and $d_{\perp-}^U$. Thus d_x^* can be expressed in terms of these two functions. We then see from (3-110) and (3-111) that $\underline{d}^U$ for scattering into the back cone can be constructed from the <u>Two-Dimensional</u> Diffraction Coefficients $d_{\perp+}^U$, $d_{\perp-}^U$, $d_\parallel^U$, and d_x^U.

78

For scattering from a knife edge, (3-112) becomes

$$d_X^* (\phi_i, \phi_s) = \frac{e^{i\pi/4}}{(2\pi)^{1/2}} \frac{\cos \frac{1}{2} \phi_s}{\cos \frac{1}{2}\phi_i \pm \sin \frac{1}{2} \phi_s} \cot \phi_s \qquad (3\text{-}114)$$

with the + sign for $\phi_i < \pi$ and the – sign for $\phi_i > \pi$.

3.2.4 BACKSCATTER

For backscatter, we have

$$\phi_i = \phi_s = \phi, \ \beta_i = -\beta_s = \beta \quad , \qquad (3\text{-}115)$$

which is a special case of scattering into the back cone. It is convenient to
define unit vectors $\underline{e}_r$, $\underline{e}_\perp$, and $\underline{e}_{\parallel}$ such that

$$\underline{e}_r^s = \underline{e}_r^i = \underline{e}_r, \quad \underline{e}_\perp^s = -\underline{e}_\perp^i = \underline{e}_\perp \quad , \quad \underline{e}_\parallel^s = \underline{e}_\parallel^i = \underline{e}_\parallel \quad . \qquad (3\text{-}116)$$

we can then express $\underline{\underline{d}}^U$ in the form

$$\underline{\underline{d}}^U = - d_\perp^U \underline{e}_\perp \underline{e}_\perp + d_\parallel^U \underline{e}_\parallel \underline{e}_\parallel - d_X^U \underline{e}_\parallel \underline{e}_\perp \qquad (3\text{-}117)$$

with

$$d_\perp^U = - \frac{e^{i\pi/4}}{2(2\pi)^{1/2}} \left\{ \frac{2\nu}{\sin \nu \pi} \left[\frac{1}{1 + \tan \nu \frac{\pi}{2} \tan \nu (2\pi - \phi)} + \frac{1}{1 + \tan \nu \frac{\pi}{2} \tan \nu\phi} \right] \right. \qquad (3\text{-}118a)$$

$$\left. - U_+ \tan (\phi - a) + U_- \tan (\phi + a) \right\}$$

$$= \frac{e^{i\pi/4}}{(2\pi)^{1/2}} \left\{ \nu \sin \nu \pi \left[- \frac{1}{1 - \cos \nu \pi} + \frac{1}{\cos \nu \pi + \cos 2\nu (\pi - \phi)} \right] \right.$$

$$\left. + \frac{1}{2} \left| U_+ \tan (\phi - a) - U_- \tan (\phi + a) \right| \right\} \quad . \qquad (3\text{-}118b)$$

$$d_{\parallel}^{U} = - \frac{e^{i\pi/4}}{2(2\pi)^{1/2}} \left[\frac{\nu}{\sin\nu\pi} \; \frac{4}{1 - \tan^2\nu\frac{\pi}{2}\tan^2\nu(\pi-\phi)} + U_+ \tan(\phi-\alpha) - U_- \tan(\phi+\alpha) \right]$$

$$\tag{3-119a}$$

$$= \frac{e^{i\pi/4}}{(2\pi)^{1/2}} \left\{ \nu \sin\nu\pi \left[- \frac{1}{1-\cos\nu\pi} - \frac{1}{\cos\nu\pi + \cos 2\nu(\pi-\phi)} \right] \right.$$

$$\left. - \frac{1}{2} \left[U_+ \tan(\phi-\alpha) - U_- \tan(\phi+\alpha) \right] \right\} \quad , \tag{3-119b}$$

$$d_{X}^{U} = - \frac{e^{i\pi/4}}{(2\pi)^{1/2}} \; \frac{2\nu}{\sin\nu\pi} \left[\frac{\cot(\phi-\alpha)}{1 - \tan\nu\frac{\pi}{2}\cot\nu(\pi+\alpha-\phi)} \right.$$

$$\left. + \frac{\cot(\phi+\alpha)}{1 + \tan\nu\frac{\pi}{2}\cot\nu(\pi-\alpha-\phi)} \right] \sin\beta \quad . \tag{3-120}$$

For a knife edge (3-117) still holds, with $d_{\perp}^{U}$ now given by (2-161), $d_{\parallel}^{U}$ by (2-163), and d_{X}^{U} by

$$d_{X}^{U} = - \frac{e^{i\pi/4}}{(2\pi)^{1/2}} \cot\frac{\phi}{2} \sin\beta \quad . \tag{3-121}$$

To verify (3-118) and (3-119) and to justify the use of (2-161) and (2-163), we first observe from (3-110) that $d_{\perp}^{U}$ and $d_{\parallel}^{U}$ are the same as for two-dimensional generalized backscatter, which has been treated in Section 2.2.6. We then obtain (3-118a) from (2-153) and (2-154); (3-119a) from (2-155); and (3-118b) and (3-119b) from (2-97), (2-156), and (2-158). To verify (3-120), we start with (3-111), use (2-118) to evaluate $d_{X}^{U}(\beta_i, \beta_i)$ and (3-112) to evaluate d_X^*, and note that (3-112) simplifies for backscatter to

$$d_{X}^{*}(\phi, \phi) = - \left[d_{\perp+}^{U}(k;\beta,\phi;\beta,\phi) \cot(\phi-\alpha) + d_{\perp-}^{U}(k;\beta,\phi;\beta,\phi) \cot(\phi+\alpha) \right] \tag{3-122}$$

with the $d_{\perp\pm}^{U}$ given by (2-153) and (2-154). To verify (3-121), we just substitute the knife edge value $\nu = \frac{1}{2}$ into (3-120) and use standard trigonometric identities.

IV SCATTERING FROM A PERFECTLY CONDUCTING
POLYGONAL PLATE

4.1 GENERAL FORMULAS

Let us now develop formulas for far-field scattering from an N-sided perfectly conducting polygonal plate which is illuminated by the incident plane wave of (2-3). A typical plate geometry is shown in Figure 6. To avoid a phase factor which has no essential bearing on the problem, we assume that the origin of coordinates lies in the plane of the plate. Following Section V of Reference 11 we make the following definitions:

S indicates both the illuminated side of the plate and the area of the plate;

$\underline{n}$ is the unit normal out of the illuminated side;

P_n, for $n = 0$ to N, is the nth corner of the plate, with n increasing in the counterclockwise direction as seen from the $+\underline{n}$ halfspace and with

$$P_N = P_0; \tag{4-1}$$

$\tilde{\underline{r}}_n$ is the position vector to P_n and is normal to $\underline{n}$;

α_n is the angle of the corner at P_n;

C_n indicates both the edge running from P_{n-1} to P_n and the length of the edge, and

$$C_0 = C_N; \tag{4-2}$$

$\underline{l}_n$ is the unit tangent to C_n, directed from P_{n-1} to P_n;

$\tilde{\underline{r}}_{Cn}$ is the center of C_n, so that

$$\bar{\underline{r}}_{Cn} = \frac{1}{2}(\bar{\underline{r}}_{n-1} + \bar{\underline{r}}_n) = \bar{\underline{r}}_{n-1} + \frac{1}{2}C_n\underline{l}_n = \bar{\underline{r}}_n - \frac{1}{2}C_n\underline{l}_n; \tag{4-3}$$

$\underline{e}$ is the unit vector along the projection of the sum vector $(\underline{e}_r^s + \underline{e}_r^i)$ (which bisects the bistatic angle) onto the plane of S, so that

$$\underline{e} = \frac{1}{2\tau}\left[\underline{n} \times (\underline{e}_r^s + \underline{e}_r^i)\right] \times \underline{n}, \tag{4-4}$$

where the parameter τ is given by
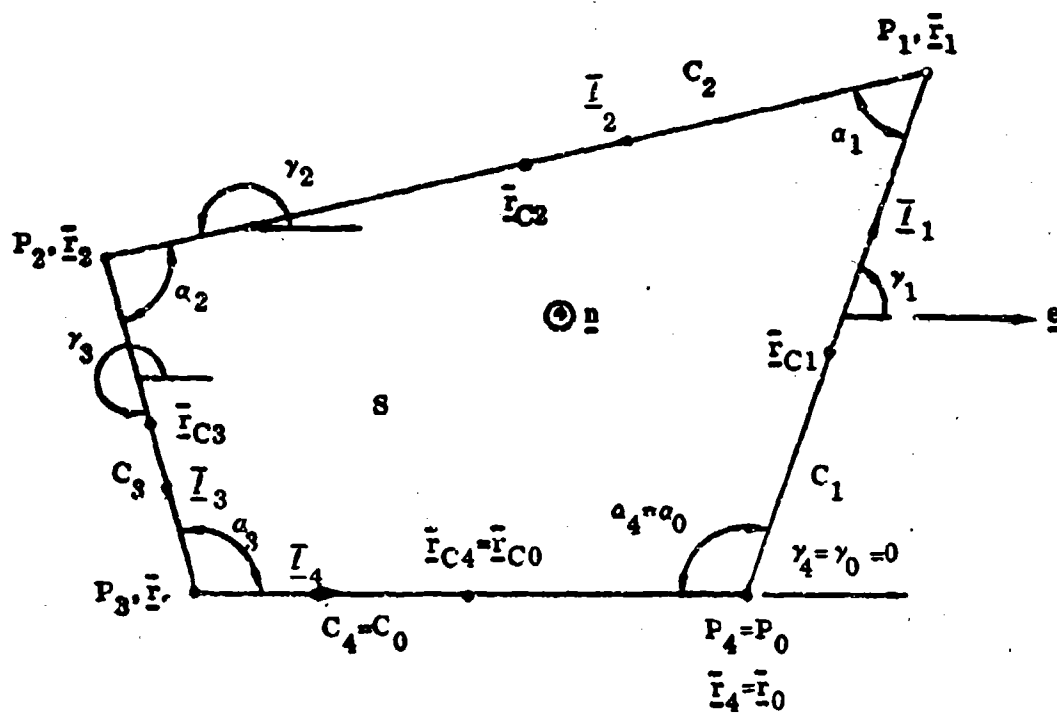
FIGURE 6   POLYGONAL PLATE

$$\tau = \frac{1}{2} |\underline{n} \times (\underline{e}_r^s + \underline{e}_r^l)| \qquad (4\text{-}5)$$

and lies in the range

$$1 \geq \tau \geq 0 ; \qquad (4\text{-}6)$$

γ_n is the angle measured counterclockwise from $\underline{e}$ to $\overline{I}_n$, so that

$$\cos \gamma_n = \underline{e} \cdot \overline{I}_n, \quad \sin \gamma_n = \underline{n} \cdot (\underline{e} \times \overline{I}_n) ; \qquad (4\text{-}7)$$

$\underline{Y}_n$ is a parameter proportional to the phase difference between far-field returns from the two ends of C_n and is given by

$$\overline{Y}_n = \tau k C_n \cos \gamma_n. \qquad (4\text{-}8)$$

We note that $\tau = 0$ for forward scattering and for all cases in which $\underline{n}$ bisects the bistatic angle, including backscatter at normal incidence. The quantities $\underline{e}$ and γ_n are not defined for $\tau = 0$ but this fact does not lead to any difficulties.

If we consider the edge C_n to be a segment of an infinitely long edge, then we can define values of β_l, β_s, ϕ_s, and ϕ_l on C_n. Indeed, we readily find that

$$\sin \beta_{ln} = \underline{e}_r^l \cdot \overline{I}_n, \quad \sin \beta_{sn} = - \underline{e}_r^s \cdot \overline{I}_n \qquad (4\text{-}9)$$

with β_{ln} and β_{sn} in the range $-\pi/2$ to $\pi/2$, that

$$\cos \phi_{ln} = \frac{1}{\cos \beta_{ln}} \underline{e}_r^l \cdot (\underline{n} \times \overline{I}_n) \qquad (4\text{-}10)$$

with

$$\pi > \phi_{ln} > 0 \qquad (4\text{-}11)$$

because we have specified that $\underline{n}$ points out of the illuminated side, and that

$$\cos \phi_{sn} = \frac{1}{\cos \beta_{sn}} \underline{e}_r^s \cdot (\underline{n} \times \underline{l}_n) \text{ with } \begin{cases} \pi > \phi_{sn} > 0 \text{ for } \underline{e}_r^s \cdot \underline{n} > 0 \\ 2\pi > \phi_{sn} > \pi \text{ for } \underline{e}_r^s \cdot \underline{n} < 0 \end{cases} . \quad (4\text{-}11\text{A})$$

Furthermore, we can define unit polarization vectors $\underline{e}_{\perp n}^i$, $\underline{e}_{\parallel n}^i$, $\underline{e}_{\perp n}^s$, and $\underline{e}_{\parallel n}^s$ by using (2-5), (2-14), and (2-15) with $\underline{t}$ replaced by $\underline{l}_n$.

If we neglect edge interactions and also neglect distortion of the fringe wave currents near the corners, then the field scattered from the plate can be represented as the sum of the physical optics scattering from S plus the integral around the edge of the Ufimtsev ILEDC with proper phase weighting. We can express the radiation vector $\underline{F}$ in the form

$$\underline{F} = E_0 \frac{1}{k} \underline{\underline{D}} \cdot \underline{p} , \quad (4\text{-}12)$$

where the three-dimensional diffraction coefficient $\underline{\underline{D}}$ is the sum

$$\underline{\underline{D}} = \underline{\underline{D}}^{PO} + \underline{\underline{D}}^U \quad (4\text{-}13)$$

of a physical optics coefficient and a fringe-wave coefficient. If we introduce the notation

$$\sigma = \sigma (\underline{q}, \underline{p}; \underline{e}_r^s, \underline{e}_r^i; k) , \quad (4\text{-}14)$$

with $\underline{q}$ a real unit vector, to designate the radar cross-section (RCS) seen by a linearly polarized antenna which is sensitive to the component of $\underline{E}^{scat}$ parallel to $\underline{q}$, then we have

$$\sigma = \frac{4\pi}{k^2} \left| \underline{q} \cdot \underline{\underline{D}} \cdot \underline{p} \right|^2 . \quad (4\text{-}15)$$

Thus the problem of determining the RCS reduces to the problem of determining $\underline{\underline{D}}$ or, equivalently, determining both $\underline{\underline{D}}^{PO}$ and $\underline{\underline{D}}^U$.

* * *

The fringe-wave coefficient $\underline{\underline{D}}^U$ can be represented either as the sum of N edge contributions or as the sum of N corner contributions. To obtain the edge

84

contribution form, we use (3-10) and observe that $\bar{r}_o$ corresponds to $\bar{r}_{Cn}$,

T corresponds to C_n, and X corresponds to $|\bar{Y}_n|$ because

$$2\,\tau\cos\gamma_n = 2\,\tau\,\underline{e}\cdot\bar{I}_n = (\underline{e}_r^i + \underline{e}_r^s)\cdot\bar{I}_n = \sin\beta_{in} - \sin\beta_{sn}. \qquad (4\text{-}16)$$

We thus obtain

$$\underline{\underline{D}}^U = \frac{e^{-i\pi/4}}{(2\pi)^{1/2}}\,k\,\sum_{n=0}^{N-1}\exp\left\{-2i\,\tau\,k\underline{e}\cdot\bar{r}_{Cn}\right\}C_n\,\frac{\sin\gamma_n}{\gamma_n}\underline{\underline{d}}_n^U, \qquad (4\text{-}17)$$

where $\underline{\underline{d}}_n^U$ is the knife edge Ufimtsev ILEDC for C_n. From (2-96) we see that $\underline{\underline{d}}_n^U$ has the three-element form

$$\underline{\underline{d}}_n^U = d_{\perp n}^U\,\underline{e}_{\perp n}^s\,\underline{e}_{\perp n}^i + d_{xn}^U\,\underline{e}_{\|n}^s\,\underline{e}_{\perp n}^i + d_{\|n}^U\,\underline{e}_{\|n}^s\,\underline{e}_{\|n}^i \qquad (4\text{-}18)$$

where $d_{\perp n}^U$, d_{xn}^U, and $d_{\|n}^U$ are functions of k, β_{in}, ϕ_{in}, β_{sn}, and ϕ_{sn}
which can be found using the material of Section 3.2.2 to 3.2.4. The individual terms
in the sum (4-17) remain finite as $\tau \to 0$.

In computing the data of Section 4.2, $\underline{\underline{D}}^U$ was calculated using (4-17).

By rearranging the terms of (4-17), we obtain an expression for $\underline{\underline{D}}^U$
as the sum of N corner contributions,

$$\underline{\underline{D}}^U = \sum_{n=0}^{N-1}\exp\left\{-2i\,\tau\,k\underline{e}\cdot\bar{r}_n\right\}\underline{\underline{c}}_n^U, \qquad (4\text{-}19)$$

where the flat plate corner diffraction coefficient $\underline{\underline{c}}_n^U$ is given by

$$\underline{\underline{c}}_n^U = -\,\frac{e^{i\pi/4}}{2(2\pi)^{1/2}\,\tau}\left(\frac{1}{\cos\gamma_{n+1}}\,\underline{\underline{d}}_{n+1}^U - \frac{1}{\cos\gamma_n}\,\underline{\underline{d}}_n^U\right). \qquad (4\text{-}20)$$

The representation (4-19) corresponds to a physical interpretation of the fringe
wave scattering in terms of rays diffracted from the corners of the plate.
Note that the diffraction from a corner does not depend on the lengths of the edges
which meet there.

The representation (4-19) is valid if and only if the condition

$$(\underline{e}_r^{\,s} + \underline{e}_r^{\,l}) \cdot \overline{l}_n \neq 0 \text{ for all } n \tag{4-21}$$

is satisfied. This condition excludes all cases in which one or more edges are normal to the bisector $(\underline{e}_r^{\,s} + \underline{e}_r^{\,l})$ of the bistatic angle and thus also normal to $\underline{e}$. It also excludes the case of forward scattering, for which

$$\underline{e}_r^{\,s} + \underline{e}_r^{\,l} = 0. \tag{4-22}$$

The condition (4-21) is necessary because two or more of the $\underline{c}_n^{\,U}$ are infinite when (4-21) does not hold. A correct result can be obtained, however, by taking the limit as the left-hand side of (4-21) approaches zero.

$$* \quad * \quad *$$

The physical optics coefficient $\underline{\underline{D}}^{PO}$ has been studied in Section V of Reference 11. Like $\underline{\underline{D}}^{U}$, it can be represented either as the sum of N edge contributions or as the sum of N corner contributions. The edge contribution form is

$$\underline{\underline{D}}^{PO} = \frac{e^{-i\pi/4}}{(2\pi)^{1/2}} \, k \left[\sum_{n=0}^{N-1} \exp\left\{-2i\tau k\underline{e} \cdot \overline{r}_{Cn}\right\} C_n \frac{\sin \overline{\gamma}_n}{\overline{\gamma}_n} \, d_n^{PO} \right] \underline{\underline{J}}_0, \tag{4-23}$$

where

$$d_n^{PO} = \frac{e^{i\pi/4}}{2(2\pi)^{1/2}\tau} \, \sin \gamma_n, \tag{4-24}$$

$$\underline{\underline{J}}_0 = -\underline{e}_r^{\,s} \times \left\{ \underline{e}_r^{\,s} \times \left[\underline{n} \times (\underline{e}_r^{\,l} \times \underline{\underline{l}}) \right] \right\}, \tag{4-25}$$

and $\underline{\underline{l}}$ is the unit dyadic. The corner contribution form is

$$\underline{\underline{D}}^{PO} = \left[\sum_{n=0}^{N-1} \exp\left\{-2i\tau k\underline{e} \cdot \overline{r}_n\right\} c_n^{PO} \right] \underline{\underline{J}}_0, \tag{4-26}$$

where c_n^{PO} is related to the d_n^{PO} in the same way that $\underline{c}_n^{\,U}$ is related to the $\underline{\underline{d}}_n^{\,U}$ in (4-20), that is

$$c_n^{PO} = -\frac{e^{i\pi/4}}{2(2\pi)^{1/2}\tau} \left(\frac{1}{\cos\gamma_{n+1}} d_{n+1}^{PO} - \frac{1}{\cos\gamma_n} d_n^{PO} \right). \tag{4-26A}$$

Upon substituting from (4-24) into (4-26A), we obtain the much simpler expression

$$c_n^{PO} = - \frac{1}{8\pi\tau^2} (\tan \gamma_{n+1} - \tan \gamma_n). \tag{4-27}$$

The edge contribution form (4-23) is valid for all cases in which $\tau \neq 0$ and approaches the correct limit

$$\underline{\underline{D}}^{PO} = - \frac{1}{2\pi} k^2 \ S \ \underline{\underline{J}}_0 \tag{4-28}$$

as $\tau \to 0$. The corner contribution form (4-26), like the corner contribution form (4-19) for $\underline{\underline{D}}^U$, is valid if and only if (4-21) holds, and a limiting process will yield the correct result when (4-21) does not hold.

In computing the data of Section 4.2, $\underline{\underline{D}}^{PO}$ was calculated using (4-23) except at normal incidence.

$$* \quad * \quad *$$

If we combine the fringe wave and physical optics contributions, we obtain the edge contribution form

$$\underline{\underline{D}} = \frac{e^{-i\pi/4}}{(2\pi)^{1/2}} k \sum_{n=0}^{N-1} \exp\left\{-2i\tau k \, \underline{e} \cdot \underline{\overline{r}}_{Cn}\right\} C_n \frac{\sin \overline{\gamma}_n}{\overline{\gamma}_n} \ \underline{\underline{d}}_n \tag{4-29}$$

with

$$\underline{\underline{d}}_n = \underline{\underline{d}}_n^U + d_n^{PO} \ \underline{\underline{J}}_0, \tag{4-30}$$

which is valid when $\tau \neq 0$, and the corner contribution form

$$\underline{\underline{D}} = \sum_{n=0}^{N-1} \exp\left\{-2i\tau k \, \underline{e} \cdot \underline{\overline{r}}_n\right\} \underline{\underline{c}}_n \tag{4-31}$$

with

$$\underline{\underline{c}}_n = - \frac{e^{i\pi/4}}{2(2\pi)^{1/2}\tau} \left(\frac{1}{\cos \gamma_{n+1}} \ \underline{\underline{d}}_{n+1} - \frac{1}{\cos \gamma_n} \ \underline{\underline{d}}_n\right) \tag{4-32a}$$

$$= \underline{\underline{c}}_n^U + c_n^{PO} \ \underline{\underline{J}}_0, \tag{4-32b}$$

which is valid when (4-21) holds.

The physical meaning of (4-31) is that, to the order of approximation we are using here, the total scattering from the plate can be represented in terms of rays diffracted from the corners of the plate, with the diffraction from a corner independent of the lengths of the edges which meet there. This statement would still be true if we were to take into account the distortion of the fringe wave currents near the corners but is no longer true when we take into account edge interactions.

*   *   *

It should be noted that the method of Ryan and Peters (Reference 10) can be applied to the polygonal plate problem and leads to a result which can be written in the form (4-29), but with a different expression for $\underline{\underline{d}}_n$. It can be shown that the Ryan-Peters method gives accurate results in many cases for which standard Geometrical Theory of Diffraction is not satisfactory but that there is a much larger class of problems which can be solved accurately by using the value of $\underline{\underline{d}}_n$ developed in this report.

For scattering bodies other than polygonal plates, a similar observation can be made as to the relative ranges of usefulness of standard GTD, the Ryan-Peters method, and the form of PTD used in this report.

4.2 TYPICAL RESULTS

Figures 7 to 11 compare calculated and experimental values of radar cross-section for diamond-shaped and trapezoidal plates. The calculations were made as described in Section 4.1. All data are for backscatter, $\underline{e}_r^s = \underline{e}_r^i = \underline{e}_r$, with receiver polarization the same as incident polarization, $\underline{q} = \underline{p}$. The orientation of $\underline{e}_r$ is given by the angle α, measured in a plane normal to the plate and including the axis marked Z in the figures. For $\alpha = -90°$, the incident wave is traveling in the +Z

88

f ≈ 10 GHz
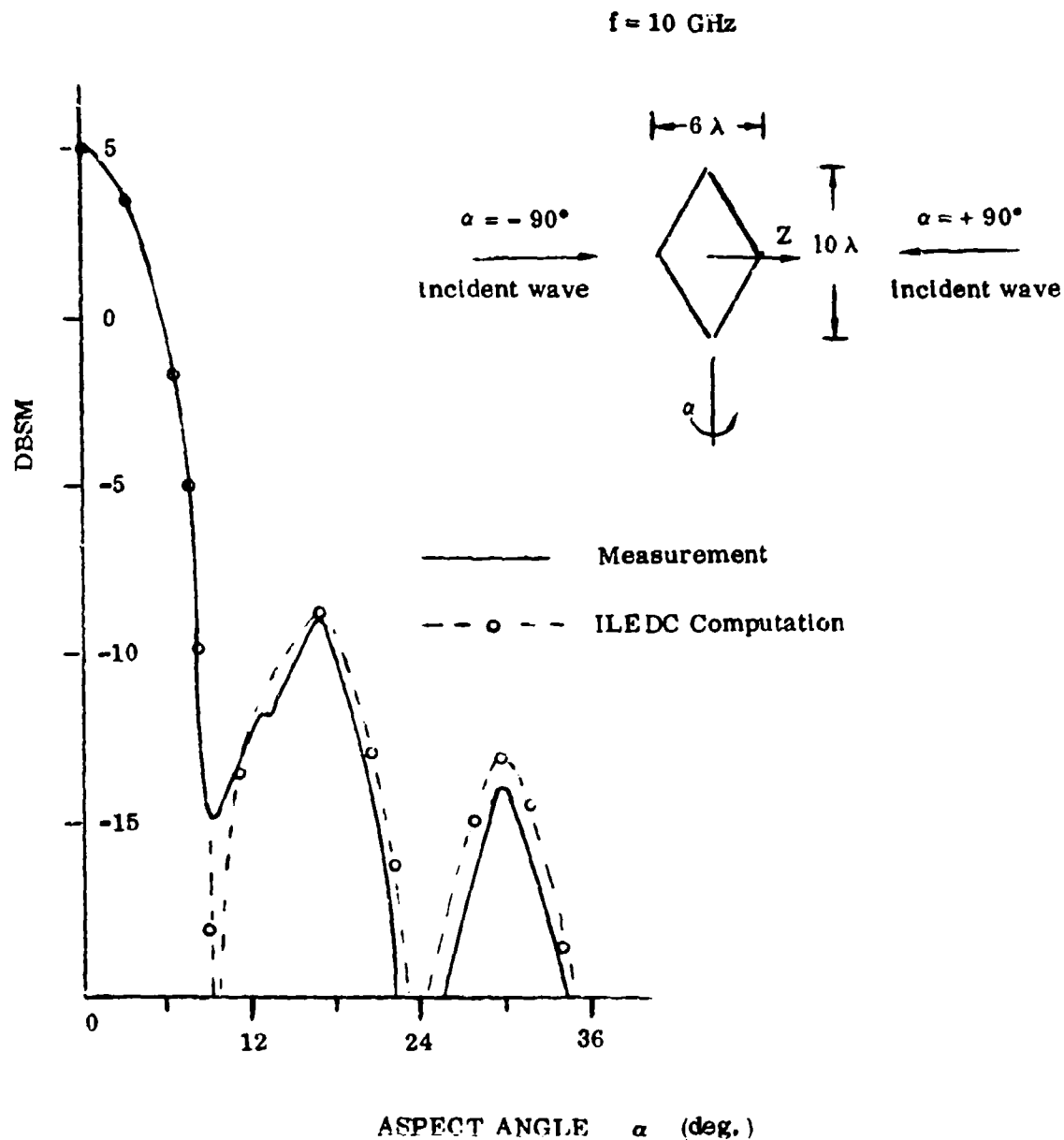
FIGURE 7   RCS OF DIAMOND SHAPED PLATE IN PLANE NORMAL
TO 10 λ DIAGONAL,   VV POLARIZATION

$f = 10$ GHz

$\alpha = -90°$

Incident wave

10λ

Z

6λ

$\alpha = +90°$

Incident wave

α

Measurement

- - o - - ILEDC Computation

DBSM

10

0

-10

-20

-30

0
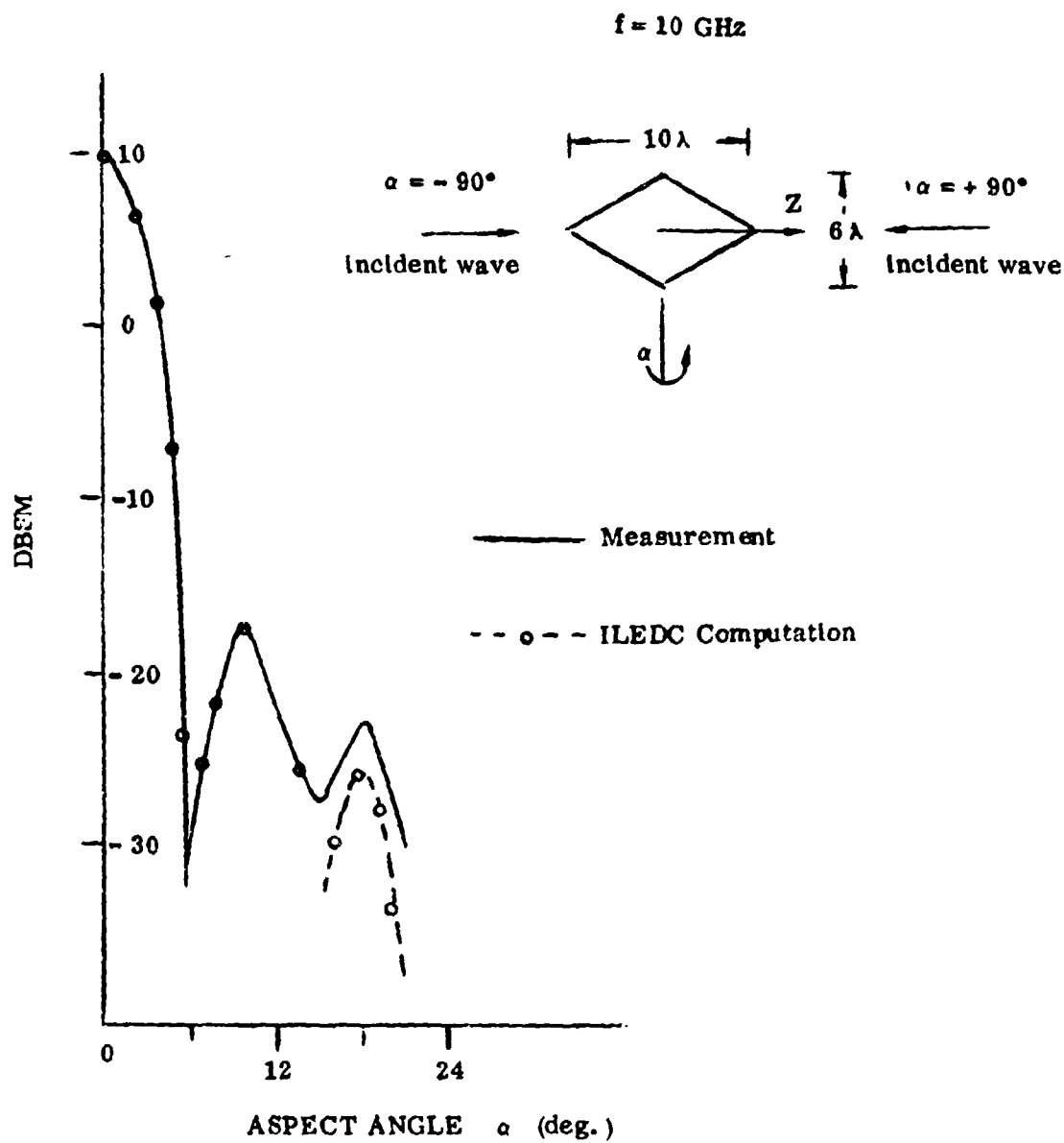
12

24

ASPECT ANGLE α (deg.)

FIGURE 8   RCS OF DIAMOND SHAPED PLATE IN PLANE NORMAL
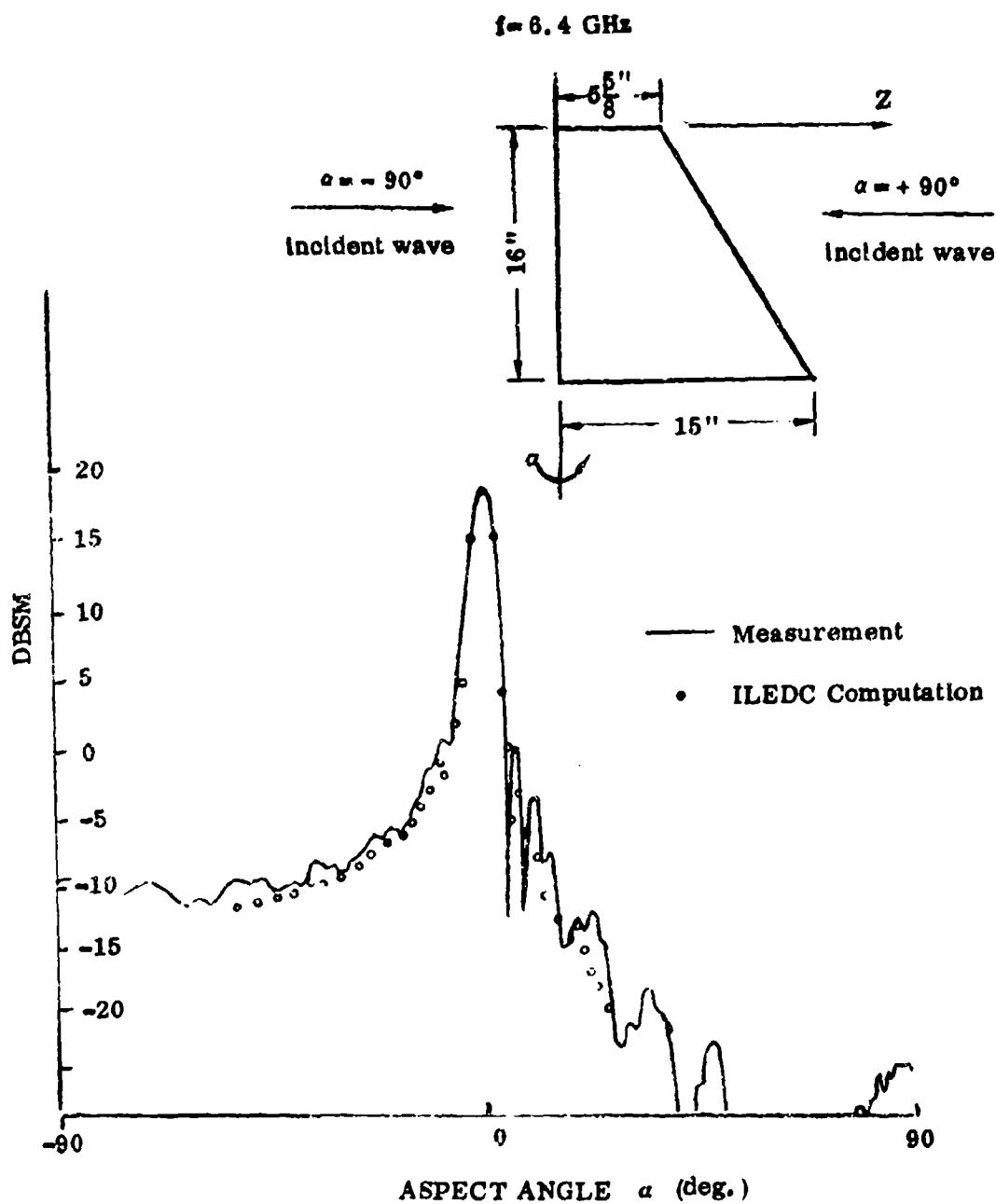TO 6 λ DIAGONAL, HH POLARIZATION

FIGURE 9   RCS OF TRAPEZOIDAL PLATE IN PLANE NORMAL
TO 16" SIDE, VV POLARIZATION
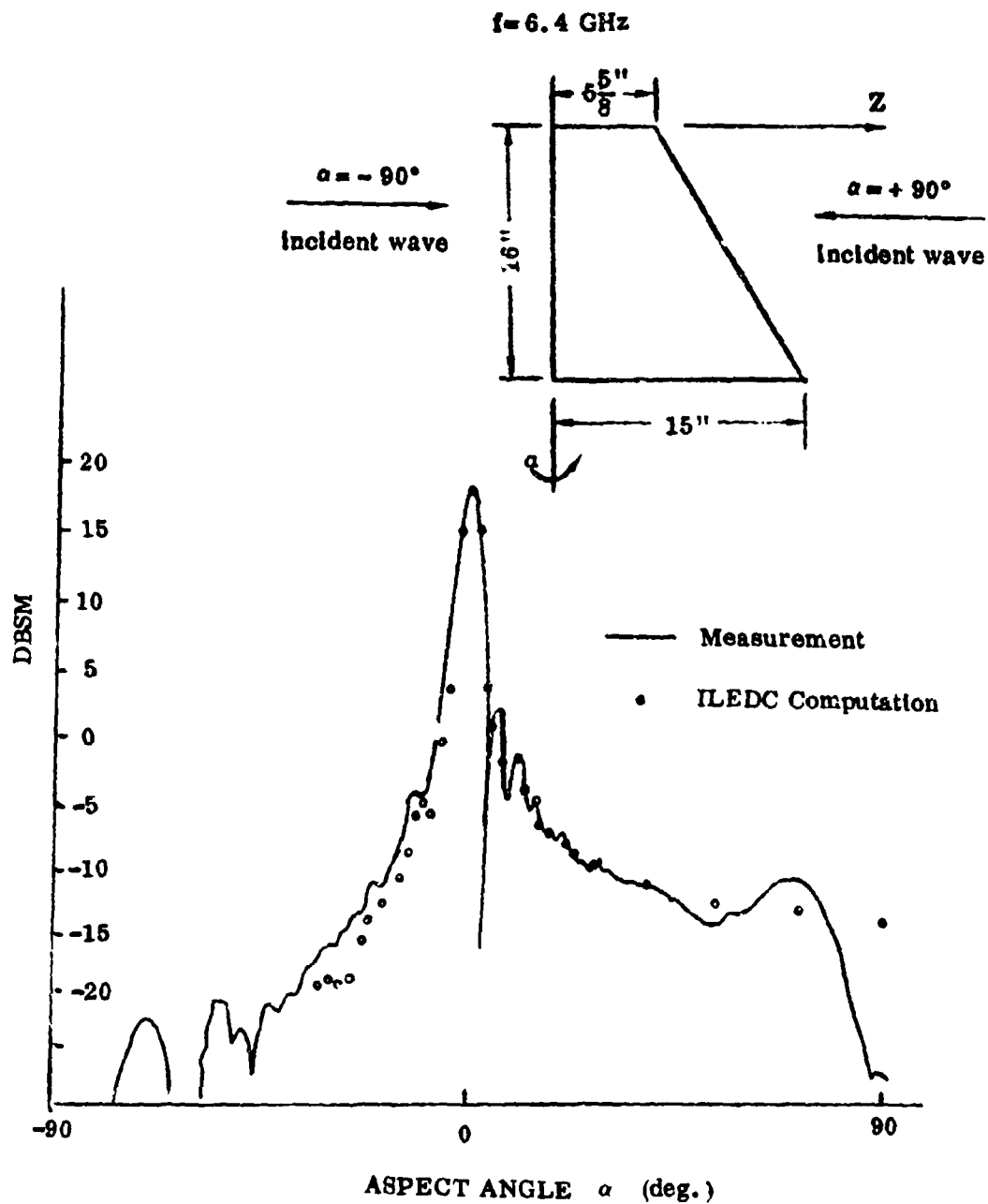
FIGURE 10 RCS OF TRAPEZOIDAL PLATE IN PLANE NORMAL TO 16" SIDE, HH POLARIZATION

92
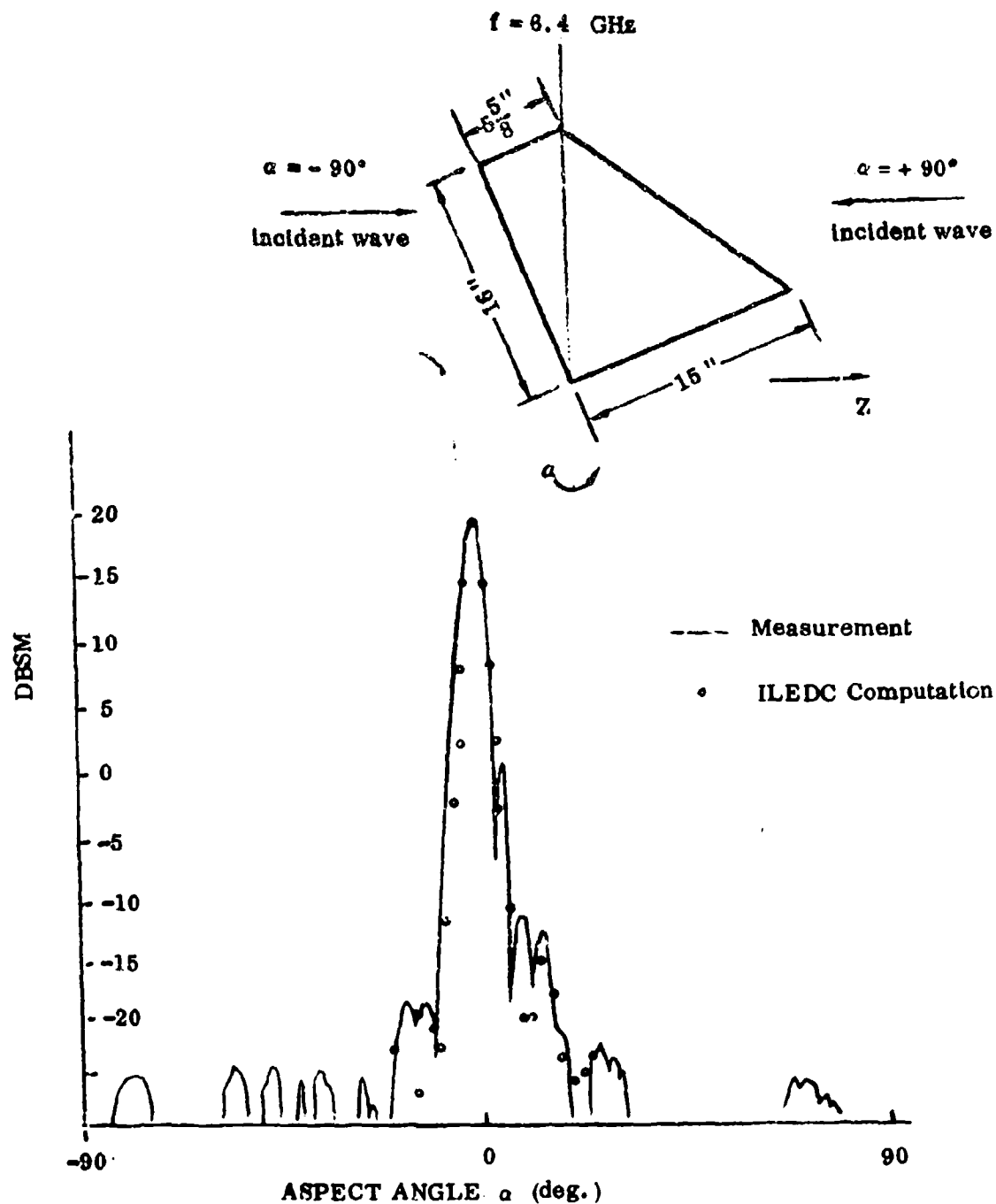
FIGURE 11   RCS OF TRAPEZOIDAL PLATE IN PLANE NORMAL TO
SHORT DIAGONAL,   HH POLARIZATION

direction and $\underline{e}_r$ thus points in the $-Z$ direction. For $\alpha = 0°$, the wave is incident normal to the plate and, for $\alpha = 90°$, it is travelling in the $-Z$ direction. Vertical polarization V corresponds to $\underline{p}$ and thus $\underline{E}_0$ normal to the Z- axis, and horizontal polarization corresponds to $\underline{H}_0$ normal to the Z- axis. Data are given for $\alpha = 0°$ to $90°$ for the diamond plate case, $\alpha = -90°$ to $+90°$ for the trapezoidal plate.

Experimental data were normalized so that they agree with calculated results at normal incidence, $\alpha = 0°$. These experimental data were obtained by sweeping α through $360°$, which gives a pattern which should in principle repeat four times for the diamond plate case, twice for the trapezoidal plate case. The plotted data are for one non-repeating part of the experimental pattern, with no attempt to average out those variations which were observed between parts. Examination of these variations indicates that main lobe data are quite reliable, the positions and peak values of the first few sidelobes are fairly reliable, and hardly any of the data on nulls are reliable.

In light of these shortcomings in the experimental data, plus the fact that even the first sidelobes are so many dB down from the peak value of σ, the agreement between calculated and experimental data is quite good. The divergences which arise as we approach grazing incidence in the problems of Figure 9 and Figure 10 can probably be removed by taking into account edge interactions and corner current distortions.

V. SUMMARY AND CONCLUSIONS

In Section I, we have given an overview of the Physical Theory of Diffraction (PTD) and the role which the Incremental Length Diffraction Coefficient (ILDC) in general and the Ufimtsev Incremental Length Edge Diffraction Coefficient in particular play in the theory. The actual formulas for expressing far-field scattering in terms of ILDC's are given in Sections 3.1.1 and 3.1.2. General formulas for the ILDC as a function of the effective surface currents are summarized in Sections 3.1.3 to 3.1.5, with these sections drawing heavily on material presented earlier in Sections 2.1.3 to 2.1.6. The Ufimtsev ILEDC $\underline{d}^U$ is developed in Section 3.2. Then PTD and the Ufimtsev ILEDC are used in Section IV to solve the problem of far-field scattering of a plane wave from a perfectly conducting polygonal plate. The data in Section 4.2 show how well problems can be solved by PTD with use of the Ufimtsev ILEDC, even when edge interactions and current distortion near the corners are neglected.

These neglected effects can be accounted for within the framework of PTD, and the results thus obtained will remain accurate nearer to grazing incidence. Even without such further development of PTD, a great variety of problems involving flat plates, finite cylinders, doubly curved surfaces, and bodies with flat faces can be solved satisfactorily by simply using the Ufimtsev ILEDC of Section 3.2 in conjunction with the physical optics material of References 11 and 12.

* * *

Before treating the ILEDC in Section III, we develop the simpler theory of the Two-Dimensional Diffraction Coefficient (2-D DC) in Section II. Sections 2.1.1 and 2.1.2 show how to express the far-field scattering from an infinite cylinder in terms of the 2-D DC. Sections 2.1.3 to 2.1.6 give general formulas for the 2-D DC as a function of the effective surface currents; as already noted, many of

these formulas are also used for the ILEDC. Section 2.2 gives the 2-D DC's for Ufimtsev's and Keller's approaches to scattering from a conducting wedge. The material of Section II is supplemented by a thorough study in the Appendix of scattering from an infinite cylinder. Some of the material in the Appendix can be used in extending the approach given here to the case in which source and observer are not both at infinity.

<p style="text-align:center">*   *   *</p>

A list of key equations for expressing fields in terms of diffraction coefficients and for evaluating the various edge diffraction coefficients is given at the end of Section I.

Some additional comments are appropriate on the equations for the ILEDC $\underline{d}^U$ in Section 3.2.1. Equations (3-56) to (3-60) have been verified as correct when f and g are defined by the integral expressions (3-52) and (3-53). For $-1 < V \leq 1$, it has been verified that f and g are given by (3-65) to (3-74). But further verification is still needed that (3-75) to (3-78) are correct evaluations of the integrals of (3-52) and (3-53) for the cases $V \leq -1$ and $V > 1$.

APPENDIX. SCATTERING FROM AN INFINITE CYLINDER

I.1 OBLIQUE INCIDENCE AND EXPONENTIAL VARIATION ALONG AN AXIS

Our main objective in this Appendix is to verify the material of Sections 2.1.2 to 2.1.6 for far-field scattering from an infinite cylinder when the plane wave of (2-3) is incident. We shall follow the notation of Section 2.1, as illustrated in Figure 1, with one exception: we use the symbol β in place of both β_i and β_s because, as we shall show, $\beta_i = \beta_s$ for an infinite cylinder problem.

The plane wave of (2-3) has exponential variation along the cylinder axis. To show this, we substitute (2-2) and (2-8) into (2-3), obtaining

$$\underline{E}_o = \hat{\underline{E}}_o \exp\left\{-ik_t t\right\} , \quad Z_o \underline{H}_o = Z_o \hat{\underline{H}}_o \exp\left\{-ik_t t\right\} , \tag{I-1}$$

with $\hat{\underline{E}}_o$ and $\hat{\underline{H}}_o$ independent of t and given by

$$\hat{\underline{E}}_o = E_o \underline{p} \exp\left\{-i k \cos\beta \, \hat{\underline{e}}_r^i \cdot \underline{\rho}\right\} ,$$

$$Z_o \hat{\underline{H}}_o = - E_o \underline{e}_r^i \times \underline{p} \exp\left\{- ik \cos\beta \, \hat{\underline{e}}_r^i \cdot \underline{\rho}\right\} , \tag{I-2}$$

and with the <u>axial wave number</u> k_t given by

$$k_t = k \sin\beta. \tag{I-3}$$

We are interested in scattering from an infinite cylinder, aligned with the t-axis, which either is composed of material invariant in the t-direction or is described by boundary conditions with no t-dependence. When a field with exponential t-dependence is scattered from such a cylinder, there is nothing in the scattering process which affects the t-dependence of the field. The scattered field thus has the same exponential t-dependence as the incident field. By factoring out the t-dependence, we can reduce the original three-dimensional problem to a two-dimensional problem. This is the approach we shall take here.

We begin in Section I.2, by developing important basic material: the Maxwell and Helmholtz equations and the Green's function for fields with exponential t-dependence; integral representations for the field produced in free space by current sources with exponential t-dependence; and a more general representation for far-field radiation from such sources. Then in Section I.3 we apply the material to scattering problems. Although emphasis is on verifying the material of Sections 2.1.2 to 2.1.6, there is also much useful material for the cases of source or observation point or both at finite distance from the scatterer.

I.2 FIELDS WITH EXPONENTIAL VARIATION ALONG AN AXIS

I.2.1 THE MAXWELL AND HELMHOLTZ EQUATIONS

Let us consider a homogeneous region of space, with cylindrical boundaries parallel to the t-axis. Let this region be filled with a homogeneous medium with wave number k and wave impedance Z, and let the region contain an electric current source distribution $\underline{K}_{eo}^{v}$ (amperes/m^2) and a magnetic current source distribution $\underline{K}_{mo}^{v}$ (volts/m^2) which have exponential t-dependence:

$$\underline{K}_{qo}^{v} = \hat{\underline{K}}_{qo}^{v} (\rho) \exp\left\{-i k_t t\right\} \qquad \text{for } q = e, m \quad . \tag{I-4}$$

Here the axial wave number k_t is not restricted by (I-3), but is an arbitrary complex number.

Under appropriate conditions on the behavior of the field at the boundary, the composition of adjoining regions, and the sources in these regions, the field $(\underline{E}, \underline{H})$ in the region of interest will have the same t-dependence as the $\underline{K}_{qo}^{v}$:

$$\underline{E} = \hat{\underline{E}} (\rho) \exp\left\{-i k_t t\right\} \quad , \quad \underline{H} = \hat{\underline{H}} (\rho) \exp\left\{-i k_t t\right\} \quad . \tag{I-5}$$

For such a field, Maxwell's equations

$$\nabla \times \underline{H} + \frac{ik}{Z} \underline{E} = \underline{K}_{eo}^{v} \quad , \tag{I-6}$$

$$\nabla \times \underline{E} - ikZ \underline{H} = - \underline{K}_{mo}^{v} \quad , \tag{I-7}$$

take the form

$$\nabla \times \hat{\underline{H}} - ik_t \underline{t} \times \hat{\underline{H}} + \frac{ik}{Z} \hat{\underline{E}} = \hat{\underline{K}}^v_{eo} \quad , \tag{I-8}$$

$$\nabla \times \hat{\underline{E}} - ik_t \underline{t} \times \hat{\underline{E}} - ikZ\hat{\underline{H}} = -\hat{\underline{K}}^v_{mo} \quad . \tag{I-9}$$

Now let us introduce the notation

$$\underline{f} = f_t \underline{t} + \underline{f}_\rho \tag{I-10}$$

to represent a vector $\underline{f}$ as the sum of an axial component $f_t \underline{t}$ and a transverse component $\underline{f}_\rho$. By using the identity

$$\nabla \times \underline{f}(\underline{\rho}) = -\underline{t} \, \nabla \cdot \left[\underline{t} \times \underline{f}_\rho(\underline{\rho}) \right] - \underline{t} \times \nabla f_t(\underline{\rho}), \tag{I-11}$$

we can decompose (I-8) and (I-9) to obtain

$$\nabla \hat{H}_t + ik_t \hat{\underline{H}}_\rho + \frac{ik}{Z} \underline{t} \times \hat{\underline{E}}_\rho = \underline{t} \times \hat{\underline{K}}^v_{eo\rho} \quad , \tag{I-12}$$

$$\nabla \hat{E}_t + ik_t \hat{\underline{E}}_\rho - ikZ \underline{t} \times \hat{\underline{H}}_\rho = -\underline{t} \times \hat{\underline{K}}^v_{mo\rho} \, ; \tag{I-13}$$

$$\nabla \cdot (\underline{t} \times \hat{\underline{E}}_\rho) + ikZ \hat{H}_t = \hat{K}^v_{mot} \quad , \tag{I-14}$$

$$\nabla \cdot (\underline{t} \times \hat{\underline{H}}_\rho) - \frac{ik}{Z} \hat{E}_t = -\hat{K}^v_{eot} \quad . \tag{I-15}$$

By appropriate manipulation of (I-12) and (I-13), we get

$$\nabla \hat{H}_t - \frac{\hat{k}^2}{ikZ} \underline{t} \times \hat{\underline{E}}_\rho - \frac{k_t}{kZ} \underline{t} \times \nabla \hat{E}_t - \underline{t} \times \hat{\underline{K}}^v_{eo\rho} - \frac{k_t}{k\overline{Z}} \hat{\underline{K}}^v_{mo\rho} \tag{I-16}$$

and

$$\nabla \hat{E}_t + \frac{\hat{k}^2 Z}{ik} \, \underline{t} \times \hat{\underline{H}}_\rho + \frac{k_t Z}{k} \, \underline{t} \times \nabla \hat{H}_t = -\underline{t} \times \hat{\underline{K}}^{\,v}_{mo\rho} - \frac{k_t Z}{k} \, \hat{\underline{K}}^{\,v}_{eo\rho} , \qquad (I-17)$$

where the <u>transverse wave number</u> $\hat{k}$ is related to k and k_t by

$$\hat{k}^2 = k^2 - k_t^2. \qquad (I-18)$$

The pair of equations (I-8) and (I-9), the four equations (I-12) to (I-15), and the four equations (I-14) to (I-17) are three equivalent forms of Maxwell's equations for fields with exponential t-dependence.

If now we take the divergence of (I-16) and (I-17) and make use of (I-14), (I-15), and the identity

$$\nabla \cdot \left[\, \underline{t} \times \nabla g(\underline{\rho}) \, \right] = 0, \qquad (I-19)$$

we obtain the Helmholtz equations

$$(\nabla^2 + \hat{k}^2) \, \hat{H}_t = \frac{\hat{k}^2}{ikZ} \, \hat{\underline{K}}^{\,v}_{mot} - \underline{t} \cdot \nabla \times \hat{\underline{K}}^{\,v}_{eo\rho} - \frac{k_t}{kZ} \, \nabla \cdot \hat{\underline{K}}^{\,v}_{mo\rho} \qquad (I-20)$$

and

$$(\nabla^2 + \hat{k}^2) \, \hat{E}_t = \frac{\hat{k}^2 Z}{ik} \, \hat{\underline{K}}^{\,v}_{eot} + \underline{t} \cdot \nabla \times \hat{\underline{K}}^{\,v}_{mo\rho} - \frac{k_t Z}{k} \, \nabla \cdot \hat{\underline{K}}^{\,v}_{eo\rho} . \qquad (I-21)$$

In conjunction with these equations, it is useful to express $\hat{\underline{E}}_\rho$ and $\hat{\underline{H}}_\rho$ as functions of $\hat{H}_t$ and $\hat{E}_t$ by the equations

$$\hat{\underline{E}}_\rho = \frac{1}{i\hat{k}^2} \left[k_t \nabla \hat{E}_t + kZ \, \underline{t} \times \nabla \hat{H}_t + k_t \, \underline{t} \times \hat{\underline{K}}^{\,v}_{mo\rho} + kZ \, \hat{\underline{K}}^{\,v}_{eo\rho} \right] \qquad (I-22)$$

and

$$\hat{\underline{H}}_\rho = \frac{1}{i\hat{k}^2} \left[k_t \nabla \hat{H}_t - \frac{k}{Z} \, \underline{t} \times \nabla \hat{E}_t - k_t \, \underline{t} \times \hat{\underline{K}}^{\,v}_{eo\rho} + \frac{k}{Z} \, \hat{\underline{K}}^{\,v}_{mo\rho} \right] , \qquad (I-23)$$

which are just rearrangements of (I-16) and (I-17).

Thus far, our results are valid for arbitrary values of k and k_t, and $\hat{k}$ has only appeared in the form $\hat{k}^2$. We now restrict k to be real and positive and restrict k_t to <u>not</u> be a real number with absolute value greater than or equal to k. Furthermore, we define $\hat{k}$ to be the root of $\hat{k}^2$ which has a positive real part. It is readily seen that such a root exists for all admissible values of k_t in the complex plane· pure imaginary roots

correspond to the forbidden values of k_t, which in turn, correspond to surface wave problems rather than scattering or radiation problems. We can readily confirm that

$$\hat{k}_R \hat{k}_I = -k_{tR} k_{tI} , \quad \hat{k}_R > |k_{tI}| , \qquad (I-24)$$

where subscripts R and I indicate real and imaginary parts respectively.

For k_t real and $|k_t| \sim k$, we can use the notation of (I-3) with β real and in the range $-\frac{\pi}{2} < \beta < \frac{\pi}{2}$. We then have

$$\hat{k} = k \cos \beta . \qquad (I-24A)$$

For any admissible values of k_t and $\hat{k}$, we have

$$k_t = k \sin \beta , \quad \hat{k} = k \cos \beta \qquad (I-24B)$$

for some value of β in the open strip

$$-\frac{\pi}{2} < \beta_R < \frac{\pi}{2} , \quad \beta_I \text{ arbitrary} . \qquad (I-24C)$$

The problems of ultimate interest in this Appendix are scattering problems, more specifically problems which involve scattering from an infinitely long cylinder of finite or infinite cross section into an infinite region of free space (or other homogeneous lossless material). In this type of problem it is useful to consider the total field ($\underline{E}$, $\underline{H}$) in the region outside the scattering body as the sum of an incident field ($\underline{E}_0$, $\underline{H}_0$) and a scattered field ($\underline{E}^{scat}$, $\underline{H}^{scat}$):

$$\underline{E} = \underline{E}_0 + \underline{E}^{scat} , \quad \underline{H} = \underline{H}_0 + \underline{H}^{scat} . \qquad (I-25)$$

The incident field ($\underline{E}_0$, $\underline{H}_0$) we define as the field which would be produced in free space, that is, in the absence of the scattering body, by the sources exterior to the scattering body. We include the effect of sources at infinity, such as those which give rise to plane waves (see Reference 4, Section 2.2.6).

It follows that the scattered field has no sources exterior to the scattering body. One consequence of this is that $\hat{E}_t^{scat}$ and $\hat{H}_t^{scat}$ satisfy homogeneous Helmholtz

101

equations,

$$(\nabla^2 + \hat{k}^2)\, \hat{E}_t^{scat} = 0 \ , \quad (\nabla^2 + \hat{k}^2)\, \hat{H}_t^{scat} = 0 \ , \tag{I-26}$$

in the region exterior to the scattering body. But these equations would still be valid if there were sources at infinity. To exclude such sources and to thus obtain a uniquely defined scattered field it is necessary to impose a condition on the behavior of the field at infinity, a condition which guarantees that the direction of power flow at infinity is away from the scattering body.

When the cylinder cross section is of finite maximum dimension, the appropriate condition is that both $\hat{E}_t^{scat}$ and $\hat{H}_t^{scat}$ must satisfy a two-dimensional radiation condition of the form

$$\lim_{P_o \to \infty} P_o^{1/2} \left[\frac{\partial}{\partial P_o} F(\underline{\rho}) - i\,\hat{k}\, F(\underline{\rho}) \right] = 0 \ , \tag{I-27}$$

where

$$P_o = |\underline{\rho}| \tag{I-28}$$

is distance from the origin in the transverse direction. There are also many problems involving cylinders with cross section extending to infinity--such as the wedge problem discussed in Section 2.2--in which $\hat{E}_t^{scat}$ and $\hat{H}_t^{scat}$ satisfy (I-27) for some or all directions of scattering.

The condition (I-27) tells us that the behavior of the field F for P_o large is essentially the same as the behavior of a cylindrical wave with propagation constant $\hat{k}$. It is important to realize that (I-27) is a radiation condition because we have required that $\hat{k}$ have a positive real part and that an equation of form (I-27) would not be a radiation condition if $\hat{k}_R$ were zero or negative. We shall verify in Section I.2.3 that $\hat{k}_R > 0$ does indeed characterize a radiating field, that is, a field which carries energy away from the origin.

The quantity $\hat{k}_I$ can be positive, negative, or zero. When $\hat{k}_I$ is negative, $\hat{E}_t^{scat}$ and $\hat{H}_t^{scat}$ increase exponentially with P_o for P_o sufficiently large. This behavior, strange as it appears at first look, does not violate any physical principle. The physically meaningful quantities are $\underline{E}$ and $\underline{H}$, not $\hat{\underline{E}}$ and $\hat{\underline{H}}$, and, as we shall see in Section I.2.3,

the fields $\underline{E}$ and $\underline{H}$ propagate energy at an angle to the cylinder axis and the fields do not increase in the direction of energy propagation. Waves with negative $\hat{k}_I$ are called **leaky waves**.

Since the scattered field has no sources outside the scattering body, it mus necessarily have sources within or on the surface of the scattering body. We shall show that the effective surface currents on the scattering cylinder act as the sources of the scattered field.

I.2.2 THE TWO-DIMENSIONAL GREEN'S FUNCTION

Let us now introduce the two-dimensional scalar Green's function

$$\overline{G} \ (\underline{\rho}, \ \underline{\rho}'; \hat{k}) = \overline{G} \ (\hat{k} \, P) = \frac{1}{4} \ H_0^{(1)} \ (\hat{k} \ P) \ , \tag{I-29}$$

where we are using the notation $H_n^{(1)}$ for the Hankel function of first kind and order n, and

$$P = \left| \underline{\rho} - \underline{\rho}' \right| \tag{I-30}$$

is the distance from source point $\underline{\rho}'$ to observation point $\underline{\rho}$. The function G satisfies the Helmholtz equation

$$(\nabla^2 + \hat{k}^2)\overline{G} = - \ \delta \ (\underline{\rho} - \underline{\rho}') \ , \tag{I-31}$$

where δ is the Dirac delta function for a point singularity in a two-dimensional space.

We can readily show that

$$\nabla P = -\nabla' P = \underline{\sigma} \tag{I-32}$$

and

$$\nabla \nabla P = \nabla' \nabla' P = -\nabla \nabla' \ P = -\nabla' \nabla \ P = \frac{1}{P}(\underline{I}_\rho - \underline{\sigma} \, \underline{\sigma} \ ), \tag{I-33}$$

where

$$\underline{\sigma} = (\underline{\rho} - \underline{\rho}') / \ P \tag{I-34}$$

is a unit vector pointing from $\underline{\rho}'$ to $\underline{\rho}$ and

$$\underline{\underline{I}}_\rho = \underline{e}_x \underline{e}_x + \underline{e}_y \underline{e}_y \tag{I-35}$$

acts as a unit dyadic for vectors normal to $\underline{t}$. Using (I-32) and (I-33), we obtain

$$\nabla \overline{G} = -\nabla' \ \overline{G} = -\frac{i\hat{k}}{4} H_1^{(1)} \left(\hat{k} \ P\right) \underline{\sigma} \tag{I-36}$$

and

$$\nabla \nabla \overline{G} = \nabla' \ \nabla' \ \overline{G} = -\nabla\nabla' \ \overline{G} = -\nabla'\nabla \ \overline{G} \tag{I-37}$$

$$= -\frac{i\hat{k}}{4 \ P} \left\{ H_1^{(1)} \left(\hat{k} \ P\right) \left(\underline{\underline{I}}_\rho - 2 \ \underline{\sigma} \ \underline{\sigma}\right) + \hat{k} \ P \ H_0^{(1)} \left(\hat{k} \ P\right) \ \underline{\sigma} \ \underline{\sigma} \right\} \ . \tag{I-38}$$

For
$$\hat{k}_R > 0, \ \left|\hat{k}\right| P \gg 1$$

we have the approximations

$$\overline{G} \approx \overline{G}_R = \frac{e^{i\pi/4}}{2 \ (2\pi\hat{k} \ P)^{1/2}} \ e^{i\hat{k} \ P} \ , \tag{I-39}$$

where the value of the square root with positive real part is chosen,

$$\nabla \overline{G} = -\nabla' \ \overline{G} \approx \ i \hat{k} \ \overline{G}_R \ \underline{\sigma} \quad , \tag{I-40}$$

and

$$\nabla \nabla \overline{G} = \nabla'\nabla' \ \overline{G} = -\nabla\nabla' \ \overline{G} = -\nabla'\nabla \ \overline{G} = -\hat{k}^2 \ \overline{G}_R \ \underline{\sigma} \ \underline{\sigma} \ . \tag{I-41}$$

These approximations, obtained by using the asymptotic expansion of the Hankel function, are useful in both the radiating near-field region and the far-field region as defined in the IEEE Antenna Standard (Reference 7). It can readily be shown that $\overline{G}_R$ satisfies a radiation condition of the form of (I-27).

Let us write $\underline{\rho}$ in the form

$$\underline{\rho} = P_0 \hat{\underline{e}}_r^s \quad , \tag{I-42}$$

where $P_0 = \left|\underline{\rho}\right|$ as in (I-28) and $\hat{\underline{e}}_r^s$ is thus a unit vector. (We shall show in Section I.2.3 that the $\hat{\underline{e}}_r^s$ of (I-42) is the same as the $\hat{\underline{e}}_r^s$ of (2-13).) Then, for $\hat{k}$ real and

$$\hat{k} \, \underline{P}_0 \gg 1 \quad , \quad \hat{k} \left| \underline{\rho}' \right|^2 \ll \underline{P}_0 \quad , \quad \left| \underline{\rho}' \right| \ll \underline{P}_0 \quad , \tag{I-43}$$

we have the approximations

$$\overline{G} \approx \overline{G}_\infty = \overline{G}_0 \, \exp \left\{ -i\hat{k} \, \hat{\underline{e}}_r^s \cdot \underline{\rho}' \right\} \quad , \tag{I-44}$$

$$\nabla \overline{G} = - \nabla' \, \overline{G} = i \hat{k} \, \overline{G}_\infty \, \hat{\underline{e}}_r^s \quad , \tag{I-45}$$

$$\nabla \nabla \overline{G} = \nabla' \nabla' \, \overline{G} = - \nabla \nabla' \, \overline{G} = - \nabla' \nabla \overline{G} = - \hat{k}^2 \, \overline{G}_\infty \, \hat{\underline{e}}_r^s \, \hat{\underline{e}}_r^s \quad , \tag{I-46}$$

with

$$\overline{G}_0 = \frac{e^{i\pi/4}}{2(2\pi \hat{k} \, P_0)^{1/2}} \, e^{i\hat{k} P_0} \quad . \tag{I-46A}$$

These can be derived from the more general expressions (I-39) to (I-41). The approximations (I-44) to (I-46) are useful for far-field problems. Note that they depend on the choice of origin but (I-39) to (I-41) do not.

We could also define far-field approximations for complex $\hat{k}$ but these are not of as much practical interest.

I.2.3   THE FIELD DUE TO SOURCES IN FREE SPACE

We shall now show how to calculate the field produced in free space by current sources with exponential t-variation. This material is intrinsically useful, for example in calculating the incident field due to a source distribution. Much more important, it will form the basis for our treatment of scattered fields as functions of effective surface currents.

Consider a current source distribution $\underline{K}_{eo}{}^v$, $\underline{K}_{mo}{}^v$ of the form of (I-4). We designate as D the region of the (x, y) plane in which the functions $\hat{\underline{K}}_{eo}{}^v(\rho)$ and $\hat{\underline{K}}_{mo}{}^v(\underline{\rho})$, which describe the transverse variation of the source distribution, are non-zero. (In mathematical terminology, D is the <u>support</u> of the functions $\hat{\underline{K}}_{eo}{}^v$ and $\hat{\underline{K}}_{mo}{}^v$.)

Let us restrict D to be of finite extent, that is, to have a finite maximum dimension, so that there are no sources at infinity. We can then obtain an expression for the field component $\hat{E}_t$ as a function of $\hat{\underline{K}}_{eo}{}^v$ and $\hat{\underline{K}}_{mo}{}^v$ by applying the two-dimensional Green's theorem, (48) of Reference 8, which tells us that

$$\int_A dA (f \nabla^2 g - g \nabla^2 f) = \int_B d\ell \left(f \, \frac{\partial g}{\partial n} - g \, \frac{\partial f}{\partial n} \right) \tag{I-46B}$$

for f and g functions of x and y only, A a finite area, B the boundary of A, $d\ell$ the incremental length along B, and $\partial/\partial \bar{n}$ the derivative along the unit normal $\bar{n}$ to B which points out of A. We set

$$f(\underline{\rho}') = \hat{\bar{E}}_t(\underline{\rho}'), \quad g(\underline{\rho}') = \bar{G}(\underline{\rho}, \underline{\rho}') \tag{I-46C}$$

and take the area of integration to be a disc $\bar{D}$ of radius $\bar{P}$ with center at the origin and with $\bar{P}$ large enough so that $\bar{D}$ contains D. We thus obtain the preliminary result

$$\int_{\bar{D}} dD' \left[\hat{\bar{E}}_t' (\nabla')^2 \bar{G} - \bar{G} (\nabla')^2 \hat{\bar{E}}_t' \right] = \int_{\bar{L}} d\ell' \left(\hat{\bar{E}}_t' \frac{\partial}{\partial n'} \bar{G} - \bar{G} \frac{\partial}{\partial n'} \hat{\bar{E}}_t' \right) \quad . \tag{I-47}$$

Here $\bar{L}$ is the perimeter of $\bar{D}$ and a prime denotes a function of the integration variable or a derivative with respect to the integration variable.

If now we let $\bar{P}$ approach infinity, the integral around $\bar{L}$ in (I-47) will vanish by virtue of the radiation condition (I-27). Also, the ∇^2 terms on the left hand side of (I-47) can be eliminated by making use of (I-21) and (I-31). We thus obtain

$$\hat{\bar{E}}_t = -\lim_{\bar{P}\to\infty} \int_{\bar{D}} dD' \; \bar{G} \left[\frac{\hat{k}^2 Z}{lk} \hat{\underline{K}}_{eot}^{v'} + \underline{t} \cdot \nabla' \times \hat{\underline{K}}_{mo\rho}^{v'} - \frac{k_t Z}{k} \nabla' \cdot \hat{\underline{K}}_{eo\rho}^{v'} \right]. \tag{I-48}$$

We can eliminate the derivatives of the source currents by using the two-dimensional Gauss's theorem (42) of Reference 8 and the two-dimensional Stoke's theorem (51) of Reference 8, which take the forms

$$\int_A dA \nabla \cdot \underline{P} = \int_B d\ell \; \bar{\underline{n}} \cdot \underline{P} \quad , \tag{I-48A}$$

$$\int_A dA \; \underline{t} \cdot (\nabla \times \underline{P}) = \int_B d\ell \; (\underline{t} \times \bar{\underline{n}}) \cdot \underline{P} \tag{I-48B}$$

respectively for $\underline{P}$ normal to $\underline{t}$ and independent of t . We then reduce the domain of integration from $\bar{D}$ to D because the integrand vanishes outside of D. The result is

$$\hat{E}_t = \int_D dD' \left[(\underline{t} \times \nabla'\overline{G}) \cdot \hat{\underline{K}}^{v'}_{mo\rho} - \frac{\hat{k}^2 Z}{1k} \overline{G} \hat{K}^{v}_{eot} - \frac{k_t Z}{k} \nabla'\overline{G} \cdot \hat{\underline{K}}^{v'}_{eo\rho} \right] , \qquad (I-49)$$

which is the desired integral representation of $\hat{E}_t$. The analogous equation for $\hat{H}_t$ is

$$Z\hat{H}_t = - \int_D dD' \left[Z(\underline{t} \times \nabla'\overline{G}) \cdot \hat{\underline{K}}^{v'}_{eo\rho} + \frac{\hat{k}^2}{1k} \overline{G} \hat{K}^{v'}_{mot} + \frac{k_t}{k} \nabla'\overline{G} \cdot \hat{\underline{K}}^{v'}_{mo\rho} \right]. \qquad (I-50)$$

These results are valid for any observation point ρ which is <u>bounded away from</u> <u>D</u>, that is, which does not lie within D or on the boundary of D. The situation at interior points and boundary points of D is more complicated and shall not be considered here.

We now readily obtain the expressions

$$\nabla\hat{E}_t = - \int_D dD' \left[\nabla\nabla'\overline{G} \cdot (\underline{t} \times \hat{\underline{K}}^{v'}_{mo\rho}) + \frac{\hat{k}^2 Z}{1k} \nabla\overline{G} K^{v'}_{eot} + \frac{k_t Z}{k} \nabla\nabla'\overline{G} \cdot \hat{\underline{K}}^{v'}_{eo\rho} \right] \qquad (I-51)$$

and

$$\nabla(Z\hat{H}_t) = \int_D dD' \left[Z \nabla\nabla'\overline{G} \cdot (\underline{t} \times \hat{\underline{K}}^{v'}_{eo\rho}) - \frac{\hat{k}^2}{1k} \nabla\overline{G} K^{v'}_{mot} - \frac{k_t}{k} \nabla\nabla'\overline{G} \cdot \hat{\underline{K}}^{v'}_{mo\rho} \right] \qquad (I-52)$$

for ρ bounded away from D, which is a sufficient condition to justify taking the ∇ operator inside the integral sign. By substituting (I-51) and (I-52) into (I-22) and (I-23), we obtain integral representations for $\hat{\underline{E}}_\rho$ and $\hat{\underline{H}}_\rho$ (Note that the source terms in (I-22) and (I-23) vanish because ρ is outside D.)

When ρ is sufficiently far from all points ρ' of D so that the inequality (I-38) holds for all such ρ', then we say that ρ lies in the <u>radiating near-field region</u> of the source distribution. By use of (I-39) to (I-41), we can readily show that in this region we have

$$\hat{\underline{E}} = ik \int_D dD' \ \bar{G}_R \underline{V} \ (k; \ Z\hat{\underline{K}}_{eo}^{v'}, \ \hat{\underline{K}}_{mo}^{v'} \ ; k_t; \ \underline{\sigma} \ ; \underline{\rho}'), \tag{I-53}$$

$$Z\hat{\underline{H}} = ik \int_D dD' \ \bar{G}_R \left| \underline{u}_r \ (k, \ k_t, \ \underline{\sigma}) \ \times \underline{V} \ (k; \ Z\hat{\underline{K}}_{eo}^{v'}, \ \hat{\underline{K}}_{mo}^{v'} \ ; k_t; \ \underline{\sigma}; \ \underline{\rho}'), \tag{I-54}$$

with

$$\underline{V} \ (k; \ Z\hat{\underline{K}}_e^{v'}, \ \hat{\underline{K}}_m^{v'} \ ; \ k_t; \ \underline{\sigma}; \ \underline{\rho}') = - \left[Z \underline{u}_r \times (\underline{u}_r \times \hat{\underline{K}}_e^{v'}) + \underline{u}_r \times \hat{\underline{K}}_m^{v'} \right]$$

$$= V_\perp \ (k; \ Z\hat{\underline{K}}_e^{v'}, \ \hat{\underline{K}}_m^{v'}; k_t; \ \underline{\sigma}; \ \underline{\rho}') \underline{u}_\perp \ (\underline{\sigma})$$

$$+ V_\| (k; \ Z\hat{\underline{K}}_e^{v'}, \ \hat{\underline{K}}_m^{v'}; k_t; \ \underline{\sigma}; \ \underline{\rho}') \underline{u}_\| \ (k, \ k_t, \ \underline{\sigma}) , \tag{I-55}$$

$$V_\perp \ (k; \ Z\hat{\underline{K}}_e^{v'}, \hat{\underline{K}}_m^{v'}; k_t; \ \underline{\sigma}; \ \underline{\rho}') = \underline{u}_\perp \ (\underline{\sigma}) \cdot (Z\hat{\underline{K}}_{e\rho}^{v'}) + \frac{\hat{k}}{k} \hat{K}_{mt}^{v'} + \frac{k_t}{k} \ \underline{\sigma} \cdot \hat{\underline{K}}_{m\rho}^{v'} , \tag{I-56}$$

$$V_\| \ (k; \ Z\hat{\underline{K}}_e^{v'}, \ \hat{\underline{K}}_m^{v'}; k_t; \ \underline{\sigma}; \ \underline{\rho}') = - \underline{u}_\perp \ (\underline{\sigma}) \cdot \hat{\underline{K}}_{m\rho}^{v'} + \frac{\hat{k}}{k} Z\hat{K}_{et}^{v'} + \frac{k_t}{k} \ \underline{\sigma} \cdot (Z\hat{\underline{K}}_{e\rho}^{v'}) , \tag{I-57}$$

$$\underline{u}_\perp (\underline{\sigma}) = \underline{t} \times \underline{\sigma} , \tag{I-58}$$

$$\underline{u}_\| \ (k, \ k_t, \ \underline{\sigma}) = \frac{1}{k} (\hat{k} \underline{t} + k_t \underline{\sigma}) , \tag{I-59}$$

$$\underline{u}_r \ (k, \ k_t, \ \underline{\sigma}) = \frac{1}{k} (\hat{k} \underline{\sigma} - k_t \underline{t}) . \tag{I-60}$$

These results are valid for k, k_t, and $\hat{k}$ restricted as in the discussion preceding (I-24).

The arguments $\widehat{Z\underline{K}}_e^{v'}$, $\widehat{\underline{K}}_m^{v'}$, and $\underline{\sigma}$ are of course themselves functions of the argument ϱ'.

The vector $\underline{u}_\perp$ is always real and of unit length. The vectors $\underline{u}_\parallel$ and $\underline{u}_r$ are real and of unit length for k_t real and $|k_t| < k$. For $k_{tI} \neq 0$, we still have

$$\underline{u}_\parallel \cdot \underline{u}_\parallel = \underline{u}_r \cdot \underline{u}_r = 1 \tag{I-60A}$$

but the length of $\underline{u}_\parallel$ and of $\underline{u}_r$, as defined by (2-4) is greater than unity. In all cases, the three vectors $\underline{u}_\perp$, $\underline{u}_\parallel$, and $\underline{u}_r$ are mutually perpendicular and

$$\underline{u}_\perp \times \underline{u}_\parallel = \underline{u}_r \ , \quad \underline{u}_\parallel \times \underline{u}_r = \underline{u}_\perp \ , \quad \underline{u}_r \times \underline{u}_\perp = \underline{u}_\parallel \quad . \tag{I-61}$$

These vectors are generalizations of the vectors $\underline{e}_\perp^s$, $\underline{e}_\parallel^s$, $\underline{e}_r^s$ defined in Section 2.1.2.

Let us now consider the case in which the sources are concentrated at the origin:

$$\widehat{\underline{K}}_{qo}^v (\varrho) = \underline{I}_{qo} \delta(\underline{\ }) \text{ for } q = e, m \ , \tag{I-62}$$

where $\delta(\varrho)$ is the Dirac delta function as in (I-31). We then have

$$\widehat{\underline{E}} = \widehat{E}_\perp \ \underline{u}_\perp (\widehat{\underline{e}}_r^s) + \widehat{E}_\parallel \underline{u}_\parallel (k, k_t, \widehat{\underline{e}}_r^s),$$

$$Z\widehat{\underline{H}} = \underline{u}_r (k, k_t, \widehat{\underline{e}}_r^s) \times \widehat{\underline{E}} = -\widehat{E}_\parallel \ \underline{u}_\perp (\widehat{\underline{e}}_r^s) + \widehat{E}_\perp \underline{u}_\parallel (k, k_t, \widehat{\underline{e}}_r^s) \tag{I-63}$$

in the radiating near-field region, with

$$\widehat{E}_p = - \frac{e^{i\widehat{k}P_o}}{P_o^{1/2}} \frac{ke^{-i\pi/4}}{2(2\pi\widehat{k})^{1/2}} \ V_{oop} \quad \text{for} \quad p = \perp, \parallel \quad . \tag{I-64}$$

Here P_o and $\widehat{\underline{e}}_r^s$ are defined as in (I-42). The quantities $V_{oo\perp}$ and $V_{oo\parallel}$ are the coefficients of $\delta(\varrho)$ in the expressions for $V_\perp$ and $V_\parallel$ which we obtain substituting (I-62) into (I-56) and (I-57).

We can readily confirm that $\widehat{\underline{E}}$ and $\widehat{\underline{H}}$ of (I-63) satisfy the radiation condition (I-27). We can also readily verify that these functions increase exponentially with P_o for $\widehat{k}_I < 0$, the leaky wave condition. We now want to show that the field $\underline{E}$, $\underline{H}$ whose transverse variation is given by (I-63) indeed carries energy away from the origin--as a radiating

109

field by definition should--and that the field amplitude does not grow exponentially with distance <u>in the direction of energy propagation.</u>

To this end we recall that the time average power flow (watts/m^2) is given by the real part $\underline{S}_R$ of the complex Poynting vector

$$\underline{S} = \underline{E} \times \underline{\widetilde{H}} \quad , \tag{I-65}$$

where $\sim$ indicates the complex conjugate. Thus the direction of $\underline{S}_R$ is the direction of power flow and energy flow and furthermore the condition

$$\hat{\underline{e}}_r^s \cdot \underline{S}_R > 0 \quad \text{at} \quad \underline{\rho} = P_0 \, \hat{\underline{e}}_r^s \quad \text{for} \quad P_0 \text{ sufficiently large} \tag{I-66}$$

characterizes a radiating field.

For the field with transverse dependence given by (I-63), we have

$$\underline{S} = \hat{\underline{E}} \times \hat{\underline{\widetilde{H}}} = \frac{1}{Z} \left[(\hat{E}_\perp \underline{u}_\perp + \hat{E}_\parallel \underline{u}_\parallel) \times (-\hat{\widetilde{E}}_\parallel \underline{u}_\perp + \widetilde{\hat{E}}_\perp \widetilde{\underline{u}}_\parallel) \right]$$

$$= \frac{1}{Z} \left[|\hat{E}_\perp|^2 \widetilde{\underline{u}}_r + |\hat{E}_\parallel|^2 \underline{u}_r - \frac{2i}{k^2} \frac{k_{tI}}{\hat{k}_R} (\hat{k}_R^2 + k_{tR}^2) \hat{E}_\parallel \widetilde{\hat{E}}_\perp \underline{t} \times \hat{\underline{e}}_r^s \right]. \tag{I-67}$$

In deriving this result we have assumed that Z is real, which is compatible with our assumption that k is real, and we have used

$$\underline{u}_\parallel \times \widetilde{\underline{u}}_\parallel = -\frac{2i}{k^2} (\hat{k}_R k_{tI} - \hat{k}_I k_{tR}) \underline{u}_\perp = -\frac{2i}{k^2} \frac{k_{tI}}{\hat{k}_R} (\hat{k}_R^2 + k_{tR}^2) \underline{u}_\perp \quad . \tag{I-68}$$

Taking the real part of (I-67), we have

$$\underline{S}_R = \frac{1}{Z} \left[\frac{1}{k} (|\hat{E}_\perp|^2 + |\hat{E}_\parallel|^2) (\hat{k}_R \hat{\underline{e}}_r^s - k_{tR} \underline{t}) \right.$$

$$\left. + \frac{2}{k^2} \frac{k_{tI}}{\hat{k}_R} (\hat{k}_R^2 + k_{tR}^2) (\hat{E}_\parallel \widetilde{\hat{E}}_\perp)_I \underline{t} \times \hat{\underline{e}}_r^s \right] \quad . \tag{I-69}$$

Thus (I-66) is clearly satisfied if and only if $\hat{k}_R > 0$, which verifies our statement that the condition $\hat{k}_R > 0$ characterizes a radiating field. (We also see that there is no power

flow either away from or in toward the axis when $\hat{k}$ is pure imaginary, which confirms that these values of $\hat{k}$ correspond to surface waves.)

Next, from (I-5) and (I-6S) we have

$$\underline{E} = \underline{A}\frac{1}{P_o^{1/2}} \ \exp\left\{i(\hat{k}P_o - k_t t)\right\} = \underline{A}\frac{1}{P_o^{1/2}} \ \exp\left\{i\,(\hat{k}\,\hat{\underline{e}}_r^s - k_t\underline{t})\cdot\underline{r}\right\}$$

$$= \underline{A}\frac{1}{P_o^{1/2}} \ \exp\left\{i(\hat{k}_R\,\hat{\underline{e}}_r^s - k_{tR}\underline{t})\cdot\underline{r}\right\} \ \exp\left\{-(\hat{k}_I\,\hat{\underline{e}}_r^s - k_{tI}\underline{t})\cdot\underline{r}\right\}. \quad (I-70)$$

with

$$\underline{A} = -\frac{ke^{-i\pi/4}}{2(2\pi k)^{1/2}} \ (V_{oo\perp}\ \underline{u}_\perp + V_{oo\parallel}\ \underline{u}_\parallel) \ . \quad (I-71)$$

Now at point $\underline{r}$, the direction of energy propagation is the direction of $\underline{S}_R$. Thus, if we define

$$\Gamma = (\hat{k}_I\,\hat{\underline{e}}_r^s - k_{tI}\underline{t})\cdot\underline{S}_R \ , \quad (I-72)$$

we see from the last term of (I-70) that there will be an exponential increase in $\underline{E}$ in the direction of propagation only if $\Gamma < 0$. But use of (I-69) and (I-24) in (I-72) yields

$$\Gamma = \frac{1}{kZ} \ (|\hat{\underline{E}}_\perp|^2 + |\hat{\underline{E}}_\parallel|^2) \ (\hat{k}_R\,\hat{k}_I + k_{tR}k_{tI}) = 0 \ , \quad (I-73)$$

so there is neither an exponential increase nor an exponential decrease of the field in the direction of energy propagation.

For a source distributed over a region D of the (x, y) plane with finite maximum dimension, the corresponding results are that, <u>for P_o sufficiently large</u>, the radiating field condition (I-66) holds and there is no exponential increase or decrease of the field in the direction of propagation.

* * *

111

Let us next consider the field in the far-field region for the case of $\hat{k}$ real and less than k. We shall defer until later a general definition of the far-field region. For the moment, it is enough to say that a point $\underline{r}$ is in the far-field region of a source distribution with finite support D if ρ is sufficiently large at $\underline{r}$ so that the inequalities of (I-43) hold for all ρ' in D. Because we have assumed

$$\hat{k} < k \ , \tag{I-73A}$$

we can write

$$\hat{k} = k \cos \beta \quad , \quad k_t = k \sin \beta \quad , \tag{I-74}$$

with

$$- \frac{\pi}{2} < \beta < \frac{\pi}{2} \tag{I-75}$$

as in (I-3) and (I-24A).

One way to evaluate the field at ρ is by substituting the approximations (I-44) to (I-46) for the Green's function and its derivatives into (I-49) to (I-52) and then employing (I-22) and (I-23). A more convenient approach, however, is to replace G_R and $\underline{\sigma}$ by G_∞ and $\underline{e}_r^s$ respectively in (I-53) and (I-54) and then use (I-5) to obtain expressions for $\underline{E}$ and $\underline{H}$. In this manner we obtain, from (I-53), the result

$$\underline{E}(\underline{r}) =$$

$$- \frac{\exp\left\{ i(\hat{k} P_o - k_t t)\right\}}{(P_o / \cos \beta)^{1/2}} \quad \frac{e^{-i\pi/4}}{2(2\pi)^{1/2}} \quad \frac{k^{1/2}}{\cos \beta} \quad \int_D dD' \exp\left\{ -i \hat{k} \underline{\hat{e}}_r^s \cdot \rho' \right\} \underline{V}' \tag{I-76}$$

with

$$\underline{V}' = \underline{V}(k; Z \underline{\hat{K}}_{eo}^{v'}, \underline{\hat{K}}_{mo}^{v'}; k_t; \underline{\hat{e}}_r^s; \rho') \ . \tag{I-76A}$$

In order to put this result in a form more appropriate to the far-field case, we begin by _formally_ defining $\underline{e}_r^s$ as in (2-13), R_o and T_o as in (2-10), and $\underline{e}_\perp^s$ and $\underline{e}_{\parallel}^s$ as in (2-14) and (2-15) respectively (with β_s replaced by β in the definitions of $\underline{e}_r^s$ and $\underline{e}_{\parallel}^s$), but for the moment we place no physical interpretation on any of these quantities. We then readily find

$$P_o = R_o \cos \beta \qquad , \tag{I-77}$$

$$\hat{k}\underline{P}_o - k_t t = kR_o \cos^2 \beta - k_t (-R_o \sin \beta + T_o) = kR_o - k_t T_o ,$$ (I-78)

and thus (I-76) can be written as

$$\underline{E} = \frac{e^{ikR_o}}{R_o^{1/2}} \exp\{-ik_t T_o\}\underline{f} ,$$ (I-79)

with

$$\underline{f} =$$

$$-\frac{e^{-i\pi/4}}{2(2\pi)^{1/2}} \frac{k^{1/2}}{\cos\beta} \int_D dD' \exp\{-ik\hat{\underline{e}}_r^s \cdot \underline{\rho}'\}\underline{V}(k; Z\hat{\underline{K}}_{eo}^{v'}, \hat{\underline{K}}_{mo}^{v'} ; k\sin\beta ; \hat{\underline{e}}_r^s ; \underline{\rho}')$$ (I-80)

and

$$\underline{V}(k; Z\hat{\underline{K}}_e^{v'}, \hat{\underline{K}}_m^{v} ; k\sin\beta; \hat{\underline{e}}_r^s ; \underline{\rho}') = -\left[Z\underline{e}_r^s \times (\underline{e}_r^s \times \hat{\underline{K}}_e^{v'}) + \underline{e}_r^s \times \hat{\underline{K}}_m^{v'}\right]$$

$$= V_\perp \underline{e}_\perp^s + V_\parallel \underline{e}_\parallel^s .$$ (I-81)

$$V_\perp = \underline{e}_\perp^s \cdot (Z\hat{\underline{K}}_{e\rho}^{v'}) + \cos\beta \hat{K}_{mt}^{v'} + \sin\beta \hat{\underline{e}}_r^s \cdot \hat{\underline{K}}_{m\rho}^{v'} ,$$ (I-82)

$$V_\parallel = -\underline{e}_\perp^s \cdot \hat{\underline{K}}_{m\rho}^{v'} + \cos\beta Z\hat{K}_{et}^{v'} + \sin\beta \hat{\underline{e}}_r^s \cdot (Z\hat{\underline{K}}_{e\rho}^{v'}) .$$ (I-83)

We also have, from (I-54),

$$Z\underline{H} = \underline{e}_r^s \times \underline{E} .$$ (I-84)

Since $\hat{\underline{e}}_r^s$ is a unit vector in the (x, y) plane, it is determined if we know its azimuth angle, ϕ_s of Section 2.1.2. Also, $k\sin\beta$ is clearly determined if we know k and β. Thus we can write

113

$$\underline{V} = \underline{V}(k; \ z \, \hat{\underline{K}}_e^{\,v'}, \ \hat{\underline{K}}_m^{\,v'}; \ \beta, \ \phi_s; \ \underline{\rho}') \quad , \tag{I-85}$$

which is a more convenient set of arguments for many purposes. (This set of arguments can also be used in the radiating near-field region, in which case ϕ_s is itself a function of $\underline{\rho}'$.)

It is clear from (I-79) and (2-10) that $\underline{e}_r^{\,s}$ gives the direction of phase propagation, and it can be shown by evaluating $\underline{S}_R$ (see (I-69)) that $\underline{e}_r^{\,s}$ gives the direction of energy propagation. It then follows that the ray through $\underline{r}$ does indeed appear to originate at the point $t = T_o$ on the $\rho = 0$ axis and that R_o is the distance from the cylinder axis to $\underline{r}$ along the ray. It follows from (I-61) that $\underline{e}_\perp^{\,s}$, $\underline{e}_{\parallel}^{\,s}$, $\underline{e}_r^{\,s}$, in that order, form the basis of a right-handed Cartesian coordinate system. Thus we have justified the physical interpretation given to R_o, T_o and the three unit vectors in Section 2.1.2. It is also clear now that the definition of $\hat{\underline{e}}_r^{\,s}$ in (I-42) leads to the interpretation of $\hat{\underline{e}}_r^{\,s}$ embodied in (2-13).

We can now give a more general definition of the far-field region with respect to a source distribution of finite support D. It is the region consisting of all values of $\underline{r}$ at which the field is given accurately by (I-79) to (I-84). The region is cylindrical, since the validity of these equations depends only on ρ, not on t, but its inner boundary is not in general circular. The condition we used previously, that ρ be sufficiently large so that the inequalities of (I-43) hold for all ρ' in D, is a sufficient but not necessary condition. For finite D, the fact that (I-79) holds with $\underline{f}$ independent of R_o and T_o implies validity of (I-80). This is no longer true when D is infinite, in which case the far-field region is defined as the region in which (I-79) holds with $\underline{f}$ independent of R_o and T_o but not necessarily given by (I-80). The case of infinite D is discussed further in Section I.2.5.

* * *

It is also useful to consider far-field scattering when $\hat{k}$ is real and greater than k, that is, when

$$\hat{k} = \hat{k}_R > k. \tag{I-85A}$$

In this case k_t is pure imaginary. It is convenient to allow β to take pure imaginary values,

$$\beta = |\beta_{\text{I}}, \quad \infty > \beta_{\text{I}} > -\infty \quad , \tag{I-86}$$

so that we can still use (I-74) and we can still define vectors $\underline{e}_\perp^s$, $\underline{e}_\parallel^s$, and $\underline{e}_r^s$ by means of (2-13) to (2-15) (with β_s replaced by β). It is readily verified that the vectors $\underline{e}_\parallel^s$ and $\underline{e}_r^s$ are now complex. It is also readily confirmed that we can equivalently define $\underline{e}_\perp^s$, $\underline{e}_\parallel^s$, and $\underline{e}_r^s$ as the values of $\underline{u}_\perp$, $\underline{u}_\parallel$, and $\underline{u}_r$ of (I-58) to (I-60) for $\underline{\sigma} = \hat{\underline{e}}_r^s$.

By the same procedures which yielded (I-79), we obtain

$$\underline{E} = \cos^{1/2}\beta \, \frac{e^{i\hat{k}\,P_o}}{P_o^{1/2}} \exp\{k_{t\text{I}}t\}\, \underline{f}\,, \quad Z\underline{H} = \underline{e}_r^s \times \underline{E}\,, \tag{I-87}$$

with $\underline{f}$ as in (I-80). We find from (I-69) that energy flow is normal to $\underline{t}$, a fact which influenced our choice of notation in (I-87).

I.2.4 THE FIELD DUE TO SURFACE CURRENT SOURCES

There is a very strong analogy between scattering problems and source problems in which the sources are surface currents. For this reason, it will be useful to specialize the results of Section I.2.3 to the case in which the field is produced by surface current sources $\underline{K}_{eo}$, $\underline{K}_{mo}$, with the exponential t-dependence of (I-4), located on a cylindrical sheet S whose projection onto the (x, y) plane is the curve L. We shall restrict L to be of finite length, which assures that the maximum transverse dimension of the source region is finite.

If L is a closed curve, we define $\underline{n}$ as the unit outward normal from L. If L is an open curve, we can arbitrarily define either unit normal to be $\underline{n}$. In either case, we then define the tangent vector $\underline{t}$ so that (2-1) is satisfied and define ℓ to be the length parameter along L in the $\underline{t}$ direction.

The units of surface currents $\underline{K}_e$ and $\underline{K}_m$ are amperes/m. and volts/m. respectively. As indicated in Section 2.2.8.1 of Reference 4, a surface current $\underline{K}_q$ on S is the limit as $d \to 0$ of a current source

$$\underline{K}_q^{\;v} = \frac{1}{d}\,\underline{K}_q \tag{I-88}$$

115

flowing uniformly in a shell of thickness d with middle surface S. More mathematically, $\underline{K}_q$ is equivalent to a singular volume current density

$$\underline{K}_q^{\,v} = \underline{K}_q \ \delta_L \tag{I-89}$$

where δ_L is the symbolic function defined by

$$\int_L d\ell \, f = \int_{D_\infty} dD \ f \, \delta_L \quad \text{for all } f, \tag{I-90}$$

with D_∞ the entire (x, y) plane. Surface currents are restricted to lie in the plane of S, and thus we have

$$\underline{K}_q = K_{qt} \, \underline{t} + K_{q\ell} \, \underline{\ell} \quad \text{for } q = e, \, m \tag{I-91}$$

and a corresponding expression for $\overset{\wedge}{\underline{K}}_q$, which is related to $\underline{K}_q$ by an equation analogous to (I-4).

On the basis of these considerations, we readily find that the general expressions (I-49) to (I-52) specialize to

$$\hat{E}_t = \int_L d\ell' \, (\frac{\partial \bar{G}}{\partial n'} \hat{K}'_{mo\ell} - \frac{\hat{k}^2 Z}{ik} \bar{G} \, \hat{K}'_{eot} - \frac{k_t Z}{k} \, \frac{\partial \bar{G}}{\partial \ell'} \hat{K}'_{eo\ell}) , \tag{I-92}$$

$$Z\hat{H}_t = -\int_L d\ell' \, (Z \, \frac{\partial \bar{G}}{\partial n'} \hat{K}'_{eo\ell} + \frac{\hat{k}^2}{ik} \bar{G}\hat{K}'_{mot} + \frac{k_t}{k} \, \frac{\partial \bar{G}}{\partial \ell'} \hat{K}'_{mo\ell}) , \tag{I-93}$$

$$\nabla \hat{E}_t = \int_L d\ell' \, \left[(\nabla \frac{\partial \bar{G}}{\partial n'}) \hat{K}'_{mo\ell} - \frac{\hat{k}^2 Z}{ik} \nabla \bar{G} \, \hat{K}'_{eot} - \frac{k_t Z}{k} \, \frac{\partial}{\partial \ell'} \, (\nabla \bar{G}) \, \hat{K}'_{eo\ell} \right] , \tag{I-94}$$

$$\nabla (Z\hat{H}_t) = - \int_L d\ell' \, \left[Z(\nabla \frac{\partial \bar{G}}{\partial n'}) \, \hat{K}'_{eo\ell} + \frac{\hat{k}^2}{ik} \nabla \bar{G} \, \hat{K}'_{mot} + \frac{k_t}{k} \, \frac{\partial}{\partial \ell'} \, (\nabla \bar{G}) \hat{K}'_{mo\ell} \right] . \tag{I-95}$$

Equivalent expressions which differ in the last term of the integrand can be obtained using

$$\int_L d\ell' \, \frac{\partial \bar{G}}{\partial \ell'} \, \hat{K}'_\ell = - \int_L d\ell' \, \bar{G} \, \frac{\partial}{\partial \ell'} \hat{K}'_\ell \ . \tag{I-96}$$

In order to make (I-96) valid even for discontinuous $\hat{K}_\ell$ and for open curves L, we define $\frac{\partial}{\partial \ell} \hat{K}_\ell$ to include impulse functions at the discontinuities of $\hat{K}_\ell$ on L and impulse functions at the end points of an open curve. The impulse functions at the end points are calculated by considering L to be part of a closed curve with $\hat{K}_\ell = 0$ on the

116

rest of the curve.

Note that (I-92) to (I-95) are still valid if the signs of $\underline{n}$ and $\underline{\ell}$ are reversed. This is why we can designate either unit normal to L as $\underline{n}$.

In the <u>radiating near-field region</u>, the equations equivalent to (I-53) to (I-57) are

$$\hat{\underline{E}} = ik \int_L d\ell' \, \overline{G}_R \, \underline{W} \, (k; \, Z \hat{\underline{k}}'_{eo}, \, \hat{\underline{K}}'_{mo}; \, k_t; \, \underline{\sigma}; \ell') \qquad , \tag{I-97}$$

$$Z\hat{\underline{H}} = ik \int_L d\ell' \, \widetilde{G}_R \, \underline{u}_r \, (k, \, k_t, \, \underline{\sigma}) \times \underline{W} \, (k; \, Z \hat{\underline{k}}'_{eo}, \, \hat{\underline{K}}'_{mo}; \, k_t; \, \underline{\sigma}; \ell') \, , \tag{I-98}$$

$$\underline{W} \, (k; \, Z \hat{\underline{k}}'_e, \, \hat{\underline{K}}'_m; \, k_t; \, \underline{\sigma}; \ell') = - \left[Z \underline{u}_r \times (\underline{u}_r \times \hat{\underline{k}}'_e) + \underline{u}_r \times \hat{\underline{K}}'_m \right]$$

$$= W_\perp \, (k; \, Z \hat{\underline{k}}'_e, \, \hat{\underline{K}}'_m; \, k_t; \, \underline{\sigma}; \ell') \underline{u}_\perp \, (\underline{\sigma})$$

$$+ W_{\parallel} \, (k; \, Z \hat{\underline{k}}'_e, \, \hat{\underline{K}}'_m; k_t; \, \underline{\sigma}; \ell') \, \underline{u}_{\parallel} (k, \, k_t, \, \underline{\sigma}) \quad , \tag{I-99}$$

$$W_\perp \, (k; \, Z \hat{\underline{k}}'_e, \, \hat{\underline{K}}'_m; \, k_t; \, \underline{\sigma}; \ell') = (\underline{\sigma} \cdot \underline{n}') \, Z \hat{K}'_{e\ell} + \frac{\hat{k}}{k} \hat{K}'_{mt} - \frac{k_t}{k} \underline{u}_\perp (\underline{\sigma}) \cdot \underline{n}' \, \hat{K}'_{m\ell} \, , \tag{I-100}$$

$$W_{\parallel} \, (k; \, Z \hat{\underline{k}}'_e, \, \hat{\underline{K}}'_m; \, k_t; \, \underline{\sigma}; \ell') = - (\underline{\sigma} \cdot \underline{n}') \, \hat{K}'_{m\ell} + \frac{\hat{k}}{k} Z \hat{K}'_{et} - \frac{k_t}{k} \underline{u}_\perp (\underline{\sigma}) \cdot \underline{n}' \, Z \hat{K}'_{e\ell} \, , \tag{I-101}$$

with $\underline{u}_\perp, \underline{u}_{\parallel}$, and $\underline{u}_r$ given by (I-58) to (I-60). By virtue of (I-96), we see that (I-97) and (I-98) still hold if $\underline{W}$ is replaced by a vector $\overline{\underline{W}}$ with elements

$$\overline{W}_\perp = (\underline{\sigma} \cdot \underline{n}') \, Z \hat{K}'_{e\ell} + \frac{\hat{k}}{k} \hat{K}'_{mt} + \frac{1}{ik} \frac{k_t}{k} \frac{\partial}{\partial \ell'} \, \hat{K}'_{m\ell} \qquad , \tag{I-102}$$

$$\overline{W}_{\parallel} = - (\underline{\sigma} \cdot \underline{n}') \, \hat{K}'_{m\ell} + \frac{\hat{k}}{k} \, Z \hat{K}'_{et} + \frac{1}{ik} \frac{k_t}{k} \frac{\partial}{\partial \ell'} \, (Z \hat{K}'_{e\ell}) \qquad . \tag{I-103}$$

In the far-field region, (I-79), (I-84) and (I-87) are still valid, but $\underline{\ell}$ is given by

117

$$\underline{f} = -\frac{e^{-i\pi/4}}{2(2\pi)^{1/2}} \frac{k^{1/2}}{\cos\beta} \int_L d\ell' \exp\left\{-ik\hat{\underline{e}}_r^s \cdot \underline{\rho}'\right\} \underline{W}\left(k; Z\hat{\underline{K}}_{eo}^{v'}, \hat{\underline{K}}_{mo}^{v'}; k\sin\beta; \hat{\underline{e}}_r^s; \ell'\right),$$ (I-104)

and $\underline{W}$, $W_\perp$, and $W_{\parallel}$ of (I-99) to (I-101), evaluated for $k_t = k\sin\beta$ and $\underline{\sigma} = \hat{\underline{e}}_r^s$, are given by

$$\underline{W} = -\left[Z\underline{e}_r^s \times (\underline{e}_r^s \times \hat{K}_{e\ell}') + \underline{e}_r^s \times \hat{K}_{m\ell}'\right] = W_\perp \underline{e}_\perp^s + W_{\parallel} \underline{e}_{\parallel}^s,$$ (I-105)

$$W_\perp = (\hat{\underline{e}}_r^s \cdot \underline{n}') Z\hat{K}_{e\ell}' + \cos\beta \hat{K}_{mt}' - (\underline{e}_\perp^s \cdot \underline{n}') \sin\beta \hat{K}_{m\ell}',$$ (I-106)

$$W_{\parallel} = -(\hat{\underline{e}}_r^s \cdot \underline{n}') \hat{K}_{m\ell}' + \cos\beta Z\hat{K}_{et}' - (\underline{e}_\perp^s \cdot \underline{n}') \sin\beta Z\hat{K}_{e\ell}'.$$ (I-107)

Again W can be replaced by $\tilde{W}$, and the components of $\tilde{W}$ are

$$\tilde{W}_\perp = (\hat{\underline{e}}_r^s \cdot \underline{n}') Z\hat{K}_{e\ell}' + \cos\beta \hat{K}_{mt}' + \frac{1}{ik}\tan\beta \frac{\partial}{\partial\ell'} \hat{K}_{m\ell}',$$ (I-108)

$$\tilde{W}_{\parallel} = -(\hat{e}_r^s \cdot \underline{n}') \hat{K}_{m\ell}' + \cos\beta Z\hat{K}_{et}' + \frac{1}{ik}\tan, \qquad {}_{e\ell'} .$$ (I-109)

Analogously to (I-85), we can write $\underline{W}$ as a function of a different and frequently more convenient set of arguments,

$$\underline{W} = \underline{W}(k; Z\hat{\underline{K}}_e', \hat{\underline{K}}_m'; \beta, \phi_s; \ell') ,$$ (I-110)

and we can write $\tilde{W}$ in the same manner.

I.2.5 A MORE GENERAL APPROACH TO FAR-FIELD RADIATION

In this section, we shall only consider the case of $\hat{k}$ real and less than k.

118

We have already seen that, if all sources are confined to a region of finite extent in the (x, y) plane, then the far-field radiation is given by

$$\underline{E} = \frac{e^{ikR_0}}{R_0^{1/2}} e^{-ik_t T_0} \underline{f} \quad , \quad Z\underline{H} = \underline{e}_r^{s} \times \underline{E} \quad . \tag{I-111}$$

where $\underline{f}$ is independent of R_0 and T_0 and is normal to $\underline{e}_r^{s}$. In (I-80), we have given an integral representation of $\underline{f}$, and in (I-104) we have given a specialized form of this representation, valid when the sources are surface currents. For any azimuth ϕ_s, there will be a value of R_0 beyond which the far-field expressions have a given

degree of accuracy, and furthermore there is some value of R_0 beyond which the far-field expressions have that degree of accuracy for all ϕ_s.

The situation is much more complicated when the source distribution extends to infinity. It is still true that, if the integral of (I-80) or of (I-104) exists for a given azimuth angle ϕ_s, then this integral gives the correct value of $\underline{f}$ for radiation in the indicated azimuth direction. However, there are also cases in which the integral does not exist for some value of ϕ_s, but there nevertheless exists an $\underline{f}$, independent of $\underline{R}_0$, which makes (I-111) valid for that azimuth. As a simple example, consider a constant surface current distribution on an infinite half plane. The integral representation (I-104) for $\underline{f}$ involves the integral

$$I = \int_0^\infty d\ell' \exp\{-ik* \ell\} \quad , \tag{I-112}$$

with k^* a function of ϕ_s. This integral is not uniquely defined but, nevertheless, the function $\underline{f}$ of (I-111) exists for all azimuth directions except the two directions normal to the half-plane.

The fact that (I-111) can hold independent of whether (I-80) or (I-104) holds follows from the theory of the two-dimensional Helmholtz equation, which tells us that, under a wide variety of conditions, the solution has the form

119

$$Q = \frac{e^{ik P_0}}{P_0^{1/2}} \, q \, , \tag{I-113}$$

with q independent of P_0, for ϕ_s fixed and P_0 sufficiently large. By setting

$$Q = Z\hat{H}_t \, , \quad q = \cos^{3/2}\beta \quad f_\perp \, , \quad \text{and} \quad Q = \hat{E}_t, \quad q = \cos^{3/2}\beta \quad f_\parallel \, , \tag{I-113A}$$

and then calculating the corresponding values of $\hat{\underline{E}}_\rho$ and $\hat{\underline{H}}_\rho$, we find that (I-111) is a consequence of the existence of solutions of form (I-113).

When the source distribution extends to infinity, there may be values of ϕ_s for which the representation (I-111) never becomes valid, no matter how large we make P_0. In physical terms, we can never travel far enough away in the ϕ_s direction so that we are in the far field region of the sources. In the case of the constant surface current source on an infinite half-plane, this is the situation in the two directions normal to the half-plane.

Finally, for a source distribution of infinite extent, the far-field conditions may be approached non-uniformly, so that no matter how large we make R_0, increasing R_0 will increase the range of angles ϕ_s over which (I-111) is valid to a given degree of accuracy. This is the case when there are isolated directions for which (I-111) never becomes valid. Thus, for the constant surface current on an infinite half-plane, increasing R_0 will decrease but never eliminate the angular region about each normal direction in which (I-111) cannot be used.

I.3 SCATTERING OF FIELDS WITH EXPONENTIAL VARIATION

I.3.1 THE SCATTERED FIELD AS A FUNCTION OF EFFECTIVE SURFACE CURRENTS

Let us now consider the field $(\underline{E}^{scat}, \underline{H}^{scat})$ scattered from a cylinder which has its cross section bounded by a curve L of finite length in the (x, y) plane. The geometry is illustrated in Figure L. We use the same geometrical notation as in Section I.2.4, where L defined the surface on which a source distribution is located.

We begin by applying the two-dimensional Green's theorem to $\hat{E}_t^{scat}$ and $\bar{G}$. We proceed as in the derivation of (I-49) except that we exclude the region interior to L from the domain of integration and we thereby introduce a line integral over L. The line integral involves $\frac{\partial}{\partial n} \hat{E}_t^{scat}$, which we eliminate by use of (I-17). We also make use of the fact that $\hat{E}_t^{scat}$ has no sources in the domain of integration. We obtain the result

$$\hat{E}_t^{scat}(\underline{r}) = \int_L d\ell' \left(\frac{\partial \bar{G}}{\partial n'} \hat{E}_t^{scat'} - \frac{\hat{k}^2 Z}{ik} \bar{G} \hat{H}_\ell^{scat'} - \frac{k_t Z}{k} \bar{G} \frac{\partial}{\partial \ell'} \hat{H}_t^{scat'} \right), \quad (I-114)$$

for $\underline{r}$ outside L. Similarly, if we apply the two-dimensional Green's theorem to $\bar{G}$ and the source field $\hat{E}_{ot}$ with the domain of integration taken as the region interior to L, we find

$$\int_L d\ell' \left(\frac{\partial \bar{G}}{\partial n'} \hat{E}_{ot}' - \frac{\hat{k}^2 Z}{ik} \bar{G} \hat{H}_{o\ell}' - \frac{k_t Z}{k} \bar{G} \frac{\partial}{\partial \ell'} \hat{H}_{ot}' \right) = 0 \quad (I-115)$$

when the argument $\underline{r}$ of $\bar{G}$ is a point outside L. Upon adding (I-114) and (I-115) and expressing the result in terms of effective surface currents, we obtain

$$\hat{E}_t^{scat} = \int_L d\ell' \left(\frac{\partial \bar{G}}{\partial n'} \hat{K}_{m\ell}' - \frac{\hat{k}^2 Z}{ik} \bar{G} \hat{K}_{et}' + \frac{k_t Z}{k} \bar{G} \frac{\partial}{\partial \ell'} \hat{K}_{e\ell}' \right) . \quad (I-116)$$

There are no impulse functions in $\frac{\partial}{\partial \ell} \hat{K}_{e\ell}$ because L is a closed curve and $\hat{K}_{e\ell}$ is continuous even at an edge, that is, a point where the tangent to L is discontinuous.

(See Section II of Reference 5, which also gives the dual result that $\widehat{K}_{m\ell}$ is continuous.) Thus we can apply (I-96) and obtain

$$\widehat{E}_t^{scat} = \int_L d\ell' \left(\frac{\partial \bar{G}}{\partial n'} \widehat{K}_{m\ell}' - \frac{\widehat{k}^2 Z}{ik} \bar{G} \widehat{K}_{et}' - \frac{k_t Z}{k} \frac{\partial \bar{G}}{\partial \ell'} \widehat{K}_{e\ell}' \right) . \qquad (I-117)$$

But this is just (I-92) with $\widehat{E}_t$ replaced by $\widehat{E}_t^{scat}$ and $\widehat{\underline{K}}_{eo}$ and $\widehat{\underline{K}}_{mo}$ replaced by $\widehat{\underline{K}}_e$ and $\widehat{\underline{K}}_m$ respectively. Indeed, we can readily show that all the integral representations (I-92) to (I-95) and the radiating near field formulas (I-97) and (I-98) still hold with $\widehat{\underline{E}}$, $\widehat{\underline{H}}$, $\widehat{\underline{K}}_{eo}$, and $\widehat{\underline{K}}_{mo}$ replaced by $\widehat{\underline{E}}^{scat}$, $\widehat{\underline{H}}^{scat}$, $\widehat{\underline{K}}_e$, and $\widehat{\underline{K}}_m$ respectively and with $\underline{W}$ and the alternative form $\bar{W}$ still given by (I-99) to (I-103). We can similarly show that the far-field scattering is given by (I-104) and (I-111) with $\underline{E}$, $\underline{H}$, $\widehat{\underline{K}}_{eo}$, and $\widehat{\underline{K}}_{mo}$ replaced by $\underline{E}^{scat}$, $\underline{H}^{scat}$, $\widehat{\underline{K}}_e$, and $\widehat{\underline{K}}_m$ respectively. (We retain the notation $\underline{f}$ for the radiation vector in both cases.) It should be noted that $\widehat{\underline{K}}_e$ and $\widehat{\underline{K}}_m$ are functions of ℓ and linear functionals of the functions $Z\widehat{H}_{ot}(\ell)$ and $\widehat{E}_{ot}(\ell)$.

We now have a complete set of representations in which the effective surface currents on the scattering body act as the sources of the scattered field. These representations hold even when the tangent to L has discontinuities, because the resulting infinities in $\widehat{K}_{et}$ and $\widehat{K}_{mt}$ are integrable (See Section II of Reference 5).

The representations also hold for scattering from thin cylindrical sheets. The path L in this case is traced in one direction on one face of the sheet and in the other direction on the other face, enclosing zero area. A simpler formulation can be obtained, however, by using the same equations but with L now an open path running along the sheet from one edge to the other and $\widehat{K}_e$ and $\widehat{K}_m$ now the sum of the effective surface currents on the two faces, which is proportional to the jump in tangential field across the sheet.

Regardless of whether L is of finite extent or extends to infinity, the following principle (a form of Huygens' Principle) holds:

If an incident field ($\underline{E}_o$, $\underline{H}_o$) produces effective surface currents ($\underline{K}_e$, $\underline{K}_m$) on the surface of the scattering cylinder, with $\underline{K}_e$ and $\underline{K}_m$ having the exponential t - dependence of (I-4), and if identical surface current <u>sources</u> ($\underline{K}_e$, $\underline{K}_m$) would produce a radiated field ($\underline{E}^{scat}$, $\underline{H}^{scat}$) in the absence of the scattering cylinder and of other sources, then ($\underline{E}^{scat}$, $\underline{H}^{scat}$) is the scattered field produced by ($\underline{E}_o$, $\underline{H}_o$).

122

On the basis of this principle, we see that the considerations of Section I.2.5 also apply to scattered fields.

Now let us consider a pair of functions, $\hat{\underline{K}}_{ej}$, $\hat{\underline{K}}_{mj}$, which are either (1) approximations to $\hat{\underline{K}}_e$, $\hat{\underline{K}}_m$; or (2) contributions to $\hat{\underline{K}}_e$, $\hat{\underline{K}}_m$ in the sense that $\hat{\underline{K}}_e$ and $\hat{\underline{K}}_m$ are represented as sums and $\hat{\underline{K}}_{ej}$, $\hat{\underline{K}}_{mj}$ are terms in these sums; or (3) approximations to contributions. Then the formulas we have already cited can be used to calculate quantities $\underline{E}_j^{scat}$, $\underline{H}_j^{scat}$, $\hat{\underline{E}}_j^{scat}$, $\hat{\underline{H}}_j^{scat}$, $\underline{f}_j$, and $\underline{W}_j$ which are the corresponding approximations or contributions to $\underline{E}^{scat}$, $\underline{H}^{scat}$, $\hat{\underline{E}}^{scat}$, $\hat{\underline{H}}^{scat}$, $\underline{f}$, and $\underline{W}$. For example, if $\hat{\underline{K}}_{ej}$, $\hat{\underline{K}}_{mj}$ are the physical optics contributions to $\hat{\underline{K}}_e$, $\hat{\underline{K}}_m$, then $\underline{E}_j^{scat}$, $\underline{H}_j^{scat}$ are the physical optics contributions to the scattered field. The considerations of Section I.2.5 apply individually to each contribution, but the behavior for large R_0 of an approximation or contribution may not be the same as that of the true field. For example, in the case of scattering of a normally incident plane wave from an infinite half-plane, the radiation vector $\underline{f}$ is not defined in the back-scatter and forward-scatter directions. However, the contribution $\underline{f}_j$ corresponding to the fringe wave current is defined for these directions.

I.3.2   THE PERFECT CONDUCTOR CASE

A perfect conductor problem is characterized by the boundary condition

$$\widehat{\underline{K}}_m = 0 \quad . \tag{I-118}$$

By applying this condition and (I-22), we find that the boundary conditions on $\widehat{E}_t$ and $\widehat{H}_t$ at L are

$$\widehat{E}_t = 0 \tag{I-119}$$

and

$$\partial \widehat{H}_t / \partial n = 0. \tag{I-120}$$

We thus obtain two uncoupled scattering problems and can calculate $\widehat{E}_t$ and $\widehat{H}_t$ independently of each other. A corollary observation is that $\widehat{H}_{ot}$ does not produce any $\widehat{E}_t^{scat}$ and $\widehat{E}_{ot}$ does not produce any $\widehat{H}_t^{scat}$.

It is convenient to represent the surface current and the scattered field as the sum of a term which depends on $\widehat{H}_{ot}$ but not on $\widehat{E}_{ot}$ plus a term which depends on $\widehat{E}_{ot}$ but not on $\widehat{H}_{ot}$. These two terms correspond to the two principal polarizations in plane wave scattering; $\widehat{H}_{ot}$ dependence is the generalization of perpendicular polarization and $\widehat{E}_{ot}$ dependence of parallel polarization. Thus we write

$$\widehat{\underline{K}}_e = \widehat{\underline{K}}_e^{\perp} + \widehat{\underline{K}}_e^{\parallel} \quad , \tag{I-121}$$

where

$$\widehat{\underline{K}}_e^{\perp} = \widehat{K}_{et}^{\perp}\, \underline{t} + \widehat{K}_{e\ell}\, \underline{\ell} \tag{I-122}$$

is a function of $\widehat{H}_{ot}$ and

$$\widehat{\underline{K}}_e^{\parallel} = \widehat{K}_{et}^{\parallel}\, \underline{t} \tag{I-123}$$

is a function of $\widehat{E}_{ot}$. The fact that $\widehat{\underline{K}}_e^{\parallel}$ has no ℓ-component follows from the fact that $\widehat{E}_{ot}$ does not produce any $\widehat{H}_t^{scat}$. We use superscripts $\perp$ and $\parallel$ to avoid confusion with the dyadic elements of Section 2.1.5.

From (I-23) we find

$$\widehat{K}_{et}^{\perp} = -\frac{k_t}{\widehat{k}^2} \frac{\partial}{\partial \ell} \widehat{K}_{e\ell} \quad . \tag{I-124}$$

There are, however, very important situations in which we find it useful to represent $\hat{\underline{K}}_e^{\perp}$ in terms of contributions for which (I-124) does not hold. Use of such contributions leads to a spurious $\hat{E}_t^{scat}$ term, spurious in the sense that its sum over all contributions is zero. This complication arises, for example, in the case of a wedge with one face illuminated, if we decompose $\hat{\underline{K}}_e^{\perp}$ into physical optics and fringe wave contributions. (See Section 2.1.6.)

In light of this, we shall consider two different sets of formulas for perfect conductor problems. The first is valid for all contributions and approximations to the surface current which are used in practice. The second is a simplified version valid for the true field and for contributions and approximations for which (I-124) holds.

In perfect conductor problems, we never use non-zero contributions or approximations to $\hat{\underline{K}}_m$ and we always use contributions or approximations with $\hat{K}_{e\ell}$ independent of $\hat{E}_{ot}$. We thus find

$$\hat{E}_t^{scat} = -\frac{Z}{ik} \int_L d\ell' \, (\hat{k}^2 \, \overline{G} \hat{K}_{et}' + ik_t \frac{\partial \overline{G}}{\partial \ell'} \, \hat{K}_{e\ell}')$$

$$= -\frac{Z}{ik} \int_L d\ell' \left[\hat{k}^2 \, \overline{G} \hat{K}_{et}^{\parallel'} + (\hat{k}^2 \, \overline{G} \hat{K}_{et}^{\perp'} + ik_t \frac{\partial \overline{G}}{\partial \ell'} \hat{K}_{e\ell}') \right] \quad , \tag{I-125}$$

$$Z\hat{H}_t^{scat} = -Z \int_L d\ell' \, \frac{\partial \overline{G}}{\partial n'} \hat{K}_{e\ell}' \quad . \tag{I-126}$$

The expressions for $\nabla \hat{E}_t^{scat}$ and $\nabla Z\hat{H}_t^{scat}$ are readily found from these formulas and we shall omit them. The expressions for $\underline{W}$ and $\overline{W}$ in the various scattering formulas simplify to

$$\underline{W} = -2\underline{u}_r \times (\underline{u}_r \times \underline{\hat{K}}_{e\ell}') \quad , \tag{I-127}$$

$$W_\perp = \bar{W}_\perp = (\underline{\sigma} \cdot \underline{n}') Z \hat{K}_{e\ell}' \quad , \tag{I-128}$$

$$W_\parallel = \frac{\hat{k}}{k} Z\hat{K}_{et}' - \frac{k_t}{k} \underline{u}_\perp (\underline{\sigma}) \cdot \underline{n}' Z\hat{K}_{e\ell}' \quad , \tag{I-129}$$

and

$$\bar{W}_\parallel = \frac{\hat{k}}{k} Z\hat{K}_{et}' + \frac{1}{ik} \frac{k_t}{k} \frac{\partial}{\partial \ell'} (Z\hat{K}_{e\ell}') \quad . \tag{I-130}$$

It is convenient to introduce the notation

$$\underline{W} = \underline{W}^\dagger + W_x \underline{u}_\parallel \quad , \quad \underline{\bar{W}} = \underline{W}^\dagger + \bar{W}_x \underline{u}_\parallel \tag{I-131}$$

with

$$\underline{W}^\dagger = (\underline{\sigma} \cdot \underline{n}') Z\hat{K}_{e\ell}' \underline{u}_\perp + \frac{\hat{k}}{k} Z\hat{K}_{et}^{\parallel'} \underline{u}_\parallel \quad , \tag{I-132}$$

$$W_x = \frac{\hat{k}}{k} Z\hat{K}_{et}^{\perp'} - \frac{k_t}{k} \underline{u}_\perp (\underline{\sigma}) \cdot \underline{n}' \ Z\hat{K}_{e\ell}' \quad , \tag{I-133}$$

$$\bar{W}_x = \frac{\hat{k}}{k} Z\hat{K}_{et}^{\perp'} + \frac{1}{ik} \frac{k_t}{k} \frac{\partial}{\partial \ell'} (Z\hat{K}_{e\ell}') \quad . \tag{I-134}$$

Using these expressions for $\underline{W}$ and $\underline{\bar{W}}$, we can determine $\underline{f}$ and the radiating near-field region values of $\underline{\hat{E}}^{scat}$ on $\underline{\hat{H}}^{scat}$ by the usual formulas. Equations (I-125) to (I-134) are valid for all contributions and approximations used in practice.

When the condition (I-124) holds, (I-125) simplifies to

$$\hat{E}_t^{scat} = -\frac{\hat{k}^2 Z}{ik} \int_L d\ell' \ \bar{G} \hat{K}_{et}^{\parallel} \quad , \tag{I-135}$$

126

and the equation for $\nabla \hat{E}_t^{scat}$ simplifies in like manner. The expressions for $\hat{H}_t^{scat}$ and $\nabla \hat{H}_t^{scat}$ do not simplify.

The most important simplification is that of $\bar{\bar{W}}$. The "cross term" $\bar{\bar{W}}_x$ vanishes and thus we have

$$\bar{\bar{W}} = \underline{W}^\dagger \tag{I-136}$$

Obviously this is easier to work with than $\underline{W}$, so we shall not even consider the form which $\underline{W}$ takes.

* * *

We shall now consider the relationship of problems with $k_t \neq 0$ to equivalent normal incidence problems with k replaced by $\hat{k}$ and k_t set to zero. In doing so, we shall restrict consideration to fields for which (I-124) holds.

We begin by noting that the surface currents are functions of $\hat{k}$ and ℓ and linear functionals of the incident field. Thus we can write

$$\hat{K}_{e\ell} = L_\perp (\hat{k}; \ell, \ell') \, \hat{H}_{ot} (\ell') \tag{I-137}$$

$$Z \hat{K}_{et}^{\parallel} = L_\parallel (\hat{k}; \ell, \ell') \, \hat{E}_{ot} (\ell') \, . \tag{I-138}$$

with $L_\perp$ and $L_\parallel$ linear integral operators which convert a function of ℓ' into a function of ℓ. The fact that $\hat{K}_{e\ell}$ and $\hat{K}_{et}^{\parallel}$ depend on k and k_t only in the combination $\hat{k}$ is a consequence of the perfect conductor boundary condition. It is a very important fact, because it enables us to make meaningful comparisons between problems with the same $\hat{k}$ but different k and k_t.

We shall define an equivalent normal incidence problem in the same way we used in Section 3.3.3 of Reference 2, where the definition was motivated by the fact that it leads to equal radar cross-sections for the original and equivalent problems. Under this definition, a problem with

$$k_t = 0, \quad k = \hat{k}, \quad H_{ot} = H_{oEt}, \quad E_{ot} = 0 \tag{I-139}$$

is the equivalent of a problem with

$$k_t \neq 0, \quad k = (\hat{k}^2 + k_t^2)^{1/2} \, , \quad H_{ot} = \frac{\hat{k}}{k} H_{oEt}, \quad E_{ot} = 0 \, . \tag{I-140}$$

If the solution to the first problem is

$$\underline{H}^{scat} = H^{scat}_{Et} \, \underline{t}, \quad \underline{E}^{scat} = E^{scat}_{E\rho}, \quad \underline{K}_e = K_{E\ell} \, \underline{\ell}, \quad \underline{W}^\dagger = W^\dagger_{\perp E} \, \underline{u}_\perp(\sigma), \quad \underline{f} = f_{E\perp} \underline{e}^s_\perp, \quad (I-141)$$

then the solution to the second problem is

$$
\begin{aligned}
&\underline{\hat{H}}^{scat} = \frac{\hat{k}}{k} H^{scat}_{Et} \, \underline{t} + \frac{k_t}{ik\hat{k}} \nabla H^{scat}_{Et}, \quad \underline{\hat{E}}^{scat} = \underline{E}^{scat}_{E\rho}, \\[2mm]
&\underline{\hat{K}}_e = \frac{\hat{k}}{k} K_{E\ell} \underline{\ell} - \frac{k_t}{ik\hat{k}} \frac{\partial}{\partial \ell} K_{E\ell} \underline{t}, \quad \underline{W}^\dagger = \frac{\hat{k}}{k} W^\dagger_{\perp E} \, \underline{u}_\perp(\sigma), \\[2mm]
&\underline{f} = \left(\frac{k}{\hat{k}}\right)^{1/2} f_{E\perp} \underline{e}^s_\perp.
\end{aligned}
\right\} \quad (I-142)
$$

Similarly, a problem with

$$k_t = 0, \quad k = \hat{k}, \quad E_{ot} = E_{oEt}, \quad H_{ot} = 0 \qquad (I-143)$$

is the equivalent of a problem with

$$k_t \neq 0, \quad k = (\hat{k}^2 + k_t^2)^{1/2}, \quad \mathcal{E}_{ot} = \frac{\hat{k}}{k} E_{oEt}, \quad H_{ot} = 0. \qquad (I-144)$$

If the solution to the first problem is

$$\underline{E}^{scat} = E^{scat}_{Et} \, \underline{t}, \quad \underline{H}^{scat} = H^{scat}_{E\rho}, \quad \underline{K}_e = K_{Et} \underline{t}, \quad \underline{W}^\dagger = W^\dagger_{\parallel E} \, \underline{t}, \quad \underline{f} = f_{E\parallel} \underline{t}, \qquad (I-145)$$

then the solution to the second problem is

$$
\begin{aligned}
&\underline{\hat{E}}^{scat} = \frac{\hat{k}}{k} E^{scat}_{Et} \, \underline{t} + \frac{k_t}{ikk} \nabla E^{scat}_{Et}, \quad \underline{\hat{H}}^{scat} = \underline{H}^{scat}_{E\rho}, \\[2mm]
&\underline{\hat{K}}_e = K_{Et} \underline{t}, \quad \underline{W}^\dagger = \frac{\hat{k}}{k} W^\dagger_{\parallel E} \, \underline{u}_\parallel(k, k_t, \sigma), \quad \underline{f} = \left(\frac{k}{\hat{k}}\right)^{1/2} f_{E\parallel} \underline{e}^s_\parallel.
\end{aligned}
\right\} \quad (I-146)
$$

Verification of these equivalences is straightforward. It involves use of (I-128), (I-135), (I-24), (I-23), (I-132), and (I-104) and of the fact that (I-124) holds separately for the incident and for the scattered field.

By use of the equivalence concept, we can replace a problem involving an incident field with exponential dependence along the axis by two uncoupled problems, one for each polarization, involving fields with $k_t = 0$. Conversely, when we solve a $k_t = 0$ problem, we have in doing so effectively solved a class of oblique incidence problems. It must be emphasized, however, that the equivalence concept is a result of the special characteristics of perfect conductor problems, not a general rule for scattering problems.

L.3.3 PLANE WAVE INCIDENCE

We shall now consider the case in which the incident field is a homogeneous plane wave incident at angle $\beta_i = \beta$ (see Figure 1). We describe such a plane wave using (2-3) and the associated definitions of Section 2.1.1, and recall that an alternative description of the same wave is given by (I-1) to (I-3). We can now readily verify that, in order for the axial variation of the incident and scattered waves to match, we must have

$$\beta_s = \beta_i \ , \tag{I-147}$$

and thus our use of the same notation β for both these quantities is justified.

We have already noted that the effective surface currents are linear functions of $\hat{H}_{ot}$ and $\hat{E}_{ot}$. These in turn are linear functions of $E_o \, \underline{p}$ for plane wave incidence. Thus it follows that it is legitimate to relate the surface currents to $E_o \, \underline{p}$ by surface current dyadics $\hat{\underline{\underline{K}}}_e$, $\hat{\underline{\underline{K}}}_m$ as is done in (2-27) to (2-29) of Section 2.1.3.

The general expressions for the scattered field now become

$$\hat{E}_t^{scat} = E_o \left\{ \int_L d\ell' \left(\frac{\partial \overline{G}}{\partial n'} \, \underline{\ell}' \cdot \hat{\underline{\underline{K}}}_m' + ik \cos^2\beta \, Z\overline{G} \, \underline{t} \cdot \hat{\underline{\underline{K}}}_e' - \sin\beta \, Z \frac{\partial \overline{G}}{\partial \ell'} \, \underline{\ell}' \cdot \hat{\underline{\underline{K}}}_e' \right) \right\} \cdot \underline{p}, \tag{I-148}$$

$$Z\hat{H}_t^{scat} = - E_o \left\{ \int_L d\ell' \left(Z \frac{\partial \overline{G}}{\partial n'} \, \underline{\ell}' \cdot \hat{\underline{\underline{K}}}_e' - ik \cos^2\beta \, \overline{G} \underline{t} \cdot \hat{\underline{\underline{K}}}_m' + \sin\beta \frac{\partial \overline{G}}{\partial \ell'} \, \underline{\ell}' \cdot \hat{\underline{\underline{K}}}_m' \right) \right\} \cdot \underline{p} \ , \tag{I-149}$$

129

and corresponding expressions for $\nabla \hat{E}_t$ and $\nabla(Z\hat{H}_t)$ which can be used in (I-22) and (I-23).

For the radiating near-field region, we readily obtain

$$\hat{\underline{E}}^{scat} = E_0 \left[ik \int_L d\ell' \, \overline{G}_R \, \underline{\underline{W}}(k;\beta,\phi_1;k\sin\beta;\underline{\sigma};\ell') \right] \cdot \underline{p} \,, \tag{I-150}$$

$$Z\hat{\underline{H}}^{scat} = E_0 \left[ik \int_L d\ell' \, \overline{G}_R \, \underline{u}_r(k,k\sin\beta,\underline{\sigma}) \times \underline{\underline{W}}(k;\beta,\phi_1;k\sin\beta;\underline{\sigma};\ell') \right] \cdot \underline{p} \,. \tag{I-151}$$

with $\underline{\underline{W}}$ of the form

$$\underline{\underline{W}} = -\left[Z \underline{u}_r \times (\underline{u}_r \times \hat{\underline{K}}_e') + \underline{u}_r \times \hat{\underline{K}}_m' \right]$$

$$= W_{\perp\perp}\,\underline{u}_\perp \underline{e}_\perp^{\,t} + W_{\perp\parallel}\underline{u}_\perp \underline{e}_\parallel^{\,t} + W_{\parallel\perp}\,\underline{u}_\parallel \underline{e}_\perp^{\,t} + W_{\parallel\parallel}\,\underline{u}_\parallel \underline{e}_\parallel^{\,t} \,. \tag{I-152}$$

The elements of $\underline{\underline{W}}$ are

$$\left.\begin{array}{l} W_{\perp j} = (\underline{\sigma}\cdot\underline{n}')\,Z\hat{K}_{e\ell j}' + \cos\beta\,\hat{K}_{mtj}' - \sin\beta(\underline{u}_\perp\cdot\underline{n}')\hat{K}_{m\ell j}' \\[3mm] W_{\parallel j} = -(\underline{\sigma}\cdot\underline{n}')\,\hat{K}_{m\ell j}' + \cos\beta\,Z\hat{K}_{etj}' - \sin\beta\,(\underline{u}_\perp\cdot\underline{n}')\,Z\hat{K}_{e\ell j}' \end{array}\right\} \quad j = \perp,\ \parallel. \tag{I-153}$$

Alternatively, $\underline{\underline{W}}$ can be replaced by $\overline{\underline{\underline{W}}}$ with elements

$$\left.\begin{array}{l} \overline{W}_{\perp j} = (\underline{\sigma}\cdot\underline{n}')\,Z\hat{K}_{e\ell j}' + \cos\beta\,\hat{K}_{mtj}' + \dfrac{1}{ik}\,\tan\beta\dfrac{\partial}{\partial\ell'}\,\hat{K}_{m\ell j}' \\[4mm] \overline{W}_{\parallel j} = -(\underline{\sigma}\cdot\underline{n}')\,\hat{K}_{m\ell j}' + \cos\beta\,Z\hat{K}_{etj}' + \dfrac{1}{ik}\,\tan\beta\dfrac{\partial}{\partial\ell'}(Z\hat{K}_{e\ell j}') \end{array}\right\} \quad j = \perp,\parallel. \tag{I-154}$$

The equations (I-150) and (I-151) are the jumping-off point for the development of a diffraction coefficient representation of scattering at finite ranges. We shall not, however, pursue this line of investigation here.

We also readily verify that the far-field scattering is given by (2-19) with $\underline{f}$ of the two-component form (2-21) and given by

$$\underline{f} = E_0 \frac{1}{k^{1/2}\cos\beta} \left[-\frac{e^{-i\pi/4}}{2(2\pi)^{1/2}} k \int_L d\ell' \exp\{-ik\cos\beta\,\hat{\underline{\theta}}_r^s\cdot\underline{\rho}'\}\underline{\underline{W}}(k;\beta,\phi_1;k\sin\beta;\hat{\underline{\theta}}_r^s;\ell') \right] \cdot \underline{p} \,. \tag{I-155}$$

For far-field work, it is convenient to proceed as in (I-110) and express $\underset{\approx}{W}$ in terms of arguments β and ϕ_s instead of (k sin β) and $\hat{\underline{e}}_r{}^s$. We thus have

$$\underset{\approx}{W} = \underset{\approx}{W} \, (\, k; \beta, \phi_i; \beta, \phi_s; \, \ell \, ' \,) \tag{I-156}$$

and similarly for $\underset{\approx}{\bar{W}}$. We now see that this $\underset{\approx}{W}$ and $\underset{\approx}{\bar{W}}$ are indeed special cases for $\beta_i = \beta_s = \beta$ of the $\underset{\approx}{W}$ and $\underset{\approx}{\bar{W}}$ defined by (2-30), (2-31), and (2-33). (The notation here is a little more general than that of Section 2 in that we use an arbitrary real wave imped-ance Z instead of specifying the free space wave impedance Z_0.) Furthermore, if we define the diffraction coefficient $\underset{\approx}{d}$ as in (2-22) to (2-24), we find from (I-155) that $\underset{\approx}{d}$ is indeed given by (2-32).

To verify the basic symmetry property (2-34), from which (2-35) to (2-37) follow, we first note that replacing β by $-\beta$ will not affect the sign of $\hat{H}_{t\perp}{}^{scat}$, the contribution to $\hat{H}_t{}^{scat}$ due to the $\perp$-polarized component of the incident field, nor the sign of $\hat{E}_{t\parallel}{}^{scat}$. Then (I-22) and (I-23) tell us that the signs of $\hat{E}_{\rho\perp}{}^{scat}$ and $\hat{\underline{H}}_{\rho\parallel}{}^{scat}$ are also unchanged but the signs of $\hat{E}_{t\perp}{}^{scat}$ and $\hat{H}_{t\parallel}{}^{scat}$ reverse.

A second application of (I-22) and (I-23) tells us that $\hat{\underline{E}}_{\rho\parallel}{}^{scat}$ and $\hat{\underline{H}}_{\rho\perp}{}^{scat}$ reverse signs. Upon replacing the fields by the corresponding surface currents (See (2-26C).), we obtain (2-34).

Turning to the perfect conductor problem, we confirm from (I-118) and (I-123) that $\hat{\underset{\approx}{K}}_m$ and $\hat{K}_{e\ell\parallel}$ are zero, as stated in (2-38). The results (2-39) and (2-41) are obtained from the equivalences derived in Section I.3.2. The result (2-40) follows from (I-124) and the equivalences.

As in Section I.3.2, we have two different sets of formulas for the perfect conductor problem, the first valid for all contributions and approximations used in practice-- including those for which (2-40) does not hold-- and the second valid for the true field and for contributions and approximations which satisfy (2-40).

In the first case, (I-148) and (I-149) reduce to

$$\hat{E}_t^{scat} = - E_0 \left\{ \frac{Z}{ik} \int_L d\ell' \left[k^2 \cos^2\beta \, \bar{G} \, \hat{K}_{et\parallel}' + (k^2 \cos^2\beta \, \bar{G} \, \hat{K}_{et\perp}' + ik \sin\beta \frac{\partial \bar{G}}{\partial \ell'} \hat{K}_{e\ell\perp}') \right] \right\} \cdot \underline{\wp}, \quad \text{(I-157)}$$

$$Z\hat{H}_t^{scat} = - E_0 \left\{ Z \int_L d\ell' \, \frac{\partial \bar{G}}{\partial n'} \, \hat{K}_{e\ell\perp}' \right\} \cdot \underline{\wp} \quad , \quad \text{(I-158)}$$

and there are corresponding expressions for $\nabla \hat{E}_t^{scat}$ and $\nabla Z \hat{H}_t^{scat}$ which can be used in (I-22) and (I-23). In the radiating near-field region, (I-150) and (I-151) hold with

$$\underline{\underline{W}} = \underline{\underline{W}}^\dagger + W_X \, \underline{u}_\parallel \underline{e}_\perp^\ell \quad , \quad \bar{\underline{\underline{W}}} = \underline{\underline{W}}^\dagger + \bar{W}_X \, \underline{u}_\parallel \underline{e}_\perp^\ell \quad , \quad \text{(I-159)}$$

$$\underline{\underline{W}}^\dagger = W_{\perp\perp} \, \underline{u}_\perp \underline{e}_\perp^\ell + W_{\parallel\parallel} \, \underline{u}_\parallel \underline{e}_\parallel^\ell \quad , \quad \text{(I-160)}$$

$$W_{\perp\perp} = (\underline{\sigma} \cdot \underline{n}') \, Z \, \hat{K}_{e\ell\perp}' \quad , \quad \text{(I-161)}$$

$$W_{\parallel\parallel} = \cos\beta \, Z\hat{K}_{et\parallel}' \quad , \quad \text{(I-162)}$$

$$W_X = \cos\beta \, Z\hat{K}_{et\perp}' - \sin\beta (\underline{u}_\perp \cdot \underline{n}') \, Z \, \hat{K}_{e\ell\perp}' \quad , \quad \text{(I-163)}$$

$$\bar{W}_X = \cos\beta \, Z\hat{K}_{et\perp}' + \frac{1}{ik} \tan\beta \, \frac{\partial}{\partial \ell'} (Z \, \hat{K}_{e\ell\perp}') \quad . \quad \text{(I-164)}$$

From these formulas and the equivalences of Section I.3.2, we readily confirm that the far-field scattering is given by (2-19), (2-22), and (2-32) with $\underline{\underline{W}}$ and $\bar{\underline{\underline{W}}}$ given by (2-42), (2-43), (2-45), (2-46), (2-52), and (2-53). The expressions (2-48) and (2-49) for the d_q are consequences of the results for $\underline{\underline{W}}$.

When (2-40) holds, (I-157) simplifies to

$$\hat{E}_t^{scat} = E_0 \left\{ ik \, Z \cos^2\beta \int_L d\ell' \, \bar{G} \, \hat{K}_{\partial\ell\parallel}' \right\} \cdot \underline{\wp} \quad \text{(I-165)}$$

and there is an analogous expression for $\nabla \hat{E}_t^{scat}$. In the radiating near-field region and in the far-field region, we have

$$\bar{W}_X = 0, \quad \text{(I-166)}$$

so we can use (I-150), (I-151), (2-19), (2-22), and (2-32) with

$$\bar{\underline{\underline{W}}} = \underline{\underline{W}}^\dagger \; . \tag{I-167}$$

This result confirms (2-47) and thus (2-50). It is readily verified that W_X is given by (2-44) in the far field, but in practice we would never use $\underline{\underline{W}}$ instead of $\bar{\underline{\underline{W}}}$ when (2-40) holds.

LIST OF SYMBOLS

(We omit dummy variables, quantities which appear only in derivations, quantities which are only used within a few lines of where they are defined, and quantities which are used only in Section IV, which is short enough so that there is no problem keeping track of the notation.)

A) If A is a scalar, vector, or dyadic, then

A', when it appears under an integral sign, signifies A taken as a

function of the integration variables. There is one exception to this rule, namely $\widetilde{v}_B{}'$.

If A is a complex scalar, vector, or dyadic, then

$\widetilde{A}$ is the complex conjugate of A.

A_R is the real part of A. (Note: There is one exception, $\overline{G}_R$. Also,

R as a subscript on the real scalars ϕ and δ has another meaning.)

A_I is the imaginary part of A.

If A is a scalar, vector, or dyadic which has exponential variation along an axis, then we use the notation

$$A = \hat{A} \exp \left\{ -ik_t t \right\}$$

where

t is the length parameter along the cylinder axis.

k_t is the axial wave number (See Section I.2.1, also Sections 2.1.2 and I.1.).

$\hat{A}$ is independent of t.

If $\underline{A}$ is a vector, then

$$A_l = \underline{l} \cdot \underline{A}$$

$$A_t = \underline{t} \cdot \underline{A}$$

$$\underline{A}_\rho = \underline{t} \times (\underline{A} \times \underline{t}) = \underline{A} - A_t \, \underline{t}$$

where

$\underline{t}$ is the unit vector along the axis of a cylinder, which can be an infinite length cylinder (See Section 2.1.1.) or an incremental

135

length cylinder (See Section 3.1.1.).

$\underline{l}$ is the unit tangent to the cylinder in a plane normal to $\underline{t}$
(See (2-1).).

If $\underline{\underline{A}}$ is a dyadic, then

$$A_{\perp\perp} = \underline{e}_\perp^s \cdot \underline{\underline{A}} \cdot \underline{e}_\perp^l \qquad A_{\perp l} = \underline{e}_\perp^s \cdot \underline{\underline{A}} \cdot \underline{l} \qquad A_{l\perp} = \underline{l} \cdot \underline{\underline{A}} \cdot \underline{e}_\perp^l$$

$$A_{\perp\parallel} = \underline{e}_\perp^s \cdot \underline{\underline{A}} \cdot \underline{e}_\parallel^l \qquad A_{\perp t} = \underline{e}_\perp^s \cdot \underline{\underline{A}} \cdot \underline{t} \qquad A_{l\parallel} = \underline{l} \cdot \underline{\underline{A}} \cdot \underline{e}_\parallel^l$$

$$A_{\parallel\perp} = \underline{e}_\parallel^s \cdot \underline{\underline{A}} \cdot \underline{e}_\perp^l \qquad A_{\parallel l} = \underline{e}_\parallel^s \cdot \underline{\underline{A}} \cdot \underline{l} \qquad A_{t\perp} = \underline{t} \cdot \underline{\underline{A}} \cdot \underline{e}_\perp^l$$

$$A_{\parallel\parallel} = \underline{e}_\parallel^s \cdot \underline{\underline{A}} \cdot \underline{e}_\parallel^l \qquad A_{\parallel t} = \underline{e}_\parallel^s \cdot \underline{\underline{A}} \cdot \underline{t} \qquad A_{t\parallel} = \underline{t} \cdot \underline{\underline{A}} \cdot \underline{e}_\parallel^l$$

where

$\underline{e}_\perp^l$, $\underline{e}_\parallel^l$, $\underline{e}_\perp^s$, $\underline{e}_\parallel^s$ are unit polarization vectors defined by

(2-5), (2-14), and (2-15).

For convenience, we sometimes use the simpler notation

$A_\perp$ instead of $A_{\perp\perp}$

$A_\parallel$ instead of $A_{\parallel\parallel}$

A_X instead of $A_{\parallel\perp}$

B) Additional subscripts and superscripts which have specific meanings:

E indicates a quantity obtained from the equivalent normal incidence problem (See Section I.3.2.).

e indicates an electric current or related quantity.

i indicates a quantity related to the incident field.

K indicates a quantity for use in Keller's Geometrical Theory of Diffraction (GTD).

m indicates a magnetic current or related quantity.

PO indicates the physical optics contribution to a quantity.

s indicates a quantity related to the scattered field.

scat indicates a scattered field.

U indicates the fringe wave (Ufimtsev) contribution to a quantity.

o indicates an incident field or a current source distribution.

136

+   indicates a quantity associated with the surface S_+, which intersects the surface S_- to form an edge. For example, d_{a+} is the contribution to d_a from the current on S_+.

−   indicates a quantity associated with the surface S_- (See +.).

C) Other symbols:

$\underline{b}$ Unit vector normal to $\underline{t}$ and $\underline{n}_o$ (See (2-54) and Figure 3.).

C   An edge (See Section I and Figure 3.).

c   Speed of light.

D   Support of the functions $\hat{\underline{K}}_{eo}^v$, $\hat{\underline{K}}_{mo}^v$ (See Section I.2.3.).

$\underline{\underline{D}}$ Three-Dimensional Diffraction Coefficient (See Section 3.1.1.).

$\underline{\underline{D}}_\infty$ Value of $\underline{\underline{D}}$ calculated by assuming currents $\underline{K}_{e\infty}$, $\underline{K}_{m\infty}$ on a cylinder of finite length (See Section 3.1.2.).

d_a, d_b Scalar diffraction coefficients related to $\underline{\underline{d}}$ for a wedge (See (2-80b).).

$d_\perp$, $d_\parallel$, d_x See (A).

d_{q+}, d_{q-} for $q = \perp$, $\parallel$, x, a, b   Contribution to d_q from the current on S_+ or S_- respectively.

$d_{\parallel\perp}^*$ Quantity related to $d_{\parallel\perp}$ (See (3-32), (3-33).).

$d_{\parallel\perp}^{**}$ Quantity related to $d_{\parallel\perp}$ (See (3-42) to (3-46).).

d_x^*, d_x^{**} Alternate notation for $d_{\parallel\perp}^*$, $d_{\parallel\perp}^{**}$ respectively.

$\underline{d}$, $\underline{\underline{d}}$ $(k;\beta_i, \phi_i;\beta_s, \phi_s)$ Incremental Length Diffraction Coefficient (ILDC) (See Section III.); also, for $\beta_s = \beta_i$, Two-Dimensional Diffraction Coefficient (2-D DC) (See Section II.).

$\underline{\underline{d}}_+$, $\underline{\underline{d}}_-$ Contributions to $\underline{\underline{d}}$ from the current on S_+ and S_- respectively.

$d\underline{\underline{D}}_\infty$ Contribution to $\underline{\underline{D}}_\infty$ from an incremental length element of a cylinder (See (3-8).).

$d\underline{F}_\infty$ Radiation vector corresponding to $d\underline{\underline{D}}_\infty$ (See (3-7).).

$\hat{E}_\perp$, $\hat{E}_\parallel$ Components of $\hat{\underline{E}}$ (See (I-63).).

$\underline{E}$ Electric field.

$\underline{e}_r^s$, $\underline{e}_r^i$ Unit vectors which indicate the directions of the scattered wave ($\underline{e}_r^s$) and the incident wave ($-\underline{e}_r^i$) (See Sections 2.1.1, 2.1.2,

3.1.1.).

$\hat{\underline{e}}_r^s$, $\hat{\underline{e}}_r^i$ Unit vectors along the projections of $\underline{e}_r^s$ and $\underline{e}_r^i$ respectively onto a plane normal to the cylinder axis (See (2-   ), (2-13).).

$\underline{e}_x$ Unit vector normal to $\underline{t}$ which serves as an azimuth reference (See Section 2.1.1.). For the wedge, we use $\underline{e}_x = -\underline{n}_o$ (See Figure 3.).

$\underline{e}_y$ Unit vector normal to $\underline{t}$ and $\underline{e}_x$ (See Section 2.1.1.).

$\underline{e}_\perp^s$, $\underline{e}_\parallel^s$; $\underline{e}_\perp^i$, $\underline{e}_\parallel^i$ Polarization vectors for the scattered and incident fields (See (2-5), (2-14), and (2-15).).

$\underline{e}_\rho^+$, $\underline{e}_\rho^-$ Unit tangent vectors normal to $\underline{t}$ on S_+ and S_- respectively (See (2-56) and Figure 3.).

$\underline{F}$ Radiation vector for a three-dimensional problem (See (3-2), (3-3).).

f, $f(V, \psi)$ A function related to the ILEDC $\underline{\underline{d}}^U$ for a wedge (See (3-52), (3-56), (3-57), (3-60).).

f_+, f_- Values of f for the arguments (V_+, ψ_+) and (V_-, ψ_-) respectively (See (3-55).).

$\underline{f}$ Radiation vector for an infinite cylinder problem (See (2-19), (2-22).).

$\overline{G}$ Two-dimensional scalar Green's function (See (I-29).).

$\overline{G}_R$, $\overline{G}_o$, $\overline{G}_\infty$ Approximations to $\overline{G}$ (See (I-39), (I-44), (I-46A).).

g, $g(V, \psi)$ A function related to the ILEDC $\underline{\underline{d}}^U$ for a wedge (See (3-53), (3-58), (3-59).).

g_+, g_- Values of g for the arguments (V_+, ψ_+) and (V_-, ψ_-) respectively (See (3-55).).

$H_n^{(1)}$ Hankel function of first kind and order n.

$\underline{H}$ Magnetic field.

$h(\beta_i, \beta_s)$ Quantity related to $d_{\parallel\perp}$ (See (3-25), (3-29), (3-32).).

$\underline{\underline{I}}_\rho$ Unit dyadic for vectors normal to $\underline{t}$ (See (I-35).).

i Square root of -1; $\exp\{-i\omega t\}$ time dependence is used.

$\underline{K}_e$, $\underline{K}_m$ Effective electric and magnetic surface current respectively (See (2-25), (2-26).). On a perfect conductor, $\underline{K}_e$ is the true surface current.

$\underline{K}_{e\infty}$, $\underline{K}_{m\infty}$ The effective surface currents on an infinitely long cylinder when used as an approximation or contribution to the currents on a finite or incremental length of cylinder (See Section 3.1.2.).

$\underline{K}_e^v$, $\underline{K}_m^v$ Electric and magnetic volume current distributions (See Section I.2.3.).

$\hat{\underline{K}}_e^\perp$, $\hat{\underline{K}}_e^\parallel$ For an infinite length cylinder, the contributions to $\underline{K}_e$ induced by the $\perp$-polarized and $\parallel$-polarized components respectively of an incident wave with exponential variation along the cylinder axis (See Section I.3.2.).

$\hat{\underline{\underline{K}}}$ A surface current dyadic, either electric or magnetic.

$\hat{\underline{\underline{K}}}_e$, $\hat{\underline{\underline{K}}}_m$ Electric and magnetic surface current dyadics respectively (See (2-27).).

k   Wave number.

k_t Axial wave number (See Section I.2.1, also Sections 2.1.2 and I.1.).

$\hat{k}$ Transverse wave number (See (I-18).).

L   The curve normal to $\underline{t}$ which describes the cross section of a cylinder (See Section 2.1.1 and Figure 1.).

l Length parameter along L (See Section 2.1.1.).

$\underline{l}$ Unit tangent to L (See (2-1).).

$\underline{n}$ Unit outward normal (See Section 2.1.1.).

$\underline{n}_o$ Unit vector which bisects the wedge angle and points out of the wedge (See Section 2.2.1 and Figure 3.).

$\underline{n}_+$, $\underline{n}_-$ Unit outward normals to S_+ and S_- respectively (See (2-55).).

P, P_o These symbols are to be read as capital rho. Therefore they are included in the alphabetic listing of Greek-letter symbols.

$\underline{p}$ Polarization vector of the incident wave. (See Section 2.1.1.).

R_o Distance to a point in the far-field region. For a three-dimensional body, R_o is measured from the origin (See (3-1).). For an infinite length cylinder, R_o is measured from the axis along the unique scattered ray which passes through the far-field point (See (2-10) and Figure 2.).

$\underline{r}$ Position of a point in space.

S   The surface of a three-dimensional body.

S_+, S_- The two surfaces which intersect to form the edge C (See Section 2.2.1 and Figure 3.).

139

$\underline{S}$	Complex Poynting vector (See (I-65).).
T	Length of a finite cylinder (See Section 3.1.2.).
T_o	Point on the axis of an infinite length cylinder from which a scattered ray appears to originate (See 2.10 and Figure 2.).
$\boldsymbol{t}$	Time.
t	Length parameter along the cylinder axis (See (2.2).).
$\underline{t}$	Unit vector along the cylinder axis (See Section 2.1.1.).
U, U_+, U_-	Step functions (See (2-102), (2-103), (3-67).).
u	Real number related to v (See (3-51).).
$\underline{u}_\perp$, $\underline{u}_\parallel$, $\underline{u}_r$	Complex vectors which are generalizations of $\underline{e}_\perp^s$, $\underline{e}_\parallel^s$, $\underline{e}_r^s$ respectively (See Section I.2.3.).
V	Argument of the functions f and g (See Section 3.2.1.).
V_+, V_-	Values of V corresponding to the scattering from S_+ and S_- respectively (See (3-47), (3-48).).
$\underline{V}$	Vector field used in calculating the field produced by a volume distribution of current sources (See Section I.2.3.).
$V_{oo\perp}$, $V_{oo\parallel}$	Quantities used in calculating the field produced by a line source (See Section I.2.3.).
v, v_+, v_-	Quantities related to V, V_+, V_- by (3-50) and (3-51).
$\widetilde{v}_B$	Quantity related to f and g (See (3-52), (3-53).).
$\widetilde{v}_B{}'$	$\partial \widetilde{v}_B/\partial\psi$ (See (3-54).).
$W_{\perp\perp}{}^*$, $W_{\parallel\parallel}{}^*$	Quantities related to $W_{\perp\perp}$ and $W_{\parallel\parallel}$ for perfect conductor case (See Section 3.1.5.). (Note: There is no dyadic $\underline{\underline{W}}{}^*$.)
$\overline{W}_{\parallel\perp}{}^*$, $\overline{W}_{\parallel\perp}{}^{**}$	Quantities related to $\overline{W}$ (See Section 3.1.5.). (Note: There are no dyadics $\underline{\underline{\widetilde{W}}}{}^*$ or $\underline{\underline{\overline{W}}}{}^{**}$.)
$\underline{W}$, $\underline{\overline{W}}$, $\underline{W}^\dagger$	Surface vector quantities used in calculating the field produced by a surface current distribution (See Section I.2.4.).

$\underset{\approx}{W}$, $\underset{\approx}{\bar{W}}$ Dyadic quantities used in calculating the field produced by a surface current distribution (See Section 2.1.3.).

w   Real number related to v (See (3-51).).

X   Half of the phase difference in radians between far-field returns from the two ends of a finite cylinder (See Section I, Section 3.1.2.).

Z   Wave impedance of a medium.

Z_o Wave impedance of free space.

α Interior half-angle of a wedge (See Section 2.2.1 and Figure 3.). (Note: α is used with a different meaning in Section 4.2.)

β Used instead of β_l and β_s in Appendix, which deals only with cases for which $\beta_s = \beta_l$.

β_l Angle describing the obliquity of $\underline{e}_r^l$ to the cylinder axis (See (2-7) and Figure 1.).

β_s Angle describing the obliquity of $\underline{e}_r^s$ to the cylinder axis (See (2-11) and Figure 1.).

β_s^* Quantity related to β_s and β_l (See (3-34).).

$\delta(\underline{\rho})$ The Dirac delta function for a point singularity at $\underline{\rho} = 0$ in a two-dimensional space (See (I-31).).

δ_{S+}, δ_{R+}; δ_{S-}, δ_{R-} The angles measured from $\underline{\hat{e}}_r^s$ to each of the four shadow and reflection boundaries (See (2-71) to (2-74).).

δd_q Measure of the error introduced when $d_q(\beta_l; -\beta_l)$ is approximated by $d_q(\beta_l; \beta_l)$ (See (3-17).).

δW_q Quantity related to δd_q (See Section 3.1.4.).

ζ Number equal to v when v is real (See (3-51).).

ν	Wedge factor (See (2-58).).
P	Distance from $\underline{\rho}'$ to $\underline{\rho}$ (See (I-30).).
P_0	Radial distance from the cylinder axis to a point in the far-field region (See (I-42).).
$\underline{\rho}$	Projection of $\underline{r}$ onto a plane normal to the axis (See (2-2).).
$\underline{\rho}'$	When not under an integral sign, signifies the value of $\underline{\rho}$ at a source point (See Section L.2.2.).
$\underline{\sigma}$	Unit vector pointing from $\underline{\rho}'$ to $\underline{\rho}$ (See (I-34).).
ϕ_s, ϕ_i	Azimuth angles of $\hat{\underline{e}}_r^{\,s}$ and $\hat{\underline{e}}_r^{\,i}$ respectively (See Section 2.1.2 and Figure 1.).
ϕ_{si}	Azimuth angle from $\hat{\underline{e}}_r^{\,i}$ to $\hat{\underline{e}}_r^{\,s}$ (See (2-75).).
ϕ_{S+}, ϕ_{R+}; ϕ_{S-}, ϕ_{R-}	The azimuths of the four shadow and reflection boundaries (See Section 2.2.2.).
ϕ_Σ	The sum $(\phi_i + \phi_s)$ (See (2-76).).
ψ	Angle which is argument of f and g (See Section 3.2.1.).
ψ_+, ψ_-	Values of ψ associated with the scattering from S_+ and S_- respectively (See (3-47), (3-48).).
ω	Radian frequency.

REFERENCES

1. Ufimtsev, P. Ya., _Method of Edge Waves in the Physical Theory of Diffraction_, Air Force Systems Command, Foreign Technology Division, Document ID No. FTD-HC-23-259-71 (1971). (Translation of _Metod krayevykh voln v fizicheskoy teorii difraktsii_, Sovetskoye Radio, 1962.)

2. Oshiro, F. K., Mitzner, K. M., Locus, S. S. et al., _Calculation of Radar Cross-Section_, Interim Report AFAL-TR-71-50, May, 1971.

3. Keller, J. B., "Geometrical Theory of Diffraction," J. Opt. Soc. Am., $\underline{52}$, 116-130 (1962).

4. Oshiro, F. K., Mitzner, K. M., Locus, S. S., et al., _Calculation of Radar Cross Section_, Final Report AFAL-TR-70-21, Part II, Analytical Report, April, 1970.

5. Meixner, J., "The Behavior of Electromagnetic Fields at Edges," IEEE Trans. Antennas Propagat., $\underline{\text{AP-20}}$, 442-446 (1972).

6. Keller, J. B. and Ahluwalia, D. S., "Diffraction by a Curved Wire," SIAM J. Appl. Math., $\underline{20}$, 390-405 (1971).

7. IEEE Standard Definitions of Terms for Antennas, IEEE Trans. Antennas Propagat., $\underline{\text{AP-17}}$, 262-269 (1969).

8. Van Bladel, J., _Electromagnetic Fields_, McGraw-Hill, New York, 1964.

9. Pauli, W., "On Asymptotic Series for Functions in the Theory of Diffraction of Light," Phys. Rev., $\underline{54}$, 924-931 (1938).

10. Ryan, C. E., Jr., and Peters, L., Jr. "Evaluation of Edge-Diffracted Fields Including Equivalent Currents for the Caustic Regions," IEEE Trans. Antennas Propagat., $\underline{\text{AP-17}}$, 292-299 (1969).

11. Mitzner, K. M., _Studies in Physical Optics_, Technical Report AFAL-TR-74-22, 1974.

12. Mitzner, K. M., "Diffraction from Open Shells," to be presented at June 1974 URSI Meeting.

DOCUMENT CONTROL DATA - R & D

(Security classification of title, body of abstract and indexing annotation must be entered when the overall report is classified)

1. ORIGINATING ACTIVITY (Corporate author)	2a. REPORT SECURITY CLASSIFICATION
Northrop Corp., Aircraft Division 3901 W. Broadway, Hawthorne, Calif. 90250	Unclassified
	2b. GROUP

3. REPORT TITLE

Incremental Length Diffraction Coefficients

4. DESCRIPTIVE NOTES (Type of report and inclusive dates)

Engineering Report, December 1970 to June 1973

5. AUTHOR(S) (First name, middle initial, last name)

K. M. Mitzner

6. REPORT DATE	7a. TOTAL NO. OF PAGES	7b. NO. OF REFS
April 1974	143	12

8a. CONTRACT OR GRANT NO. F33615-70-C-1820	9a. ORIGINATOR'S REPORT NUMBER(S)
b. PROJECT NO. 7633	NOR 73-104
c. Task 13	9b. OTHER REPORT NO(S) (Any other numbers that may be assigned this report)
d.	AFAL-TR-73-296

10. DISTRIBUTION STATEMENT

Distribution limited to U.S. Government Agencies only; Test and Evaluation Data; April 74. Other requests for this document must be referred to AFAL/WRP.

11. SUPPLEMENTARY NOTES	12. SPONSORING MILITARY ACTIVITY
	Air Force Avionics Laboratory Wright-Patterson Air Force Base Ohio 45433

13. ABSTRACT

The principal goal of USAF Contract F33615-70-C-1820 is to develop a semi-automated system for computing the radar cross section (RCS) of aerospace vehicles over the frequency range of 500-20,000 MHZ. Such a system requires the use of efficient techniques for calculating the high-frequency scattering from bodies with edges such as wings and ducts.

In calculating the scattering from three-dimensional bodies with edges, it is frequently meaningful and useful to consider the scattering associated with an incremental length of the edge and to describe this scattering in terms of an Incremental Length Edge Diffraction Coefficient (ILEDC). In this report the theory of the ILEDC is developed, taking into account the actual distribution of surface current near the edge. The theory is illustrated by applying it to the problem of scattering from a perfectly conducting polygonal plate. The Incremental Length Diffraction Coefficient (ILDC), which is the generalization of the ILEDC for linear scattering features other than edges, is also treated. It is shown that two-dimensional diffraction coefficients, such as those used by Keller and Ufimtsev, can be considered as special cases of ILDC's.

DD FORM NOV 65 **1473**

14. KEY WORDS	LINK A		LINK B		LINK C	
	ROLE	WT	ROLE	WT	ROLE	WT
Radar Cross Section Electromagnetic Theory Electromagnetic Scattering Diffraction Theory						